

Seventh FRAMEWORK PROGRAMME THEME 6 Environment

Collaborative Project (Large-scale Integrating Project)

Project no. 212085

Project acronym: **MEECE**

Project title: Marine Ecosystem Evolution in a Changing Environment

D3.4 Synthesis report for Climate Simulations

Part 3: NE Atlantic / North Sea

Due date of deliverable: 30/09/2012

Actual submission date: 09/01/2013

Lead partner responsible for deliverable: AZTI-Tecnalia

Project co-funded by the European Commission within the Seventh Framework Programme, Theme 6 Environment		
Dissemination Level		
PU	Public	x
PP	Restricted to other programme participants (including the Commission)	
RE	Restricted to a group specified by the consortium (including the Commission)	
CO	Confidential, only for members of the consortium (including the Commission)	

Start date of project: 01.09.09 Duration: 54 months (including extension)

Project Coordinator: Icarus Allen, Plymouth Marine Laboratory

D3.4 Synthesis report for Climate Simulations

Part 3: NE Atlantic / North Sea

Contributors:

Sarah L. Wakelin¹ Ute Daewel², Corinna Schrum², Jason Holt¹, Momme Butenschon³, Yuri Artioli³,
Jonathan Beecham⁴, Chris Lynam⁴, Steven Mackinson⁴

¹ NERC-NOC, United Kingdom

² Geophysical Institute, University of Bergen (GFI-UIB), Bergen, Norway

³ PML, United Kingdom

⁴ Centre for Environment, Fisheries and Aquaculture Science, United Kingdom

Table of contents

1. Science questions	3
2. Models	5
2.1 Lower Trophic Level	5
2.2 Higher Trophic Level	11
3. Scenarios: model validation and projections	14
3.1. Hindcast validation	14
3.2. Climate forced projections	17
4. Metrics considered	21
5. Linkages with MEECE deliverables	22
6. Results	23
6.1. Hindcast validation	23
6.2. Climate forced simulations	32
7. Discussion	68
8. Concluding remarks	70
9. References	76

1. Science questions

Coastal and shelf seas and their ecosystems form a vital part of the environment. They support substantial economic activity, e.g. a large fraction of global fisheries occur in these seas (Watson and Pauly, 2001) and important biogeochemical cycles, e.g. many coastal and shelf seas are observed to be a net sink of atmospheric CO₂ (e.g. Thomas et al., 2004). However, this still remains a significant source of uncertainty in the global carbon budget (Borges, 2005). Fixation of carbon by photosynthesis (primary production) and consumption by zooplankton (secondary production) are two of the most fundamental processes underlying both these aspects. Hence our ability to understand and ultimately predict this process, its variability and change is key to many aspects of environmental policy, for example the European Commission's Marine Strategy Framework Directive and the indicators of Good Environmental Status therein.

The NWS is a broad temperate shelf forming the eastern margin of the northern North Atlantic. It includes several shelf sea regions that are identified in Figure 1. The dynamics of the region are controlled by the seasonal heating cycle, atmospheric fluxes, tides, river inputs and exchanges with the open-ocean. Much of the open-shelf is seasonally stratified, with tidal mixing fronts separating these regions from well mixed/sporadically stratified shallower regions either nearer the coast or on banks. River discharge plays an important role in near coastal regions, leading to regions of freshwater influence; although compared with other shelf sea regions globally, river flows are low. The large scale ocean-shelf exchange is controlled by seasonal upwelling in the south of the region (see Gomez-Gesteira et al., 2011 and references therein), and the poleward slope current and Ekman transport in the North (Holt et al., 2009; Huthnance et al., 2009). This physical background controls, to a large extent, the spatial/temporal patterns of primary production in this region.

Much of these seas are inorganic nutrient limited and hence the supply and recycling of these nutrients generally controls the primary (and hence secondary) production. In coastal regions the combined inputs of significant riverine nutrient loads and optically active constituents (suspended particulate material, SPM, and coloured dissolved organic matter, CDOM) lead to light limited regimes. While these are comparatively small in area, they can exhibit exceptionally high levels of production (e.g. Cadée and Hegeman, 2002). In the winter month's phytoplankton growth is inhibited by high levels of mixing (Huisman et al., 1999) and short day length. During spring, increasing solar irradiance and reduced mixing and consequent stratification can trigger intense phytoplankton blooms. These deplete surface nutrient supplies, but intermittent cross thermocline mixing (e.g. spring neap tidal variability; Sharples, 2008) can maintain mid-water production in stratified regions throughout the summer months, as long as the thermocline is within the euphotic zone. In well-mixed and near-coastal regions the production is more erratic, being controlled by a complex inter-play of optical, mixing and river plume conditions. During autumn, storms and surface cooling (convection) mix the (seasonally stratified) water column. This can trigger an autumn bloom. Bacterial and zooplankton consumption of phytoplankton and detrital material in both pelagic and benthic systems recycles the nutrients and can fuel further production.

Hence plankton growth in the region is controlled by a complex interplay of physical and biological processes, with vertical mixing processes tending to dominate on tidal to seasonal time scales, and horizontal transport processes setting the biogeochemical properties on longer time scales. All these physical processes potentially act as vectors of climatic variability and change. Furthermore, climate changes can potentially impact the dynamics of higher trophic level components. Especially early life stages of fish are very vulnerable to changes in environmental factors. Both, changes in temperature, wind fields and radiation can potentially change the growth and survival and fish offspring in direct (growth, transport) or indirect ways (prey fields) (Hjort, 1914). Atlantic cod (*Gadus morhua*) is one of the top-predators of the North Sea ecosystem and of great economical relevance. Within the frame of MEECE, we also examined the potential survival and growth of early life stages of Atlantic cod in response to changes in physical forcing and lower trophic level dynamics of the North Sea ecosystem. Previous studies on climate change impacts on cod survival in the North Sea indicated a close relation with temperature changes, although other processes such as transport, food availability or predation could play a more important role.

The food webs that make up the North Sea ecosystem necessarily involve very many species divided by habitat, trophic level and other aspects that make up the niche. Classically, predictive models of fish population dynamics such as MSVPA or the North Sea Ecosim model (Mackinson & Daskalov 2007, ICES 2011) have often (but not always) assumed a consistency of environmental and lower trophic level inputs which are reflected in the basic life cycle parameters commercial fish species. This approach is unsatisfactory for a number of reasons: critical parameters that are assumed to be constant, such as recruitment at a fixed population density, can be anything but constant, and potentially important influences on life history become merely a random crowd of uncertainty around the life history models. Moreover, neglecting these mechanisms prevents us from making the conceptual link between known effects of environmental change and species that influence the growth of survival of the higher trophic level species. The aim of this project, therefore, is to see how environmentally driven changes in the lower trophic level components of ecosystems affects the dynamics of different functional groups. Pertinent to this is the idea that the broad pattern of transfer of energy up the food chain will persist in spite of environmental change, which may affect the details of the behaviour and ecology of individual species. The potential richness of interconnections between higher trophic level species, lower trophic level species and the physical environment must lead to a model system that is very greedy in terms of its need for parameters and validation data. There are a number of mechanisms which are expected to be important but difficult to model, such as the migrational response to environmental change or the physiological response of higher trophic level species to changes in the physical environment. To this end, there are a number of necessary simplifications in the coupled ERSEM-EwE model.

It has been decided to model in a non-spatial way – with a single water column feeding into the non-spatial Ecosim component of EwE.

2. Models

2.1 Lower Trophic Level

POLCOMS-ERSEM model in the NE Atlantic

For all simulations, NERC-NOC/PML used the coupled hydrodynamics-ecosystem model POLCOMS-ERSEM (Allen et al. 2001).

POLCOMS (Holt and James 2001) is a three-dimensional hydrodynamic model using a quasi finite-volume approach, discretised on a B-grid in spherical-polar-terrain following coordinates. The Atlantic Margin Model (AMM; Figure 1) configuration considered here has a resolution of $1/9^\circ$ latitude by $1/6^\circ$ longitude grid (~ 12 km) with 42 s-coordinate levels (Song and Haidvogel, 1994) in the vertical. This configuration is further described by Wakelin et al (2009; 2012).

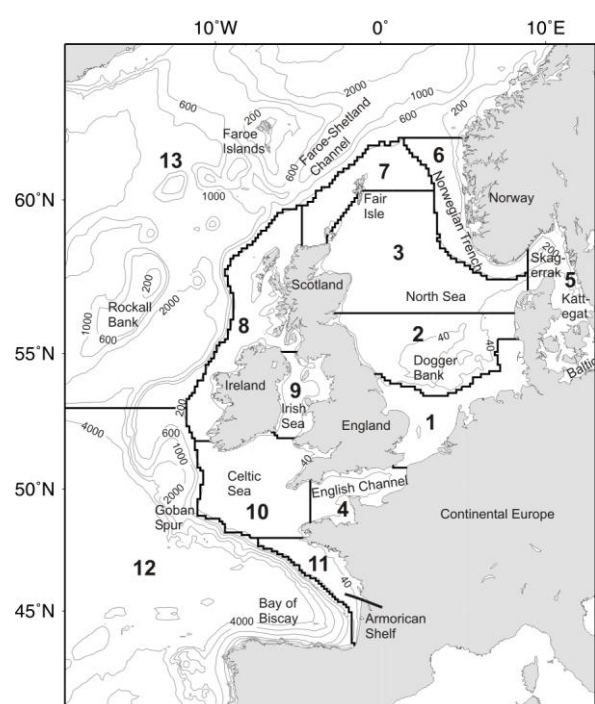


Figure 1: The POLCOMS-ERSEM model domain and regions for area integrals.

ERSEM (Figure 2) is a well established, generic lower-trophic level/biogeochemical cycling model. Eight plankton functional types are represented, including phyto-, zoo-plankton and bacteria, along with the cycling of C, N, P, Si through pelagic (Blackford et al., 2004) and benthic (Blackford, 1997) ecosystems; the latter being critical for nutrient cycling in shelf seas. The model equations can be found in these two papers. The implementation of ERSEM considered here essentially matches that described in Blackford et al. (2004) with a carbonate chemistry module (D2.2) and the treatment of abiotic (SPM, CDOM) absorption described by Wakelin et al. (2012). The parameter set matches that used by Blackford et al. (2004), except here we limit the carbon to chlorophyll ratio to better match observations (Geider et al., 1997; Artioli et al., in press). In the current model we also included a resuspension flux of particulate organic material driven by tidal and residual bottom currents, following Wakelin et al. (2012); surface wave effects are not considered.

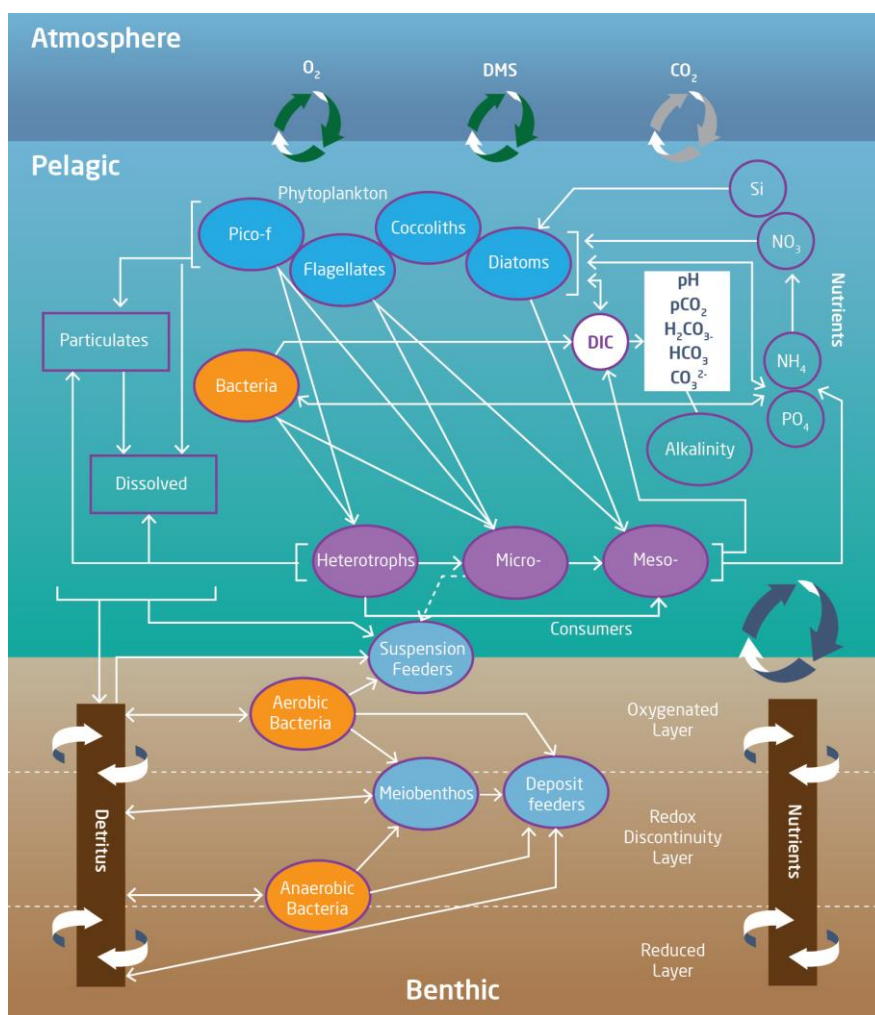


Figure 2: Pelagic and benthic components of the ERSEM model.

Parameterisation of Ocean Acidification (OA) Impacts in ERSEM

Primary production

A parameterisation to link gross primary production to atmospheric pCO₂ has been derived using data from the PEECE III mesocosm experiment are described in D2.5.

$$(*) \begin{cases} C_{enh} = 0.0005 \cdot (pCO_{2,a} - pCO_{2,a}|_{2005}) \\ gPP_{enh} = gPP \cdot (1 + C_{enh}) \\ act.resp_{enh} = asct.resp \cdot (1 + C_{enh}) \end{cases}$$

Nitrification

In ERSEM, the correlation between nitrification rate and pH is already parameterised using the linear equation found by (Huesemann et al., 2002) and described in D2.2:

$$nit = nit_{ref} \cdot \max(0; 0.6111pH - 3.8889)$$

where nit is the nitrification rate, nit_{ref} is the reference nitrification rate (set as 2.0 mmolN/m³/d), and pH is the actual pH value. This corresponds to halving the nitrification rate at approximately 7.2 pH units, and to a complete stop at 6.4 units.

Recent studies showed how the sensitivity of nitrification to pH could be significantly higher (Beman et al., 2011), but we decided to keep this conservative approach.

To estimate the direct impact of OA on nitrogen speciation, the ammonium to Dissolved Inorganic Nitrogen ratio will be used as a metrics, while the difference in the PP (particularly the relative difference between functional types) will be used as indicator of indirect effect.

Biogeography of Alien Invasive Species

The modelling of the impacts of Non indigenous Invasive Species (NIS) is a challenging task. There are many drivers influencing the onset of the invasion and the conditions which will allow the invasive species to colonize the new environment (e.g. is due to lack of predator? Or the NIS is a more efficient competitor for resources?). Furthermore the impacts of a successful invasion may also vary significantly affecting the habitat, the community or even the ecosystem functions. For this reason, any estimates of how climate change and direct anthropogenic drivers influence the probability of having a successful invasion or modulate the impact of such invasion are affected by high uncertainty.

Using a biogeographic approach we can exploit the present biogeochemical models in order to derive insights on changes in vulnerability for invasion of the ecosystem in response to climate change. The impact of an NIS on the ecosystem has been successfully monitored and classified by BioPollution Level index (BPL – Olenin et al., 2007). This index estimates the total impact combining the degree of impact in the different ecosystem compartment (communities, habitat and ecosystem functioning) with the degree of abundance and distribution range of the NIS. The aim is to use biogeochemical models to evaluate the change in abundance and distribution of the specific NIS studied, and hence to evaluate how this affect the BPL for this species. In terms of defining scenarios, because we are considering changes in habitat as a consequence of climate change, the pure climate timeslice scenarios are used (A1B 1980-2000 and 2800 to 2100) are used.

The model system used in this component is the Global Coastal Ocean Modelling System (GCOMS; Holt et al. 2009). GCOMS is derived from the oceanographic model POLCOMS (Holt and James, 2001) coupled to the biogeochemical model ERSEM (Blackford et al., 2004). In this work we have considered a coupled NW European Shelf-Baltic Sea domain. This domain and its associated boundary conditions were defined using GCOMS and has a horizontal resolution of 1/10° and 42 s-coordinates levels, with bathymetry derived from the

GEBCO 1-arcminute dataset (IOC et al., 2003). The outputs of these simulations have previously been used to explore the impacts of climate change on fisheries (Blanchard et al. 2012) and the bio-economics of fishmeal including the consequences for aquaculture (Merino et al. 2012). In this work, we analysed the monthly 2D output from these regional simulations of SST, SSS, and of average nutrient concentration by form in the mixed layer depth. Table 1 summarizes all the rules that define the physical niche, the chemical one and the condition of potential toxicity of a bloom for each of the two prototypes of harmful algae. These rules have been applied in any single grid point of the 2D outputs each month to verify if the model was predicting favourable conditions for a bloom or not.

Table 1: rules defining the physical and chemical envelope where bloom of the two plankton prototype can develop bloom. Data were largely derived from syntheses provided in Heil et al. (2004, Glibert et al. 2012, Vargo et al. 2008 and Brand et al. 2012). (SST: Sea Surface Temperature [°C]; SSS: Sea Surface Salinity; NH_4 : nitrogen concentration [$mmolN/m^3$]; NO_3 : nitrate concentration [$mmolN/m^3$]; N: dissolved inorganic nitrogen concentration [$mmolN/m^3$]; P: dissolved inorganic phosphorus concentration [$mmolP/m^3$])

		Prorocentrum-type	Karenia-type
Physical niche	temperature	15<SST<25	20<SST<30
	salinity	11<SSS<33	11<SSS<33
Chemical niche		$NH_4 > NO_3$	$NH_4 > NO_3$
Potential toxicity		N:P<5.33 or N:P>48	N:P<5.33 or N:P>48

ECOSMO model in the North Sea

ECOSMO is a coupled physical-biogeochemical model (ECOSystem Model, Schrum et al. 2006; Daewel et al., in prep.), with the hydrodynamics based on the HAMSOM (HAMBurg Shelf Ocean Model; Schrum and Backhaus 1999), a free-surface 3D baroclinic coupled sea-ice model. In the frame of MEECE, it has been applied to the combined system of the North Sea and the Baltic Sea (Figure 3). It uses a spherical grid with a horizontal resolution of 6' x 10' and 20 vertical z-levels. It has a free surface and allows for variable thickness in the last model layer, thereby resolving a realistic bathymetry. The model uses a semi-implicit method (Backhaus 1987) which allows for a relative large model time step of 20 min and hence for efficient long-term integrations.

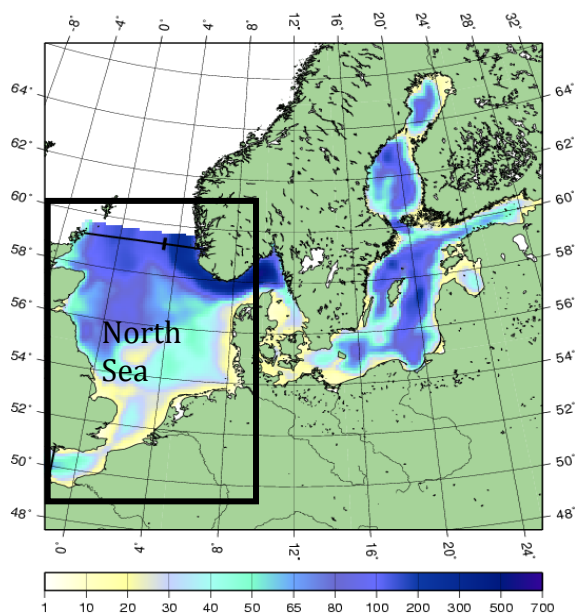


Figure 3: Model area and bathymetry [m].

In contrast to an earlier model version described by Schrum and Backhaus (1999), the current model version has been parallelized using MPI domain decomposition, based on surface decomposition ensuring load balancing, taking into account depth and hence variations in numbers of vertical grid points. Besides the parallelisation and consequent program code changes, a second order Total Variation Diminishing (TVD) scheme was implemented, i.e. a 2nd order Lax-Wendroff scheme was made TVD by a superbee-limiter (e.g. Harten (1983)). Its implementation is in more detail described by Barthel et al. (submitted). Since the TVD scheme is less diffusive, it strongly improved the model system and allows for a significantly better representation of frontal structures connected to narrow currents, such as the Norwegian Coastal current or fresh water runoff, as a comparison to FerryBox observations Hydes et al. (2010) reveals (Figure 4).

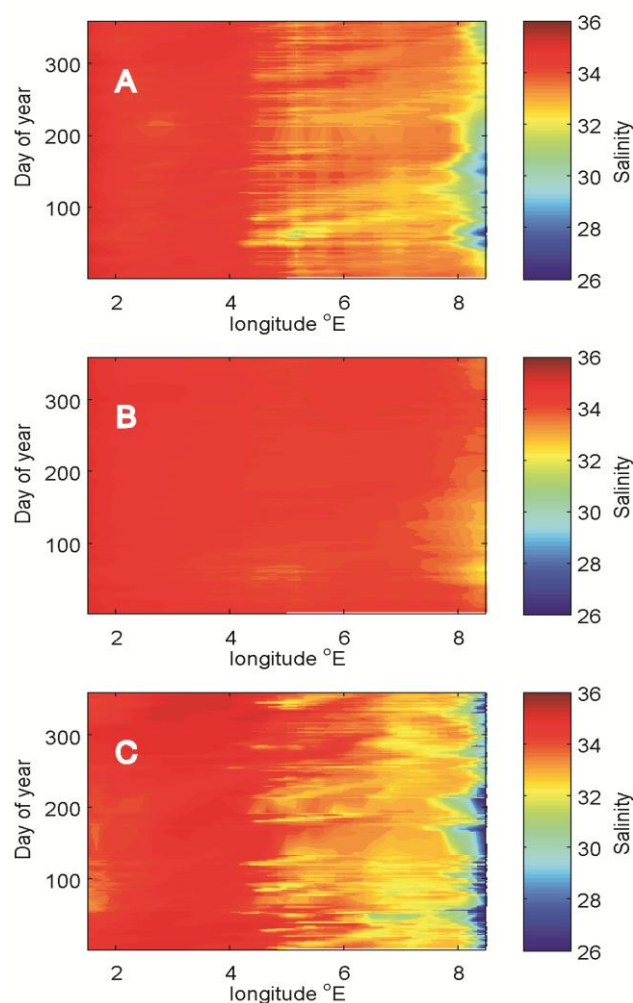


Figure 4. Hov-Möller diagram of salinity distribution along the ship transect Cuxhaven-Harwich and their temporal development from A) the simulations with the TVD scheme, B) the upwind scheme and from FerryBox observations C) ferry box observations.

After validation exercises performed on earlier model version, it deemed necessary to further improve the representation of the lower trophic level dynamics in ECOSMO to make it more applicable to a wider range of ecosystems, with particular emphasize on processes relevant in the Baltic Sea. A number of additional processes were incorporated, and a number of new state variables were introduced, namely 3 sediment groups, a third detritus group accounting for DOM and a third phytoplankton group to account for cyanobacteria. Moreover, the denitrification formulation was improved. The model formulation used here solves 16 state variables that are divided into 3 phytoplankton functional groups, 2 zooplankton functional groups, 3 detritus, 3 sediment and 4 nutrient groups plus oxygen (Figure 5). Primary production in ECOSMO is limited by either nutrients or light, and the 3 major nutrient cycles (nitrogen, phosphorus and silicate), important for simulating nutrient limitation processes in the Nordic marine ecosystems, are resolved. In addition, a module for carbon chemistry (see [D2.2](#), Blackford and Gilbert (2007)) which allows to simulate and project ocean acidification

in a high CO₂ world was incorporated in the model formulation. To solve the model properly, boundary conditions at the open boundaries as well as land- and air-borne nutrient supplies need to be considered.

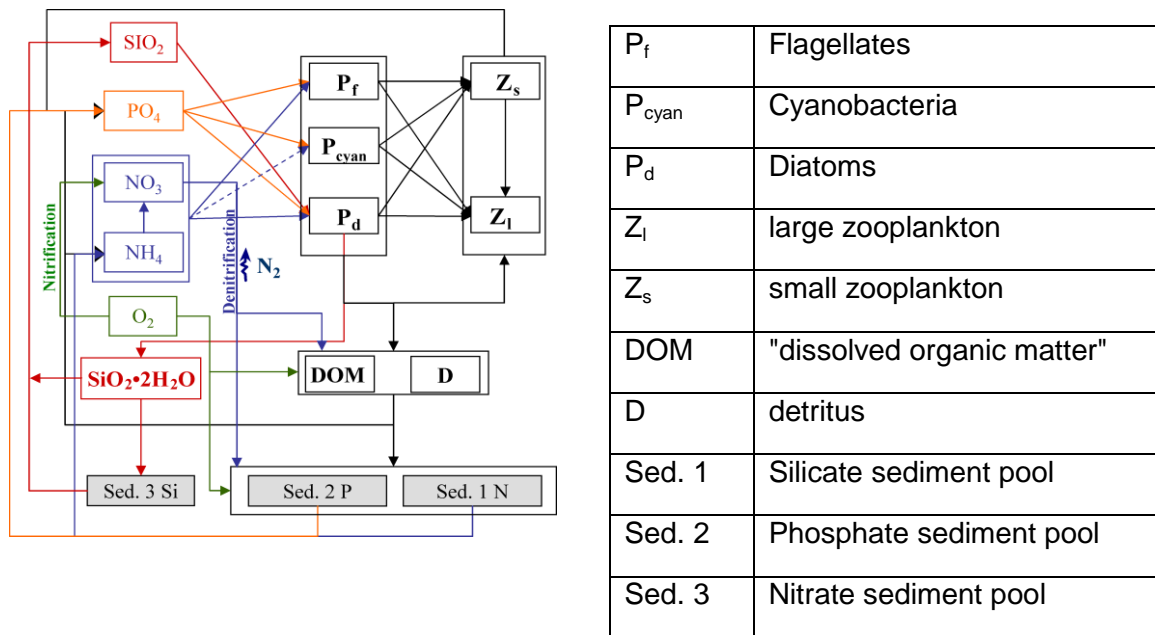


Figure 5: Schematic diagram of biological interactions in ECOSMO II.

2.2 Higher Trophic Level

IBM for Atlantic cod

To disentangle the impact of different processes potentially influencing the vital rates of cod early life stages, we developed and utilized a 3D interlinked model system that included the 3D ecosystem model (ECOSMO) as well as an individual based model (IBM, for submodel description see [D2.11](#)). The model has been described in detail by Daewel et al. (2011) and includes empirical formulations for temperature dependent development during non-feeding stages and mechanistic formulations for energy gain and loss during feeding stages of young Atlantic cod in the North Sea (Fig. 6). Here, the IBM is solved simultaneously to the hydrodynamics of ECOSMO, while prey fields are obtained from offline-performed simulations with ECOSMO (see LTL results of this report). Model setup and forcing are the same as described for the LTL ECOSMO simulations.

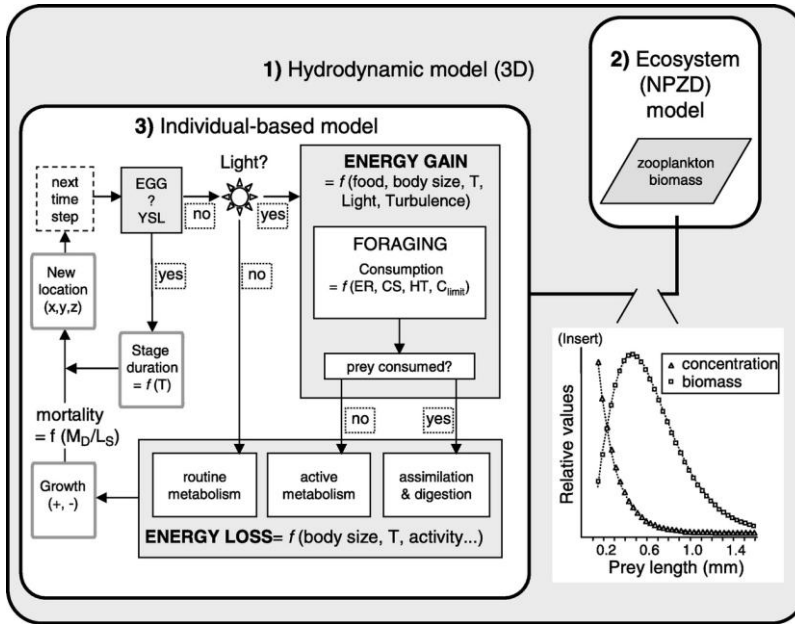


Figure 6: Spatially explicit IBM schematic diagram from Daewel et al. (2011).

In each year model, particles were released based on what is known about the spawning cycle of cod in the North Sea. On each day between 1st of January and 31st of April about 70000 particles (eggs) are released (spawned) all over the North Sea. To avoid a bias due to predefined spawning grounds the particles were dispersed homogeneously in the whole North Sea in the vertical and in the horizontal dimension (Fig. 7).

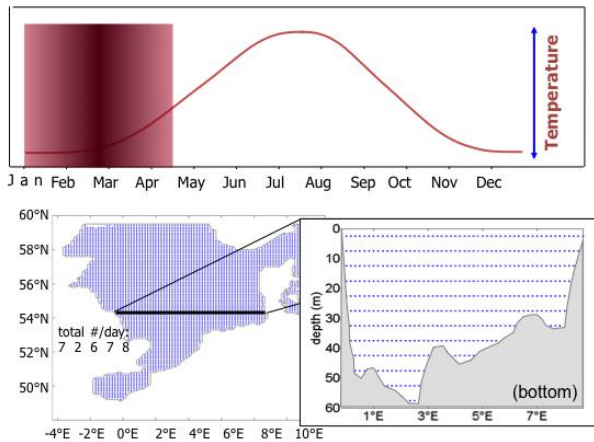


Figure 7: particle release for Atlantic cod eggs in ECOSMO-IBM.

Coupled ERSEM / ECOSIM Lower to Higher Trophic level Model

There are some 65 living groups in the higher trophic level model, some such as Cod, represent a single species, other such as *Sessile Epifauna* are composites of very many species. Details of the model are published in Mackinson and Daskalov (2007) and ICES 2011.

This model focuses on the effect on food webs of simultaneous changes in the climate and nutrients in models of phytoplankton and hence zooplankton production and possible changes in fish harvesting. We use the temporal but non-spatial model Ecosim (which is part of the EwE (Ecopath with Ecosim suite, Christensen et al. 2001)) together with the biogeochemical ERSEM model (Baretta et al. 1997) within the context of a 1 dimensional water column model GOTM (Burchard et al. 1999, 2006). In fig 8 the capabilities of the coupled model in modelling change in marine ecosystems relevant to the MEECE project are outlined. The interactions in green are those considered in this model. The interactions in yellow are those relevant to MEECE which could use this framework, although not explored here. The interactions in red are potentially important but would need modifications to the EwE code; the reasons why this might be useful are indicated in the discussion. Some of the interactions, e.g. the effect of invasive species on commercial species, could be explored with EwE on its own (EwE); others explicitly need the combined higher and lower trophic level mode (EwE GTM), or would need a 2D variant 2D ERSEM with Ecospace.

	Fishing	Invasives	Pollution	Eutrophication	Acidification	Circulation	Temperature
Biodiversity	EwE	EwE		EwE Gtm	EwE Gtm EwE	EwE Gtm (2D)	EwE Gtm EwE
Non Indigenous	EwE	EwE		EwE Gtm		EwE Gtm (2D)	
Commercial Species	EwE				EwE Gtm EwE		EwE Gtm EwE
Foodwebs	EwE	EwE		EwE Gtm	EwE Gtm EwE	EwE Gtm 2D	EwE Gtm EwE
Eutroph	-	-	-	-	-	-	X
Seabed Integ.	X	-	-	-	-	-	-
Pollution	-	-	X	-	-	-	-

Figure 8 The intereractions between drivers and the affected components within the Meece in terms of the model systems utilized to study those interactions.

The conceptual model of the linkage between the two models is shown in fig. 9. Both models have a large number of functional groups (around 65 living groups in the case of Ecosim and around 20 for ERSEM), however there is not an exact correspondence between the groups in the two models. For example, there are between 4 and 6 phytoplankton groups in the ERSEM models used (depending on whether, for example, Phaeocystis is turned on in ERSEM) and a single phytoplankton group in the EwE model of the North Sea. The linkage is primarily at the level of the Herbivorous and Omnivorous mesozooplankton, part of the pelagic model, but EwE also reads in from ERSEM the amounts of microzooplankton, bacteria, phytoplankton and detritus. However, there is no explicit benthic linkage, because

the representation of benthic components in the two models is too different. The ERSEM model is centred on 4.02 deg E and 54.41 deg N (the Oyster Ground), whereas the Ecosim model is a whole North Sea model. This distinction is quite important – a wide diversity of functional groups is achieved, in part, by incomplete mixing – e.g. by different species occupying different parts of the water column, different zones in the sea or different parts of the sea altogether (Herring is a more Northerly species than Cod, for example). In Ecosim which is completely non-spatial, incomplete mixing is modelled by use of the vulnerability index (Ahrens 2011), which is derived from the portion of a species that is vulnerable to a particular predator at a moment in time. It is not always the case, therefore, that a predator within Ecosim will need to feed off a prey population located at a different point, and so the coefficients of predator-prey interaction are adjusted seasonally to allow for the predators being somewhere else.

ERSEM carries out calculations on a ten minute timestep, and is run from real or simulated weather data. This short step is necessary to model the effect of day / night cycles / tides and ocean currents. However, the transfer of information on plankton to and from Ecosim occurs on a daily basis. The exchange of data is performed through Couplerlib, which ensures consistency of functional groups, timing and units.

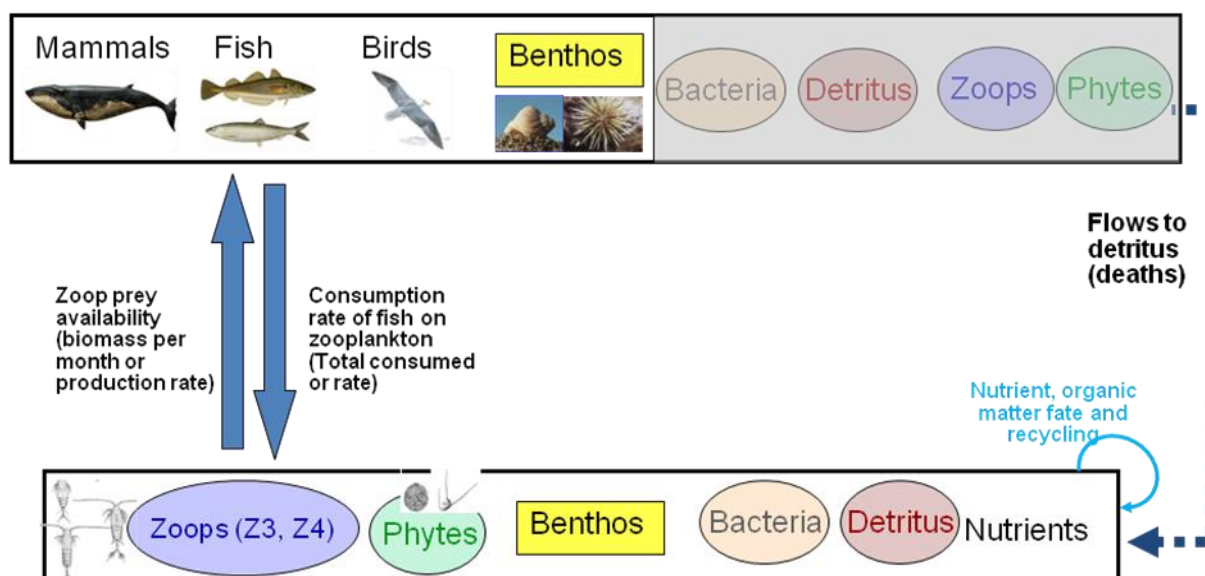


Figure 9: Conceptual diagram of links between lower and higher trophic level components.

3. Scenarios: model validation and projections

3.1. Hindcast validation

Here we consider three model experiments: a hindcast forced by ERA40 atmospheric forcing and two IPSL-CM4 forced simulations (CNTRL and A1B). We use ERA40 to explore present day variability, the difference between CNTRL and ERA40 to explore the consequences of forcing this regional model with a coarser resolution OA-GCM and the difference between

A1B and CNTRL to explore the behaviour of the system under a single example of possible future conditions. These simulations have been published by Holt et al. (2012a and b).

Lower Trophic Level: POLCOMS-ERSEM model

Hindcast simulation ERA40 is a 45-year (1960-2004) simulation with surface forcing from the ERA-40 reanalysis (until September 2001) and subsequently ECMWF operational analysis, using 6-hourly atmospheric air temperature, winds, pressure and relative humidity, and daily precipitation and short-wave radiation (the latter is modulated by the diurnal cycle). Surface fluxes are calculated by COARE v3 bulk formulae (Fairall et al., 2003) in all the experiments considered here. Lateral boundary conditions are taken from a 1° NEMO ocean reanalysis (Smith and Haines, 2009) and a North Atlantic Tidal model (providing 15 constituents; Flather, 1981). Elevation and depth mean current boundary conditions (tidal and 5 day mean residuals) are applied using a flux/radiation scheme. Temperature and salinity are relaxed to 5-daily NEMO data values in a four grid cell wide relaxation zone. Lateral boundary conditions for ERSEM use monthly values from the World Ocean Atlas (WOA; Garcia et al., 2006) for nitrate, silicate and phosphate, imposed with an up-wind advection boundary condition. Other variables use a 'zero-gradient' boundary condition. An exception is the detrital organic material fluxes, which are set to zero inflow concentration to avoid numerical instability. For freshwater fluxes, daily discharge data for 250 rivers are used from the Global River Discharge Data Base (Vörösmarty et al., 2000) and from data prepared by the Centre for Ecology and Hydrology as used by Young and Holt (2007). River nutrient loading matches that used by Lenhart et al. (2010), with raw data for the UK, Northern Ireland, Ireland, France, Norway, Denmark and the Baltic processed by van Leeuwen (CEFAS, UK) and raw data for Germany and the Netherlands was processed by Pätsch and Lenhart (2004). The Baltic exchange at the Belts is treated crudely as an inflow source using a mean annual cycle of depth averaged transport, salinity and nutrients. A constant spatial field of atmospheric nitrogen deposition (oxidized and reduced) is provided by EMEP (Cooperative Programme for Monitoring and Evolution of the Long-range transmission of Air Pollutants in Europe).

Lower Trophic Level: ECOSMO

A hindcast simulation (for outline of scenario see [D1.5](#), additional and complementary information is provided here) was performed using atmospheric boundary conditions as provided by the NCEP/NCAR re-analysis (Kalnay *et al.* 1996). Additionally, monthly means of land-based freshwater runoff and nutrient loads were required to run the model. Since no consistent high quality river runoff and load data set was available for the entire model region, we compiled fresh water runoff from a number of different sources. To fill existing gaps in the runoff and load time series we compiled average annual mean time series from the available data. For the Baltic Sea region the setup is described in the respective section. For the North Sea, we used combined sources for runoff and river load data from German continental rivers (Damm 1997; Radach and Pätsch 1997), British rivers and Norwegian sources (Morten D. Skogen, personal communication, Institute of Marine Research, Norway).

At the open boundaries to the North Atlantic Ocean sea surface variations are prescribed derived from a coarser diagnostic model (Backhaus 1987). Tidal variations were added with a 20 minutes time step accounting for the major 8 tidal constituents. Salinity is prescribed at the open boundaries based on a climatology compiled by Janssen *et al.* (1999) plus additional annual variations calculated from data available at the ICES database (<http://www.ices.dk>). For temperature, in contrast, a Sommerfeld radiation condition is applied (Orlanski 1976). Nutrient data (nitrate, silicate, ammonium and phosphate and oxygen) are taken from the World Ocean Atlas database and other biogeochemical model variables were calculated using a radiation condition.

Validation techniques. To validate the model, we adopted suggestions and methods proposed by Janssen (2002), Allen *et al.* (2007) and generally followed the MEECE model validation strategy. For the validation, we used in addition to the MEECE database, data provided by the ICES (ICES-database, www.ices.dk) and datasets compiled for validation purposes in the North Sea and Baltic Sea regions by Janssen (2002). For the North Sea, we focussed on concentrations of nitrate and phosphate from the ICES data base and present a validation for surface layer nutrients (data above 20 m, vertically averaged). Model data and observational data were co-located before calculation of error measures. We utilized a number of statistical methods to compare model and observations. Besides correlation, explained variance and RMSE (see e.g. (Janssen 2002)), we applied Taylor diagrams (Taylor 2001) to visualize model performance with respect to observations. Since this combines the centred root mean square difference, correlation coefficient and standard deviation, it allows to determine whether an error stem from differences in structure and phase or from differences in the amplitude (Taylor 2001). To make the areas better comparable in one diagram, all statistics were normalized with the standard deviation in the respective area.

Higher Trophic Level: cod IBM in the North Sea

The model runs and scenarios performed with the spatially explicit IBM were based on the LTL experiments with the NPZD model ECOSMO. Hence, the setup for the HTL experiments is the same as for the LTL experiments and prey fields were extracted directly from the ECOSMO output.

A 40 year long-term hindcast simulation 1960-1999 (for outline of scenario see [D1.5](#), additional and complementary information is provided here) was performed using atmospheric boundary conditions as provided by the NCEP/NCAR re-analysis (Kalnay *et al.* 1996).

It is challenging to validate this type of models since they only consider a subset of processes and life stages and they are not directly comparable to *in situ* observations. A discussion on that topic was given by Daewel *et al.* (2011). Here we present qualitative comparisons of observed spawning grounds (Fox *et al.* 2008) to a larval survival index back calculated from recruitment data as published by Beaugrand *et al.* (2003). These comparisons allow us to identify first, whether the results are reasonable and second,

underlying processes that determine spawning behaviour and larval survival of Atlantic cod in the North Sea.

GOTM-ERSEM Lower Trophic level Model coupled to Ecosim Higher Trophic level Model

Calibration of the HTL component of the coupled model is reported in ICES 2011, which shows how the model predictions are fitted to observation data by tuning the vulnerability parameters and inclusion of forcing functions on primary production and consumption rates of some functional groups. The fitted vulnerability parameters in the HTL define the interaction strength among predators and prey in the food web. These parameters are included in the coupled LTL-HTL model, while the driving of changes in production at lower trophic levels becomes entirely controlled by the LTL (ERSEM) model, which is turn driven by GOTM. Validation (per se) of the couple model has not been performed. However, the parameterisation of the coupled model has been directed to achieving a stable biomass dynamics of the functional groups, further details of which can be found in Beecham et al (2011).

3.2. Climate forced projections

Lower Trophic Level: POLCOMS-ERSEM model in NE Atlantic

We use the POLCOMS-ERSEM model to downscale a climate change scenario from the IPSL-CM4 20C model. We adopt a time-slice approach commonly used in climate impact studies, whereby mean conditions in a future period are compared with mean conditions in a present day reference period to give a measure of the climate change signal, on the assumption that conditions in both time-slices are approximately stationary. We use the direct forcing downscaling approach for described in D3.1, focusing on the A1B SRES scenario and consider two experiments identified as CNTRL and A1B. The CNTRL simulation is a 23-year present day simulation forced by the IPSL-CM4 20C model for the nominal present day period 1980-1999 (1980 is repeated three times before this period is simulated). The OA-GCM provides the same frequency atmospheric forcing fields as ERA40, and monthly ocean currents, sea level, temperature and salinity. Tides, rivers, abiotic absorption, and nutrient boundary conditions match those in ERA40. A1B is a future climate scenario representative of possible conditions in 2080-2100 under a business as usual emissions scenario: SRES A1B. Again the first year is repeated three times before running this period. The forcing matches CNTRL using the same OA-GCM simulation run forward to this period. This OA-GCM simulation includes the PISCES ecosystem model (Aumont et al., 2003) and we perturb the open-boundary nutrient values (nitrate, silicate and phosphate) by the fractional change between this time-slice and CNTRL using the delta change approach described in D3.1; the bias between the PISCES nutrient values and WOA data prohibits the use of an absolute change. River flows are perturbed by changes in regional rainfall from the OA-GCM, whereas riverine nutrient loads and atmospheric inputs are unchanged.

The OA-GCM has a significant negative temperature bias in the northwest European Shelf (NWS) (~-2°C), which may unduly influence changes in those processes non-linearly dependent on the temperature, e.g. growth rates and stratification. Hence we linearly correct

(D3.1) this bias in CNTRL and A1B using a time constant 3D correction field (for temperature and salinity, derived from WOA data) applied to the initial and boundary conditions, and a 2D correction to the air temperature derived from ERA40. The procedure is partially successful in removing the bias.

In all experiments we treat the first 5 years as ‘spin-up’ to allow the model to adjust to its lateral boundary and surface forcing conditions, so the results presented here are means for 40 years for ERA40 and 18 years for CNTRL and A1B.

Lower Trophic Level: ECOSMO in the North Sea

The climate change downscaling experiments were performed using results from the IPSL-ESM (D3.2). Here we followed the MEECE modelling strategy (D3.1) and applied a delta change approach (see for details D3.1). The climate change forcing was taken from IPSL 20C simulations and future scenario simulation A1B. The climate delta change signal was estimated for a 30-year period (climate time scale period) and applied to the simulations. The reference simulation and climate change simulations were both performed for a 30-year period (present day reference 1970-1999 and future simulations 2070-2099). According to the MEECE scenario definitions and MEECE approach we present the climate change results for 20 year time slices, present day: 1980-1999 and future scenario period: 2080-2099. The delta change method is applied to both the atmospheric and oceanic boundary conditions (including nutrients). River runoff and nutrient loads were not available from the GCMs and ESMS and are hence kept unchanged for the climate change experiments.

To assess the level of uncertainty of the projected changes, we performed additional model simulations forced by various GCM's and diverse scenarios. All GCMs used in this study are fully coupled 3-D atmosphere-ocean climate models although in the uncertainty assessment presented here we focus on changes in atmospheric forcing only. The GCMs selected were either part of the IPCC Fourth Assessment Report or will be included in the upcoming IPCC Fifth Assessment Report. An overview of the applied models and respective scenarios selected for our assessment is given in Table 2. All model projections were similarly applied to ECOSMO following the MEECE downscaling strategy as described above.

Table 2: IPCC AR4/AR5 GCMs and scenarios applied for uncertainty assessment.

Models	Scenarios
IPSL (AR4)	20C and A1B
BCM (AR4)	20C and A1B
ECHAM5 (AR4)	20C and A1B
NorESM (AR5)	Historical and RC4.5

Higher Trophic Level: ECOSMO in the North Sea

The forecast was, for ECOSMO, based on the fully coupled IPSL-ESM and a 30-year period (2070-2099) was simulated. To assess an estimate of potential uncertainties associated with the selection of the GCM forcing, we performed an additional experiment using NorESM instead of IPSL-ESM for the 7-year period between 2090-2096. Thus, we analysed the change of forecast relative to a control period (1990-1996).

Ocean Acidification impacts: ERSEM in the NE Atlantic

Four different simulations have been run in this work, using atmospheric forcing and oceanic boundary condition coming from the climate model IPSL-CM4 (Marti et al., 2006). We used a single member of the ensemble that is representative of the ensemble average response (Bopp, personal communication). The first one simulates present day conditions (1981-2000, called CNTRL). The remaining three runs are all far future simulations (2080-2099) that use outputs of the same ensemble member run under the IPCC AR4 A1B scenario. They differ on the parameterisation of OA impacts used:

1. A1B uses the same ERSEM parameterisation use in the PD scenario (i.e. the standard primary production model and nitrification rate depending on pH). This simulation will be used to assess the global impact of climate change and OA on the marine ecosystem and it will be used as a reference for the following scenarios.
2. ENH uses the enhanced primary production model and the pH depending nitrification rate.
3. NIT uses the standard primary production model and a nitrification rate depending only on temperature.

The diagnostic variables used are;

- the seasonal means of pH and aragonite saturation state to assess the impact on the carbonate system,
- the monthly means of net PP (calculated as particulate primary production), zooplankton biomass (both as a total and split by PFT) and the ammonium to total dissolved inorganic nitrogen ratio (NH₄:DIN) have been used to assess the broader impact on the ecosystem.

Net PP and zooplankton biomass are depth integrated on the whole water column, while all the other variables refer to surface values, where not differently specified. Seasonal mean have been calculated as mean of three consecutive months starting from January (winter=JFM, spring=AMJ, summer=JAS, autumn=OND)

GOTM-ERSEM LTL model linked to ERSEM HTL model

The Model was run with 10 different scenarios reflecting different options for future patterns of fishing, climate and eutrophication.

	No warming	A1B warming	B1 warming	A1B warming	B1 warming
Baseline N & P	½ N & P	½ N & P			
Current F	Baseline	A1BH2080B	B1H2080B	A1BL2080B	B1L2080B
F=MSY	HMSY	A1BH2080M	B1H2080M	A1BL2080M	B1L2080M

The assumptions behind the scenarios were as follows:

Warming:

- No warming – Using simulated climate data based on 1990 weather observations, this represents the approximately current meteorological conditions.
- A1B warming – The level of warming predicted by the IPCC A1B scenario – a global and industrial oriented civilization with a mix of fossil and non-fossil fuels – warming predicted 3.4 degrees.
- B1 warming – A less industrial orientated civilization – warming predicted 2.3 degrees.

Eutrophication:

- High N & P - Levels of N & P associated with current and recent historic levels of nutrients in seawater, start parameter 5.0 mmol N / m-3, 1.0 mmol P m-3.
- Low N & P – Reduced levels of N & P associated with a less industrial future (particularly less use of fertilizers); start parameter 2.5 mmol N m-3, 0.5 mmol P m-3

Fishing:

- Baseline: Calibrated to current levels of fish stocks
- MSY: Calibrated to levels of fish stocks in accordance with management practice designed to lead to exploited fish stocks at MSY

Species	Baseline	MSY
Cod	0.386	0.310
Haddock	0.458	0.309
Herring	0.219	0.19
Norway Pout	0.098	0.01
Sandeel	0.2367	0.25

Sprat	0.1573	0.350
Whiting	0.2577	0.350
Plaice	0.2710	0.171
Saithe	0.267	0.119
Sole	0.213	0.188

The scenarios marked in orange are scenarios consistent with a scenario applied consistently across all three inputs. The remainder are mixtures of different assumptions – which is reasonable because they are likely to be applied by different jurisdictions within each scenario.

4. Metrics considered

For the lower trophic level model, we used:

- Surface temperature (absolute change)
- Surface salinity (absolute change)
- Surface nutrients (fractional change)
- Surface pH (absolute change)
- Depth integrated phytoplankton biomass (fractional change)
- Depth integrated zooplankton biomass (fractional change)
- Net primary production (fractional change)
- Changes in seasonal stratification statistics and potential energy anomaly

For the higher trophic level, the model provides a number of different parameters such as egg developmental rate or growth rate. Here we focus on the potential larval survival (PLS), which serves as a proxy for climate impacts on larval survival probability due to feeding and starvation processes. As described in Daewel et al. (2011), PLS was back calculated to the time and location of particle release (egg spawning) and presented as the percentage of surviving particles per grid cell. This definition allows an estimate of the spawning grounds and times that would potentially support larval survival when predation pressure is not considered.

For the Ecosim higher trophic level food web model coupled to the ERSEM LTL model biomasses relative to the baseline scenario was produced for a variety of commercial species (such as Cod, Haddock, Plaice) and of non-commercial species / functional groups – seals, seabirds, sharks.

For non-exploited top predators (i.e. seals, whales and sharks) biomass was closely tied to production because non-predated and non-exploited populations are constrained by energy inputs and an increase in input of x% can reasonably be expected to sustain a population x%

higher. For species further down the food chain the increase in biomass may be less than the increase in production if that increase in production serves mainly to increase the amount of predation.

Species and functional groups considered in the Atlas are as follows: Cod, Whiting, Haddock, Saithe, Blue Whiting, Norway Pout, Herring, Sprat, Mackerel, Sand Eel, Plaice, Dab, Flounder, Sole, Turbot & Brill, Halibut, Catfish, Large Sharks, Small Sharks, Starry Ray, Thornback Ray, Skate, Seals, Sea birds, Omnivorous Zooplankton, Squid & Cuttlefish, Gelatinous Zooplankton, Large crabs, Nethrops, Shrimps, Sessile Epifauna, Microzooplankton, Phytoplankton.

5. Linkages with MEECE deliverables

The MEECE deliverables listed in Table 1 were used to undertake the present deliverable.

Table 1. Linkages with MEECE deliverables.

Deliverable used for LTL	Comments
D1.5	outline of model scenarios
D2.2	details of carbon submodel
D2.7	validation methods
D2.13	Sub-model alien invasive species including user guide
D3.1	outline of model scenarios and downscaling methods
D3.2	description of metrics
D3.5	data provided for the MEECE Atlas
Deliverable used for HTL	Comments
D1.3	In addition, ICES data were used to validate nutrient dynamics
D2.2	D2.2 was used to simulate acidification processes
D2.8	Coupled ERSEM-EwE model
D2.11	An IBM for Atlantic cod has been used
D3.1	The MEECE common set of forcing scenarios was used
D3.2	The MEECE common set of metrics was used
D3.3	Scientific papers are submitted and in preparation from the hindcast and climate change simulations
D3.5	Data from the hindcast and climate change simulation are delivered to compile the MEECE atlas

6. Results

6.1. Hindcast validation

Lower Trophic Level: POLCOMS-ERSEM model in the NE Atlantic

The uncertainties in the POLCOMS-ERSEM system have been extensively investigated in comparison with contemporary observations for seasonal scale simulations (Allen et al., 2007a; Holt et al., 2005; Lewis et al., 2006; Allen et al., 2007b) and detailed analysis of the representation of inter-annual variability for temperature has been published (Holt et al., In Press). Here we focus on an assessment of the mean state for temperature, salinity, nitrate and chlorophyll, drawing on the substantial volume of in-situ data for this region held at the World Ocean Data Base. We concentrate on values in the 13 regions shown in Figure 1. All the data available in the period 1981-2004 for each month are averaged onto the model grid to give 12, 3D monthly climatological mean fields for each variable and corresponding fields are calculated from the model results. For each month the surface fields are differenced (model minus observations) and these values used to calculate the statistics shown in Table 2, over each of the 13 regions. The bias is the average deviation across the region and for all months. The cost function, χ , is defined as the root mean squared (RMS) deviation divided by the standard deviation of the monthly mean observed fields in each region. Surface values are defined as the top 8 model s-levels; this ranges from 2m in 10m water depth to 37m in 4000m water depth. Hence, the mean bias indicates the overall sign and magnitude of the discrepancy between model observation and χ assesses the model's ability to reproduce the mean annual cycle and the spatial variations. Cost function values are typically ~ 1 across the regions and variables, except for temperature, which has values between 0.4 and 0.7. Hence salinity, nitrate and chlorophyll have RMS errors close to the spatial and temporal variability. The regions of the highest error for nitrate and chlorophyll are Skagerrak/Kattegat, Norwegian Trench (reflecting the poor representation of Baltic exchange), and Armorican shelf. The NE Atlantic and Shetland shelf also show high errors for chlorophyll, but there are limit number of data in these regions. There is no systematic increase in errors when comparing CNTRL with ERA40, indicating that forcing with this coarser resolution OA-GCM does not substantially degrade the simulation. However, there is a consistent negative temperature bias in the CNTRL experiment, indicating that a more sophisticated bias correction approach may be needed.

Direct measurements of the net primary production (netPP) are subject to substantial uncertainties and grossly under-sample spatial and inter-annual variation. However, accepting these limitations, we compare observed values of netPP from the literature with ERA40 and CNTRL values by region (Table 2). This demonstrates that both ERA40 and CNTRL produce annual netPP within the observed range in each region except for the Skagerrak/Kattegat. The netPP values in CNTRL tend to be less than those in ERA40. This most likely arises from both the air temperature and wind speed being less in the OA-GCM forced run than the reanalysis forced run.

Table 2: Model validation for ERA40 and CNTRL using all WOD data in the domain for the period 1981-2004. Mean Bias and cost function, χ are shown for the regions in Figure 1. This is based on ~168000 temperature and salinity observations, 62000 nitrate observations and 49000 Chl-a observations. $FC=A1B/CNTRL-1$. Values in bold indicate mean values in CNTRL and A1B are significantly different, given the inter-annual variability (tested at 95%).

ERA40	Temp.		Sal.		Nit.		Chl-a		Mean netPP	
	Mean bias	□□Mean bias	□□Mean bias	□□Mean bias	□□iERA40	Literature				
	°C	bias	bias PSU	bias	mmol/m ³		mg/m ³	gC/m ²		
1. Southern North Sea	-0.4	0.3	0.3	0.8	0.0	0.9	-3.0	1.0	149	150-300 ¹
2. Central North Sea	0.2	0.4	0.0	0.8	4.1	1.3	-1.2	1.0	118	100-150 ^{1,2}
3. Northern North Sea	0.2	0.4	0.1	0.8	2.6	1.2	-0.4	1.0	108	54-127 ³
4. English Channel	-0.2	0.4	0.2	0.9	-6.0	0.9	-2.3	1.1	151	
5. kagerrak/Kattegat	-0.6	0.4	0.7	0.5	6.1	2.3	-0.8	1.1	131	135-220 ⁷
6. Norwegian Trench	-0.2	0.5	0.5	0.8	5.5	1.8	-1.8	1.1	102	
7. Shetland Shelf	0.3	0.5	-0.1	0.9	0.4	0.9	0.2	2.0	105	
8. Irish Shelf	0.4	0.4	0.1	0.6	2.9	1.1	-0.3	0.9	131	
9. Irish Sea	0.2	0.7	0.2	0.8	2.6	1.0	0.1	0.9	145	<100-194 ⁴
10. Celtic Sea	0.9	0.7	-0.2	0.8	0.0	0.9	-0.8	1.0	143	160 ⁶
11. Armorican Shelf	-0.4	0.5	0.1	0.7	2.5	1.4	0.6	1.1	170	
12. NE Atlantic (S)	0.3	0.4	-0.2	1.1	0.6	0.7	0.0	1.0	122	
13. NE Atlantic (N)	-0.5	0.7	-0.2	0.9	-0.2	0.9	0.7	2.1	112	

CNTRL	Temp.		Sal.		Nit.		Chl-a		Mean netPP	
	Mean bias	□□Mean bias	□□Mean bias	□□Mean bias	□□CNTRL	FC				
	°C		PSU		mmol/m ³		mg/m ³	gC/m ²		
1. Southern North Sea	-1.1	0.4	0.9	0.8	-4.3	0.9	-3.3	1.1	129	3.9
2. Central North Sea	-0.7	0.4	0.3	0.9	4.0	1.3	-1.3	1.0	121	-3.2
3. Northern North Sea	-0.9	0.5	0.4	0.9	2.7	1.2	-0.3	1.1	112	-9.6
4. English Channel	-0.7	0.4	0.6	0.9	-10.2	0.9	-2.7	1.1	113	2.1
5. Skagerrak/Kattegat	-1.3	0.5	1.3	0.5	5.9	2.3	-0.8	1.2	138	3.4
6. Norwegian Trench	-1.1	0.6	0.8	0.9	5.3	1.7	-1.8	1.1	96	-3.9
7. Shetland Shelf	-0.8	0.6	0.0	0.9	0.4	0.9	0.2	1.9	105	-10.5
8. Irish Shelf	-0.7	0.5	0.2	0.7	3.6	1.3	-0.3	1.0	118	-1.6
9. Irish Sea	-0.9	0.8	0.7	1.1	0.7	1.0	-0.5	1.0	120	11.3
10. Celtic Sea	0.0	0.5	0.2	0.8	-2.6	0.9	-1.0	1.1	121	1.7
11. Armorican Shelf	-0.5	0.5	0.1	0.8	3.5	1.5	0.0	1.0	151	-2.1
12. NE Atlantic (S)	-0.8	0.5	0.0	1.0	0.9	0.7	0.2	1.2	120	-15.1
13. NE Atlantic (N)	-1.5	0.9	0.0	0.9	0.4	1.0	1.1	2.9	103	-5.4

Literature values of netPP are from: ¹ Joint and Pomeroy (1993); ²North Sea Quality Status Report (1993); ³ Steel (1956); ⁴ Gowen and Bloomfield (1996); ⁵ Gowen et al (2000); ⁶ Joint et al (2001); ⁷ Rydberg et al (2006).

Lower Trophic Level: ECOSMO in the North Sea

Climate and physical variables. Figure 10 and Figure 11 show results from a validation of modelled SST anomalies vs gridded Reynolds data are presented. The results clearly indicate the models potential to project the interannual variability of thermodynamics in the

North Sea. However, close to the coastline, the model results seem to disagree with the observations. This disagreement can partly be attributed to weaker performance of the forcing atmospheric data set close to the coast and a consequent decreasing performance in the hydrodynamic model. Another possible reason is the low resolution of the Reynolds data, which is significantly below the model resolution. The Taylor diagrams presented in Figure 13 summarize the results of the SST validation for the southern and northern North Sea separately. It indicates a better representation in modelled SST in the northern part of the North Sea. In both the northern and southern North Sea, the model performs best in the beginning of the year.

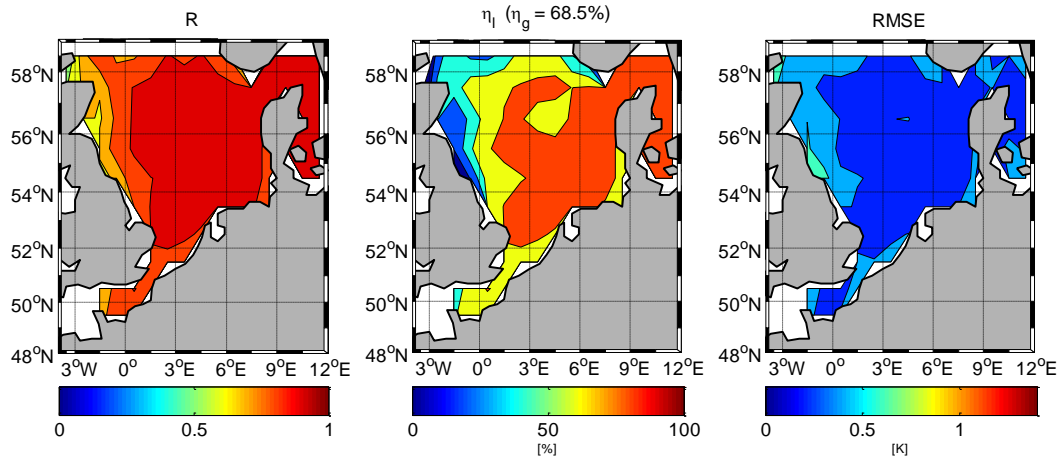


Figure 10: Error measures for the modelled summer SST. From left to right: correlation coefficient (R), explained variance (η) and RMSE. The error measures for the model data are estimated vs. gridded Reynolds SSTs. (temporal resolution of data: monthly).

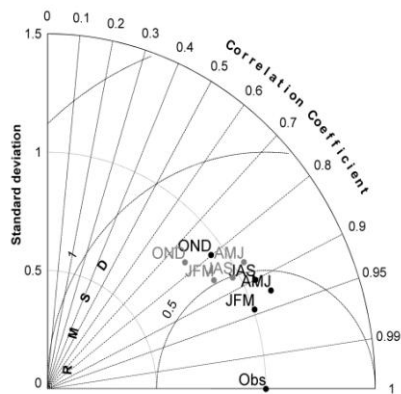


Figure 11: Taylor diagram for modelled seasonal (3 month) SST vs Reynolds SSTs. The analysis are performed for the southern (left, grey) and northern (left, black) North Sea.

The local validation of temporal changes in sea surface salinity (SSS) in a specific area of the German Bight (Figure 12) using direct rather than gridded observations showed the models potential for simulating hydrodynamic variability even in highly dynamic and frontal

active regions such as the German Bight. This validation highlights the importance to consider full resolution in observational products when validating the model.

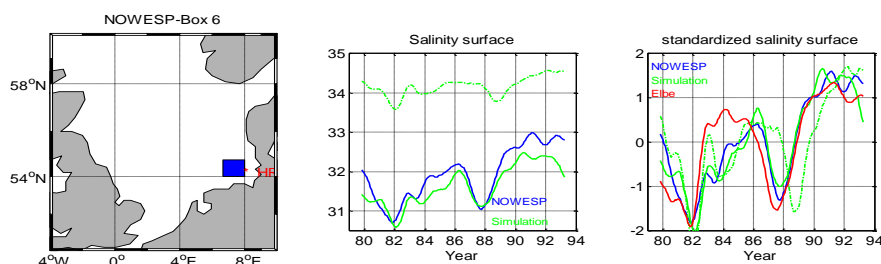


Figure 12: Salinity in the North Sea, modelled vs observed. Helgoland Roads NOWESP data (Radach et al., 1996). Right panel: location of the observations (star: Helgoland roads; box: NOWESP-box6). Mid panel: surface salinity (dashed line: averaged over the whole NOWESP box, full line: at the location of HR). Right panel: standardized surface salinity and Elbe runoff.

Lower trophic levels (LTL) and nutrients

Within MEECE, the hindcast simulation has extensively been validated against nutrient data from the ICES databases (Figure 13) and statistics are presented here in Taylor-diagrams for nitrate (Figure 13a) and phosphate (Figure 13b). The validation reveals that the model is able to describe the nutrient dynamics properly, specifically in the central and northern North Sea, while lowest agreement was found for the shallow, near coastal areas of the southern North Sea. Additional validations (not shown here) reveal that both seasonal cycle, as well as the variability and long term variations are properly described. Again, only near the continental coast the model performance is weaker (region F, G and H). In those regions, summer production seems to be too early phosphate limited, while the observations indicate phosphate limitation occurring later. There are a number of possible reasons for the disagreement in those regions. On the one hand, the regions are highly dynamic due to tides and freshwater supply and the comparison of instantaneous observations and daily mean modelled nutrients will always identify differences, which are partly caused due to the different temporal resolution of model results and data. On the other hand, nutrient dynamics in the shallow near coastal areas of the southern North Sea are known to be determined by internal sediment processes in the Wadden Sea (van Raaphorst and Veer 1990) which are not resolved in the model. A more detailed paper presenting the updated model and discussing the models performance and sensitivity is in preparation (Daewel et al., in prep).

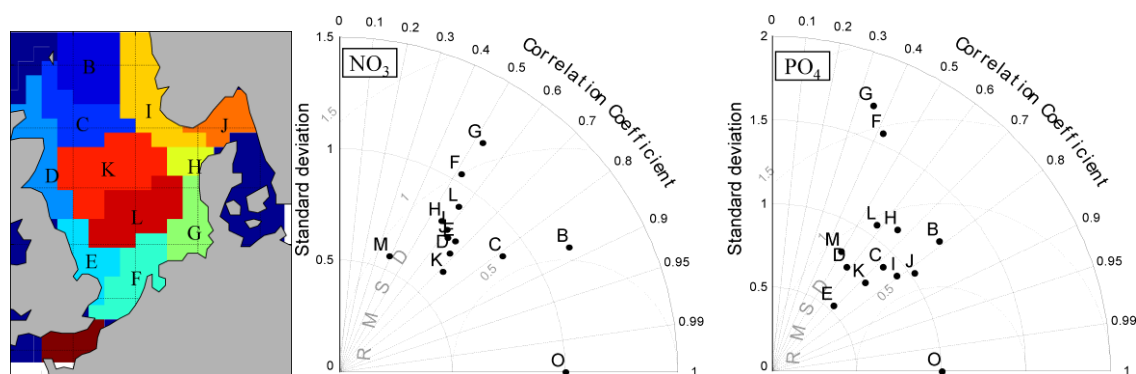


Figure 13: Taylor diagrams for model validation of nutrients. Left: Nitrate, right: Phosphate. Reference data are from the ICES database. Letters indicate different regions in the North Sea as shown in the map.

Zooplankton biomass was validated against CPR (Continuous Plankton Recorder) data for the time period 1958 onwards. Data are available from SAHFOS (Sir Alistair Hardy foundation for Ocean Science) and the sampling method has been described by e.g. (S. D. Batten et al., 2003). The CPR counts were converted into biomass (Rabea Diekmann, Univ. Hamburg personal communications) using a standard length-weight relationship for copepods/zooplankton (Peters, 1983). Modelled zooplankton biomass was co-located with CPR samples in space and time and analysed with respect to the route where they were sampled on.

In Figure 14 seasonal cycles are presented for the 12 most extensively sampled routes. The graphs indicate a general underrepresentation of CPR samples with a factor of about 10-30 when compared to model results. This underestimation of biomass by CPR data can be assigned to the CPR method and has been reported earlier by a number of authors (e.g. S. Batten, 1996; Clark, Fox, Viner, & Livermore, 2003). Besides the general underestimation, a systematic difference between modelled and observed seasonal cycle occurs early in the year specifically between March and May. We believe that the specific sampling of the CPR method is the most likely and most important reason for this deviation. The biomass estimates include only estimates for CV-CVI stages of copepods, all younger copepodite stages as well as other zooplankton species are excluded. This could explain the mismatch between modelled zooplankton biomass and the zooplankton biomass proxy derived from CPR copepod abundance estimates in late spring since early copepod stages and other species like Euphausiacea have been found dominating early in the year (Fransz, Colebrook, Gamble, & Krause, 1991).

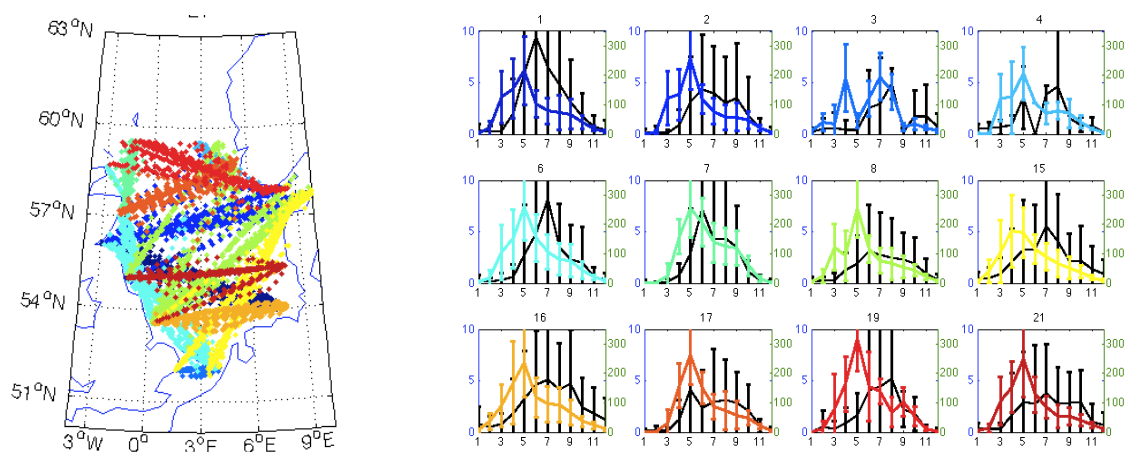


Figure 14: Right panel: Annual cycle of in situ (black, left axis: CPR-samples) and modelled (colored, right axis) zooplankton biomass. Samples were co-located in space and time and monthly means calculated. Data were partitioned based on the route the CPR recorder was sampling on (see map left panel). Only night samples were considered.

We assessed moreover the similarities of modelled biomass and CPR abundance proxy for describing interannual variability and climatic changes. Due to the principal differences in CPR abundance proxy and model estimates as outlined before, we won't expect an absolute agreement. However, such a comparison would allow us to assess whether the model in general is suitable to describe interannual and climatic changes in zooplankton biomass. We estimated relevant statistics for the time series describing changes in annually averaged biomass estimates and used the CPR tracks to group the models spatially (Figure 15). We found significant correlations between modelled biomass and CPR biomass proxies for at least four of the analysed routes (3,4,19,21).

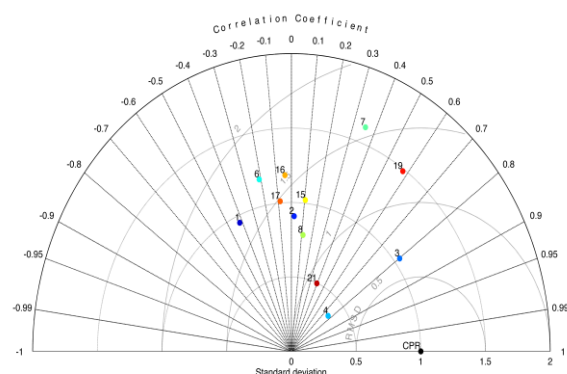


Figure 15: Taylor diagram comparing statistics of in situ (black: CPR-samples) and modelled (colored) zooplankton biomass. Samples were co-located in space and time and annual means calculated track-wise (indicated by different colors according to Figure 14). Only night samples were considered.

From the 60-year reconstruction, we assessed and compared the past climate states of primary production for two complete climate periods of 30 years. Specifically, several lower trophic levels descriptors have been analysed: average annual primary production (PP;), spring primary production (SPP), the diatom to flagellate ratio (DFR), and the mean diatom day (MDD) (Figure 17). While the spatial variability for PP recovers the general picture as already described in Schrum, Alekseeva, and St.John (2006) and has been reported for other modelling studies in the North Sea (Moll and Radach 2003), both PP and SPP show more patchiness with certain “hot-spots” at the British and along the German and Danish coastline. These “hot-spots”, at least in the German Bight, might be deduced to the circulation pattern in that area. For example, former model studies (Dippner 1993) indicate eddy formation in front of the German and Danish Coast at westerly wind condition due to an interaction between bottom topography and wind.

The time series clearly show that the model is able to reproduce regime shifts which earlier have been observed in the late 1980's as reported e.g. by Alheit *et al.* (2005) and that the model reproduce decadal changes in observed plankton dynamics. A comparison with published observational studies (Edwards *et al.* 2002; Mcquatters-Gollop *et al.* 2007; Pitois and Fox 2006) indicates that the model sufficiently represents the long-term ecosystem dynamics. While the production undergoes distinct long-term changes in the northern and southern North Sea, remain DFR and MDD in the southern North Sea rather constant throughout the period. The phenological shift in the northern North Sea is, on the other hand, accompanied by a change in PP. The estimated MDD indicates a later diatom bloom in the second period of the modelled time period.

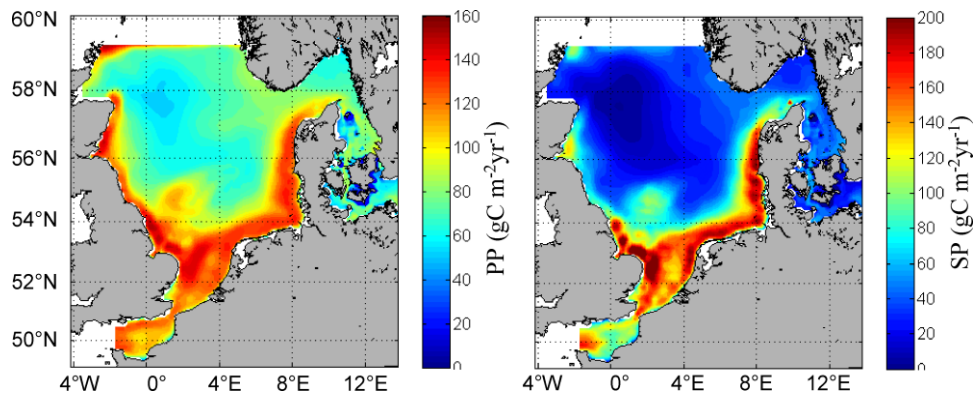


Figure 16: 60 year climatic mean annual net primary production ($\text{gC m}^{-2} \text{yr}^{-1}$) (left) and secondary production ($\text{gC m}^{-2} \text{yr}^{-1}$) (right).

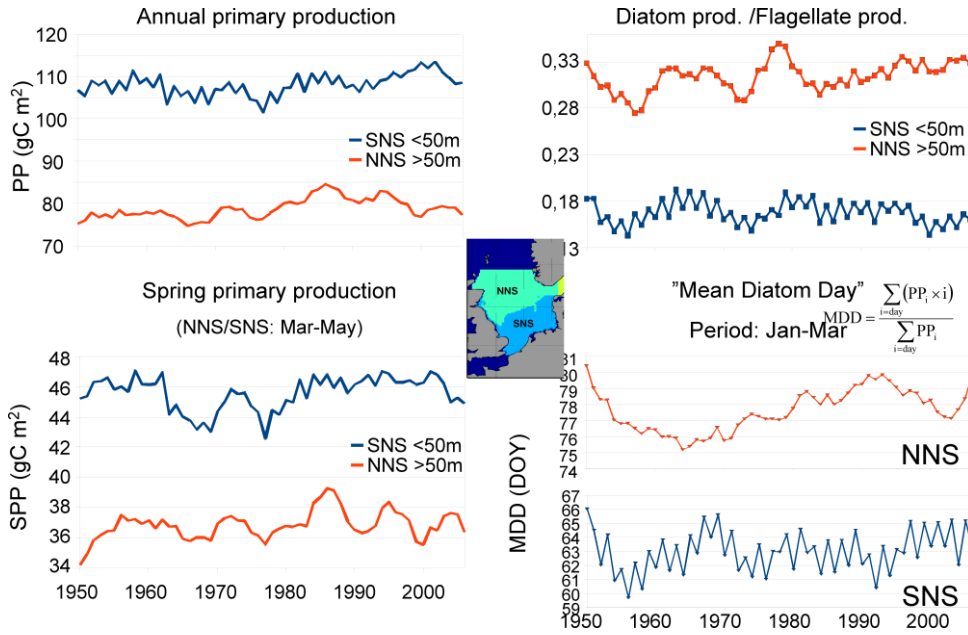


Figure 17: North Sea (Northern NS, Southern NS): Annual primary (upper, left), Spring primary production (lower, left), diatom/flagellate production (upper, right), mean diatom day (lower, right).

Higher Trophic Level: ECOSMO in the North Sea

The results from the long-term hindcast (Figure 18) indicate a decrease in PLS over the 1960-2008 period. Nonetheless, the results indicate the decrease not to be continuously but to exhibit a sudden decrease in PLS at the end of the 80's, except of two extraordinary high survival years in 1993 and 1996. The timing of the shift in PLS coincides with the time period that has earlier been identified as regime shifts in the North Sea, and also in the Baltic Sea (Alheit et al. 2005).

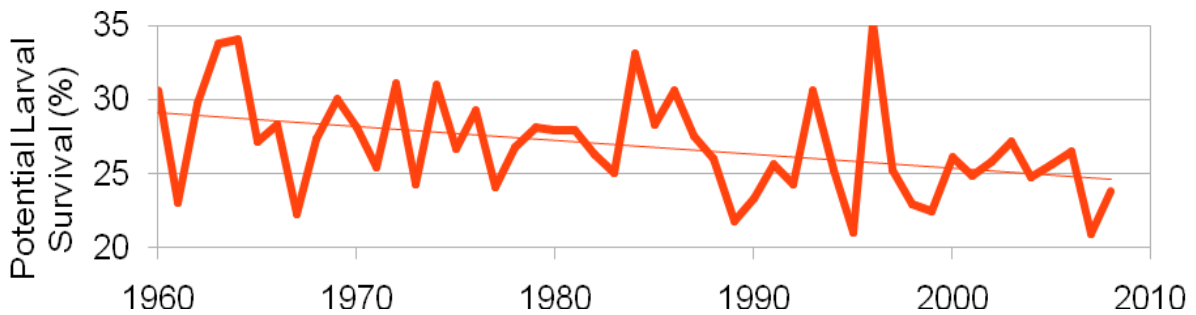


Figure 18: Annual, spatially averaged PLS (1960-2008) simulated with ECOSMO-IBM.

The comparison to the larval survival index (LSI) published by Beaugrand et al. (2003) reveals that, although the magnitude of the variability is not equally strong (with higher magnitude in the simulations), the timing of the simulated PLS and the LSI correlated positively except of a time period in the 80'ies (Figure 19). Clearly this cannot serve as validation. Not only our model includes uncertainties by the choice of considered processes, parameterisation and model setup, but also the LSI is not compiled from direct observation since it was back-calculated from recruitment data. Hence, it includes uncertainties from both the measurements as well as the model used for back calculation. However, assuming that the uncertainties are the same throughout the whole period, we can infer information from the changes in the correlation. Here, possible reasons for those changes might be the association with changes in the ecosystem dynamics (top-down vs. bottom-up controls) or with changes in the zooplankton size spectrum.

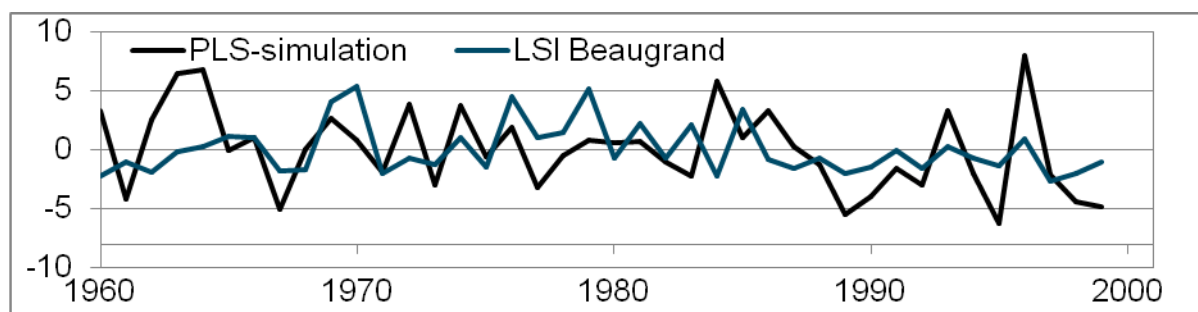


Figure 19. Variability in annual PLS (1960-2000) as simulated by the model (black) and redrawn from Beaugrand et al. (2003) (blue).

To identify processes important for PLS of Atlantic cod in the North Sea, we performed a correlation analysis between a number of potentially important environmental parameters and PLS for different seasons of the year (Figure 20). The results clearly show that water temperature plays an important role, mainly because it determines: 1) the timing of first feeding via developmental rates of non-feeding life stages, and 2) the food requirements via metabolic rates. Additionally U-current velocities and secondary production are found to be important to explain pattern in PLS. In contrast, the V-component of current velocity is of no relevance.

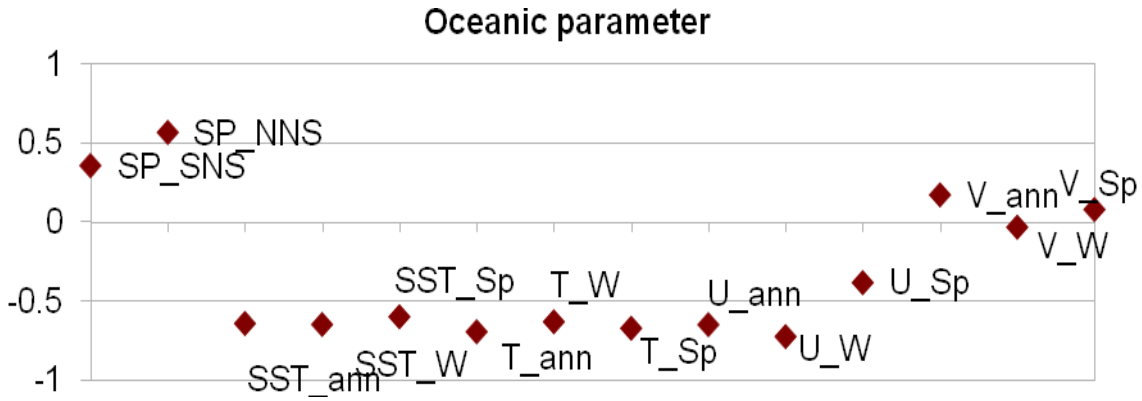


Figure 20. Linear correlation coefficients between PLS and a number of potentially important variables. (SST: sea surface temperature, T: aver. water temperature, U,V: u&v-component of current velocity, SP: secondary production). Variables where averaged over different time periods (ann: annual; Sp: spring, W: winter). SP was separated into northern (NNS) and southern NS (SNS).

6.2. Climate forced simulations

POLCOMS-ERSEM model in the NE Atlantic (climate and LTL)

The climate change signal between A1B and CNTRL is well characterised by the changes in temperature, salinity (Figure 21) and potential energy anomaly (Figure 22). The potential energy anomaly gives a measure of stratification appropriate for both shelf seas and open-ocean, and is defined as the energy required to mix the top 400m of the water column (see Holt et al. (2010) for further details). The sea surface temperature (SST) change (comparing CNTRL and A1B) shows a strong seasonal signal being larger in the summer and autumn than winter and spring. Spatially the changes are largest in the North Sea (~4°C in the central North Sea in summer) and smallest west of Biscay (~-0.5°C in winter). The sea surface salinity (SSS) change shows little seasonality, with freshening on the shelf and the open ocean south and west of Ireland and increased salinity in the open ocean north and west of Scotland. The temperature and salinity changes are accompanied by an increase in both seasonal and permanent stratification (Figure 22). There is a substantial increase in stratification in open-ocean regions of the model throughout the year. During the summer the greatest increase in oceanic stratification is towards the south of the domain. The shelf remains generally well mixed during winter, but there is a significant increase in stratification during the summer particularly in the Irish Sea, North Sea and English Channel. While there is a significant fractional change in the ‘well-mixed’ regions, values here remain low.

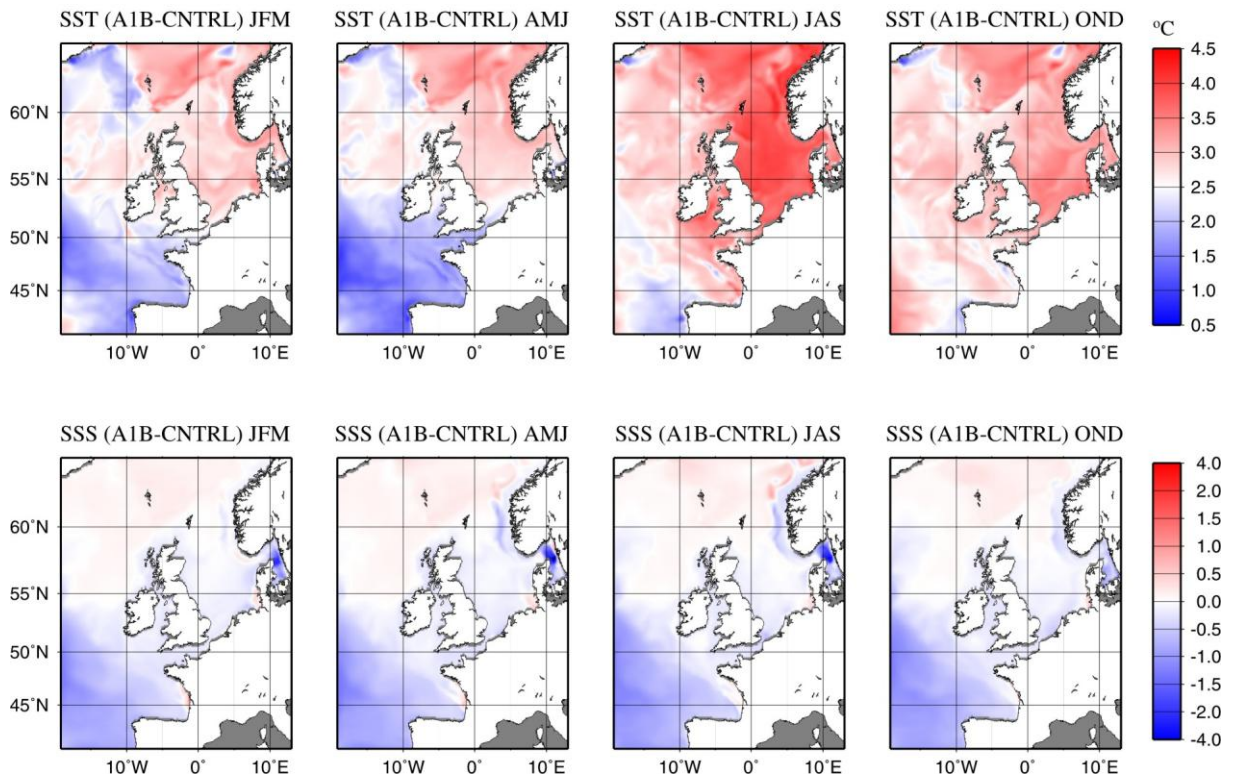


Figure 21: Change (A1B – CNTRL) in seasonal sea surface temperature and salinity.

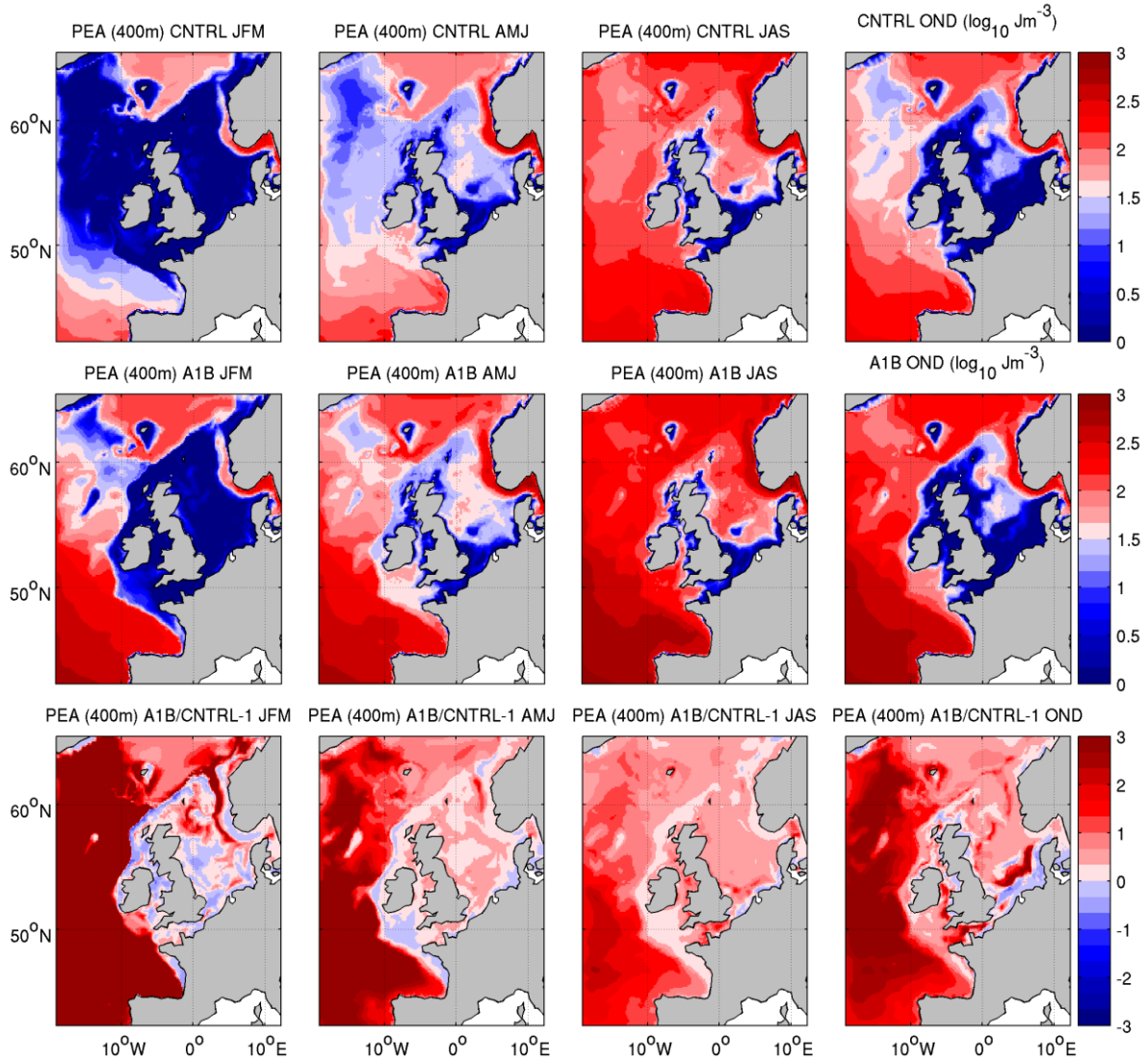


Figure 22: Seasonal mean potential energy anomaly with integration limited to 400m for CNTRL and A1B (note \log_{10} scale), and the fractional difference between them. For clarity this is limited to changes of a factor of 3, maximum change in oceanic regions is a factor of 5.7

In addition to the general increase in the strength of seasonal stratification, the stratification generally occurs earlier in A1B than for CNTRL (Figure 23), where the onset of stratification is here defined as being when the rate of reduction of surface nitrogen is a maximum (since stratification prevents the resupply from below). In A1B, stratification starts later in the Irish and Celtic Seas and shelf regions of the Bay of Biscay. Phytoplankton growth (defined as when the rate of net primary production exceeds $0.1 \text{ gCm}^{-2}\text{d}^{-1}$) tends to start earlier and end later under the A1B scenario. The change in the end of the phytoplankton bloom, defined as being when nitrogen falls below 20% of the winter value, is strongly related to the change in the start of stratification – where stratification is delayed in A1B compared to CNTRL, the bloom continues longer whilst, in regions where stratification starts earlier, the bloom also finishes earlier.

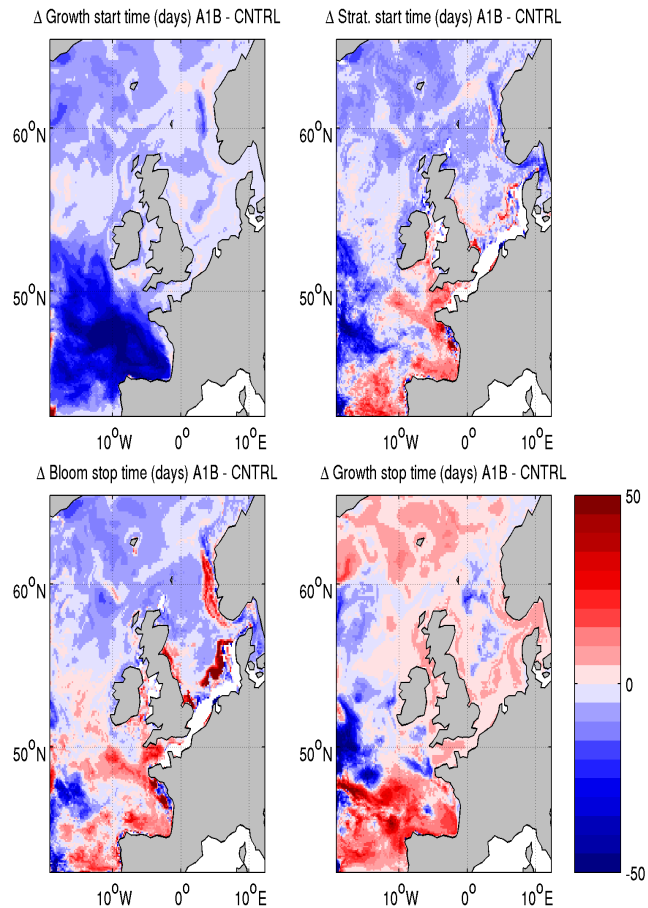


Figure 23: Changes in key times in the seasonal cycle (A1B – CNTRL): the start of phytoplankton growth; the start of stratification; the end of the phytoplankton bloom and the end of phytoplankton growth.

Compared to the CNTRL simulation, the net primary production in the future (Figure 24) increases in the Celtic and Irish Seas, the English Channel, the southern part of the North Sea, west of the Bay of Biscay, in the Faroe-Shetland Channel and in the Faroe Bank channel, west of the Faroe Islands. Elsewhere in the northeast Atlantic, net primary production reduces in the future. Changes in area mean net PP in the northern North Sea, the Shetland shelf, the Irish Sea and the deep ocean regions are significant at 95% compared to inter-annual variability (Table 2).

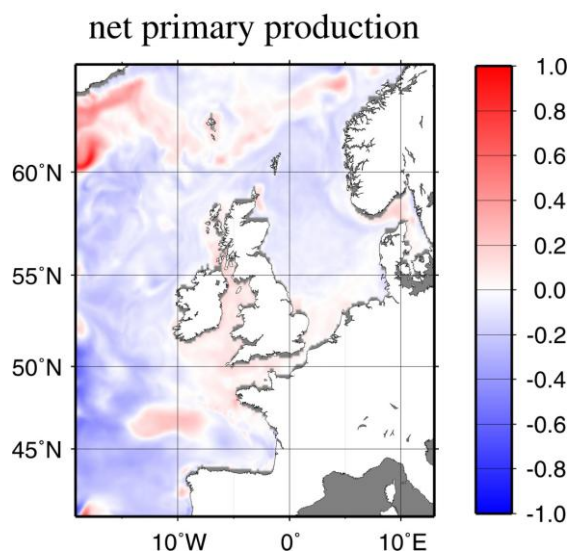


Figure 24: Fractional change ($A1B/CNTRL - 1$) in depth integrated net primary production.

Although changes in phytoplankton biomass are patchy (Figure 25), it generally decreases in the future; however, south of Iceland both large and small phytoplankton increase and there is a broad patch of increasing large phytoplankton biomass from the northwest tip of France to southern Ireland and westwards. The biomass of small zooplankton also decreases in the future scenario compared to the present day, while large zooplankton biomass mostly increases, with the largest increases being around the Faroe Islands and in the Bay of Biscay. These changes in plankton community structure most likely relate to differential response to temperature and stratification timing. A detailed analysis of the spring bloom (not shown) demonstrates that the length of the 'pre-stratification' bloom tends to increase under future conditions suggesting a more efficient use of winter nutrients (notably silicate).

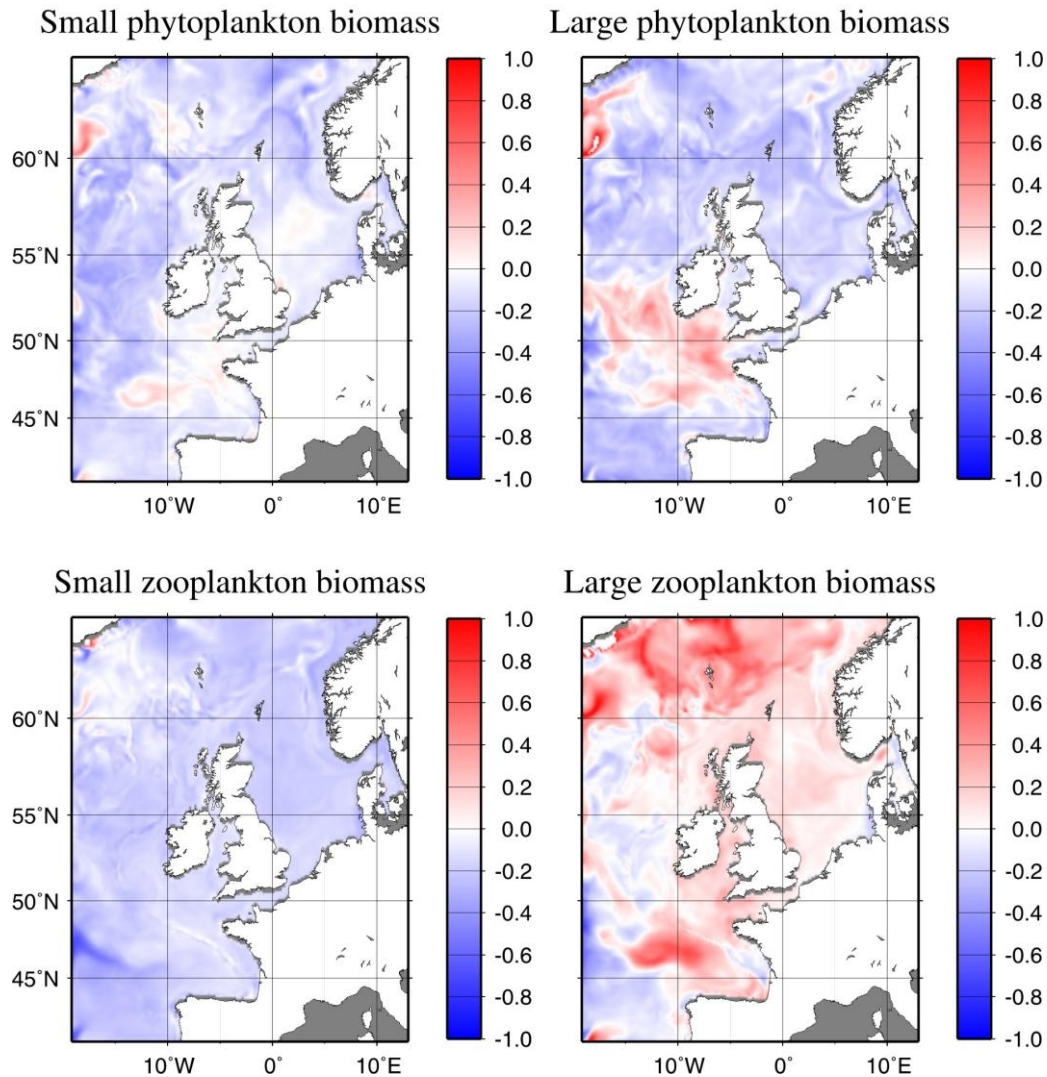


Figure 25: Fractional changes ($A1B/CNTRL - 1$) in the depth-integrated biomass of two size classes of phytoplankton and zooplankton.

There is a general reduction in surface nitrogen and phosphate in A1B compared to CNTRL (Figure 26), due to increases in stratification and a reduction in the surface nitrate and phosphate transported into the region through the boundaries. Surface silicate increases in the future scenario.

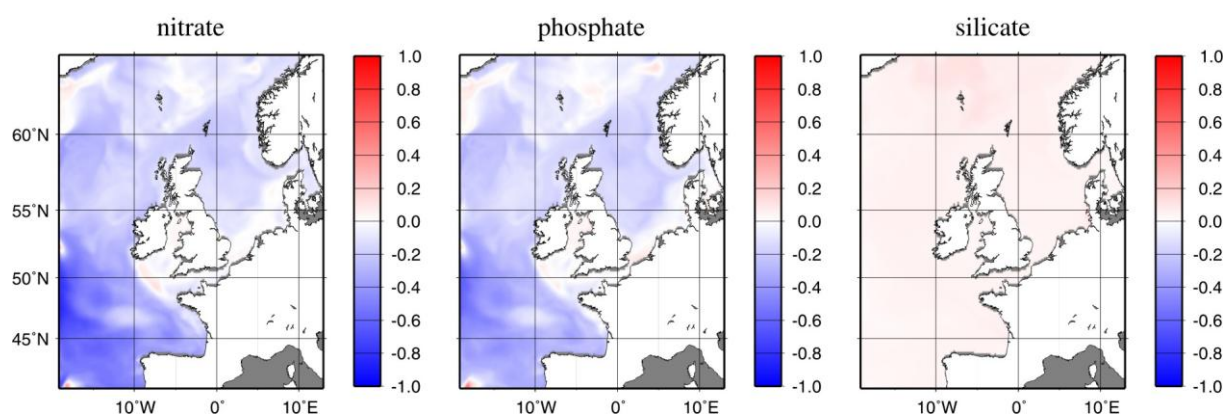


Figure 26: Fractional changes ($A1B/CNTRL - 1$) in surface nutrients levels.

Annual cycles of depth-integrated phytoplankton and zooplankton biomass, net primary production, surface pH and sea surface salinity and temperature in the CNTRL and A1B simulations are shown in Figure 27 – Figure 30. Values have been integrated over the whole model domain (Figure 1) and also over areas corresponding to Marine Strategy Framework Directive sub-regions for the northeast Atlantic; namely: the Greater North Sea, the Celtic Seas and the Bay of Biscay and Iberian Coast. With the exception of the biomass of large phytoplankton and large zooplankton in the Celtic Seas, the amplitudes of all phyto- and zooplankton biomass decrease in the future A1B simulation compared to the CNTRL. There is no discernible change in the timings of the peaks of small phyto- and zooplankton biomass, although in the Bay of Biscay, the small plankton biomass amounts are larger from January to March in the future. In all regions, peaks of both large phyto- and zoo-plankton biomass occur earlier in the year in the future simulation. The peak of net primary production reduces in the future in all regions, although the change is small in the Celtic Seas, and there is a shift towards more production earlier in the year (January to March) and reduced values from April to July. Future pH is smaller by about 0.27 with the largest changes occurring in the autumn and smallest in the spring. Future SST increases are also largest in the autumn and smallest in spring. Changes in SSS are also seasonal with the largest changes ~ 0.42 occurring in the winter in the Bay of Biscay and the smallest ~ 0.09 occurring in autumn in the Greater North Sea.

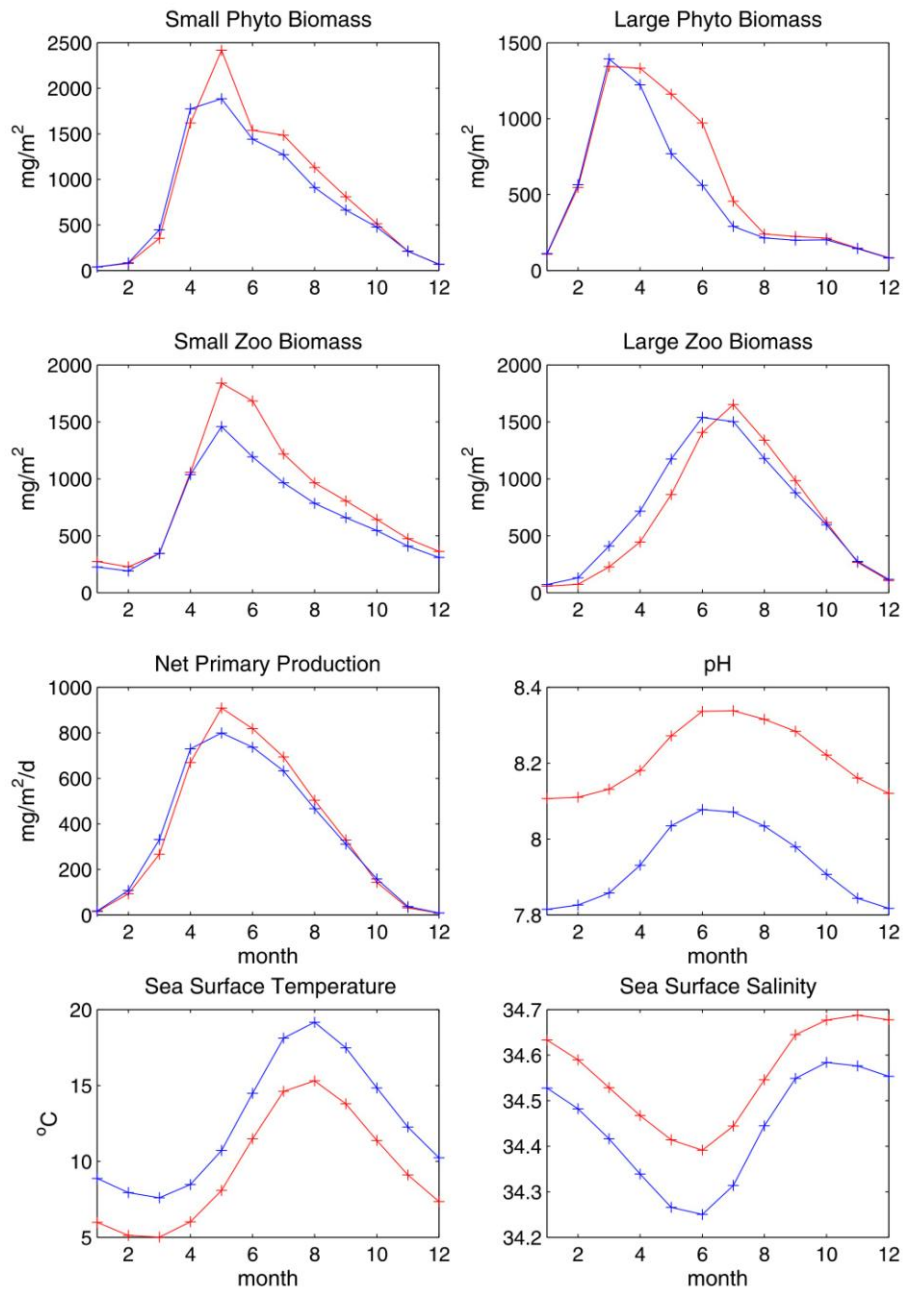


Figure 27: Annual cycles for CNTRL (red) and A1B (blue) integrated over the Greater North Sea (regions 1, 2, 3, 4, 6 and 7 in Figure 1).

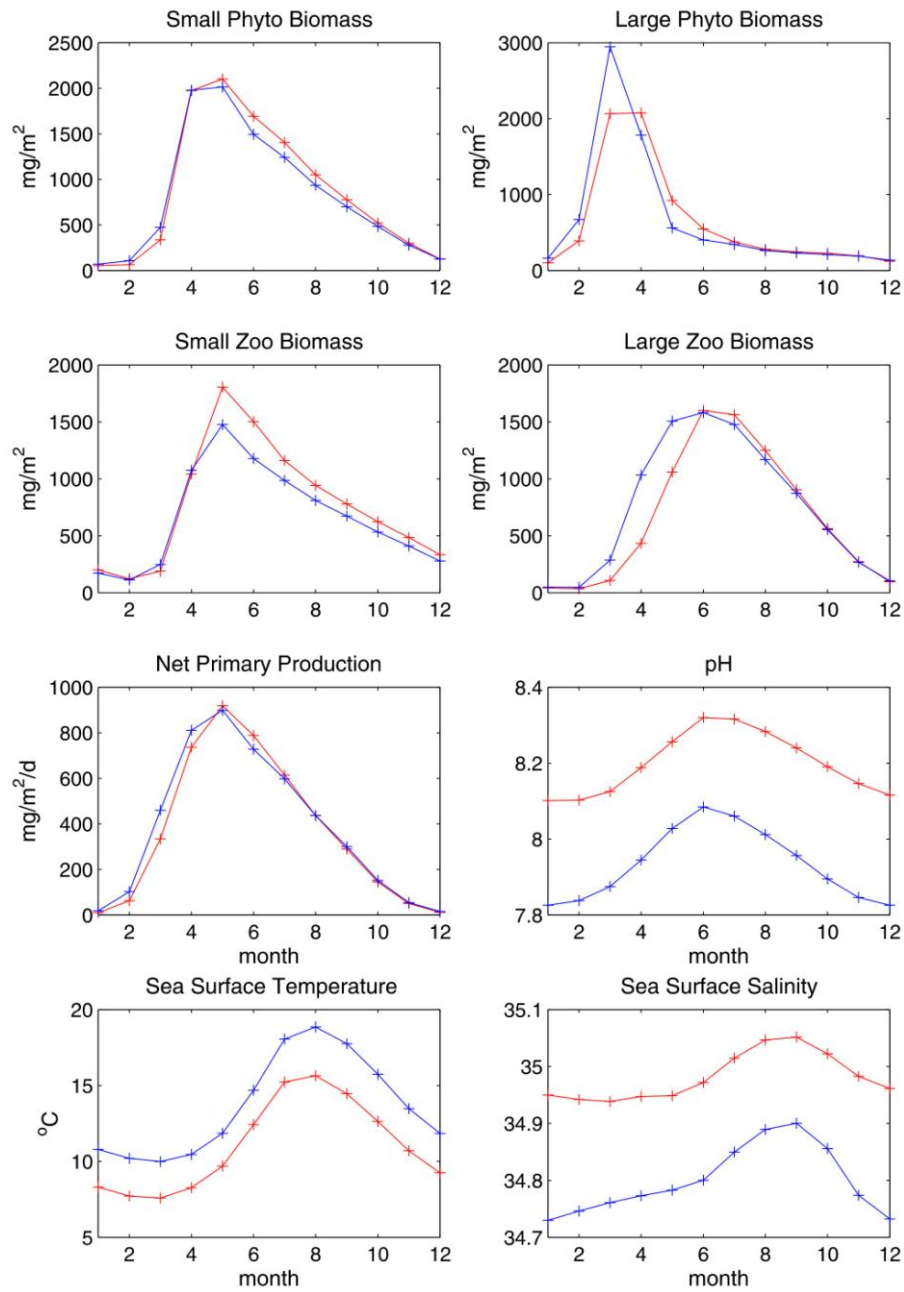


Figure 28: Annual cycles for CNTRL (red) and A1B (blue) integrated over the Celtic Seas (regions 8, 9 and 10 in Figure 1).

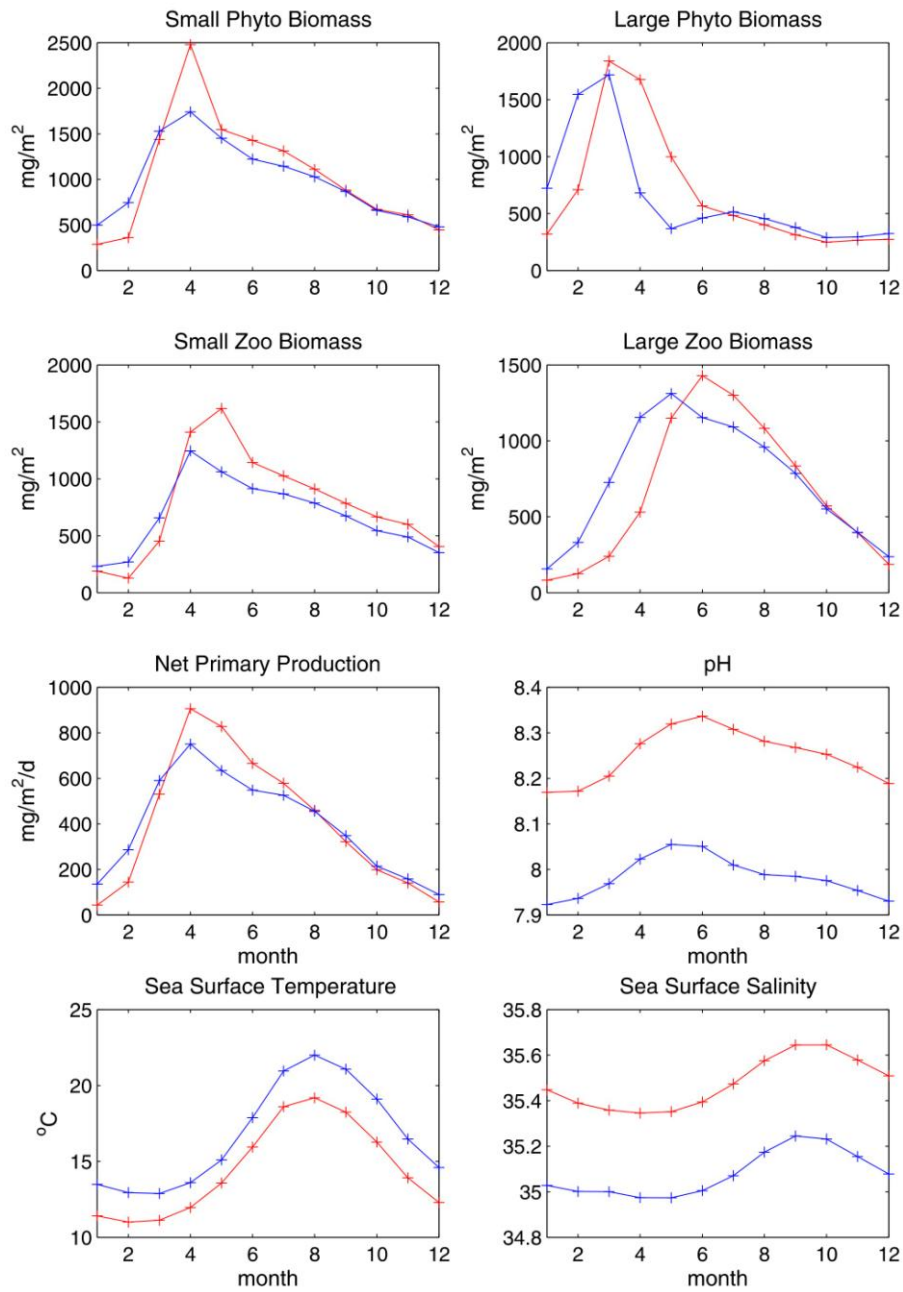


Figure 29: Annual cycles for CNTRL (red) and A1B (blue) integrated over the Bay of Biscay and Iberian Coast (region 11 in Figure 1, and westwards to 10°W).

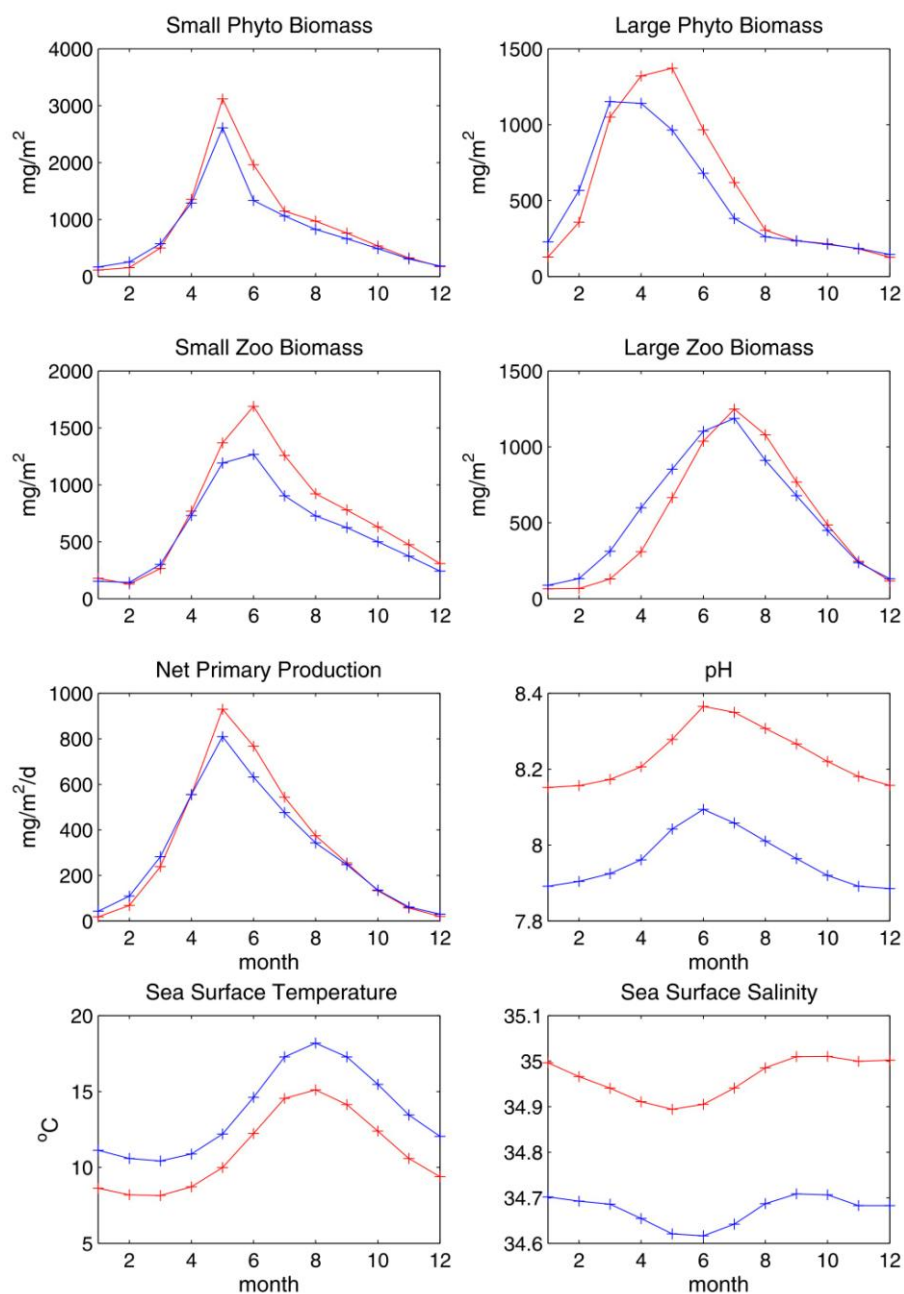


Figure 30: Annual cycles for CNTRL (red) and A1B (blue) integrated over the northeast Atlantic (Figure 1).

Impact of Ocean Acidification and climate change on the ecosystem

Here we present the differences between the outputs of the run A1B and those coming from the run CNTRL to examine how the ecosystem may change as result of both, climate change impact (e.g. increase in temperature or change in stratification) and ocean acidification (i.e. increase in atmospheric CO₂): the two processes are indeed tightly interlinked, they occur simultaneously and they cannot be disentangled.

Over the whole model domain we project a mean decrease of surface pH of about 0.27 units, but with significant spatial and temporal variability (figure 32a). Winter shows a clear

difference between the shelf and the oceanic waters, with the first one being more “acidified” by about 0.1 units. In spring the drop in pH reaches its minimum almost in the entire domain, and the spatial gradient is lower. OA impact reach its maximum in summer and autumn, with peak of more than -0.4 pH. The shelf-ocean gradient is evident also looking at future surface aragonite saturation state (figure 43b): here the difference between the two basins is even more critical as the shelf sea surface waters are close to undersaturation during winter and autumn, with localised undersaturation in the German Bight. At the same time coastal waters in the southern North Sea are fully saturated during spring and summer. Vertical gradient on the shelf is also very important. During warm seasons, indeed, the water column in central North Sea stratifies creating two contrasting environments: while the surface is oversaturated, bottom waters reach significant undersaturation on a large area (up to 0.7, figure 33). Also pH has a similar vertical gradient, with surface pH up to 0.3 units higher than in the bottom waters.

As a reference for the results that follow Figure 34 shows the spatial maps of the projected differences in primary production, NH₄:DIN ratio and zooplankton biomass. Table 1 summarizes how these changes differ among the PFTs: diatoms and flagellates are barely impacted by climate change on an annual basis, but their phenology change with an earlier bloom in March due to the temperature increase. On the contrary picophytoplankton and dinoflagellates are the groups responsible for the drop in net PP during spring and summer. Zooplankton community composition also changes, with a shift towards the meso-zooplankton (table 1).

The difference in NH₄:DIN (figure 34c) shows also a distinct seasonal cycle loosely following the changes in net PP: in winter the model projects a change only in the southernmost area with a small increase in ammonium only in the southernmost area of the domain (passing from few percent to 10-15% of DIN), and the opposite in spring when all the rest of the basin will experience an increase. In summer the model projects a decrease in the ratio in the entire domain (with an average drop of 8% in absolute term, e.g. from 30% of ammonium to 22% of ammonium) while in autumn the differences are lower in absolute value and the positive and negative sign are equally present with the former more focused on the southern part of the domain.

The consequences of the assumed enhancement of PP due to PP are analysed by comparing the output from the ENH with the A1B scenario in order to separate impact of the biological feedback from the climate change one.

The major consequences of this assumption is a general increase in net PP in most of the domain, particularly in spring, with an average increase around 100 mgC/m²/d, and in summer limited to the coastal area of the shelf, with peak of more than 200 mgC/m²/d usually close to river mouths (figure 35a). In contrast, most of the open ocean would experience a reduction of net PP of about 50mgC/m²/d during summer. Again, not all phytoplankton groups respond in the same way, with Picophytoplankton having a remarkably higher increase in spring compared to the other PFT (table 3). Zooplankton biomass tightly coupled to PP changes (figure 35b).

Changes in pH (figure 35c) mimic the pattern of changes in PP, but with much lower intensity. During spring a small increase of 0.016 pH unit on average is simulated compared to the A1B scenario in most of the domain, with peak on the coastal area close to the river mouths up to 0.1 units. In summer the coastal areas are still projected to have a higher pH than in the A1B scenario, while the rest of the domain is experiencing a low decrease. Changes in saturation state follow the same pattern but they are statistically not separable from the one due to only climate. Finally, the feedback of the enhanced PP on the nitrogen speciation is low (few percent of maximum difference) with no clear pattern except a general decrease of ammonium in summer.

The second feedback studied is the change in the nitrification rate. As expected, turning off the dependence of this process to pH will impact the NH₄:DIN ratio: this tends to decrease in winter and autumn particularly on shelf where the low pH slow down the nitrification in the A1B scenario. The magnitude of the change is at most equal than those caused by the enhanced PP, and lower than those due to climate change. This variation on nitrogen speciation does not have significant impact on the rest of the ecosystem, with very small changes (if any) in net PP, zooplankton biomass, pH and aragonite saturation state.

Table 3: seasonal mean on all the domain of the difference between the A1B scenario and the PD (A1B-PD) and the enhanced production and the A1B scenarios for primary production split into PFT and for the zooplankton biomass. Both data are depth integrated.

	Diatoms	Flagellates	Picophyto pl.	Dinoflagell ates	Mesozoopl .	Microzoopl .	Heterotr. nanoflagell ates	
	mgC/m ² /d	mgC/m ² /d	mgC/m ² /d	mgC/m ² /d	mgC/m ²	mgC/m ²	mgC/m ²	
winter	10.68	4.03	9.49	0.83	69.45	5.81	-7.71	
spring	-11.6	-1.5	-33.97	-21.4	150.97	-107	-29.36	
A1B- PD	summer	0.83	-4.73	-18.47	-19.68	-53.16	-244.2	-43.49
autumn	2.78	0.85	1.46	-0.07	-8.45	-68.97	-35.25	
annual mean	0.6725	-0.3375	-10.3725	-10.08	39.7025	-103.59	-28.9525	
winter	5.77	3.95	13.01	1.12	28.06	24.48	11.33	
spring	6.75	7.42	31.16	10.29	58.04	78.8	16.51	
ENH	summer	2.62	-0.39	6.8	2.41	5.25	4.24	-1.92
autumn	1.48	1.69	6.36	1.93	25.34	13.41	4.61	
annual mean	4.155	3.1675	14.3325	3.9375	29.1725	30.2325	7.6325	

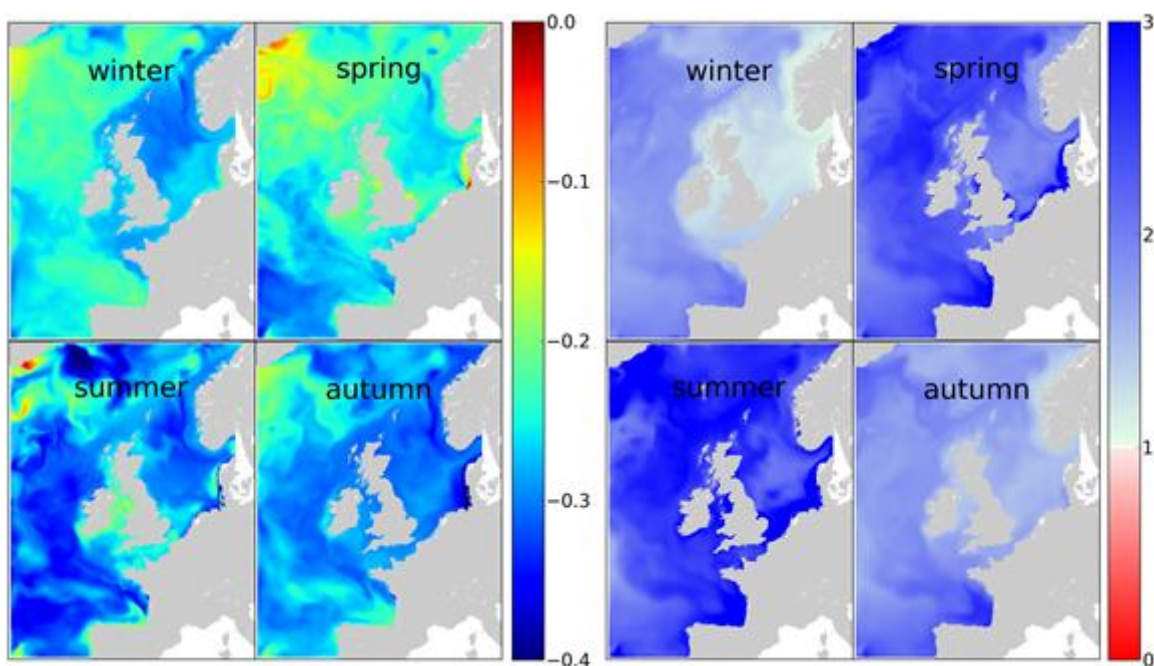


Figure 32: Impacts of climate change and OA in the carbonate system as projected by the A1B scenario: on the left (a) absolute difference in surface pH compared to the present day scenario, on the right (b) future surface saturation state of aragonite

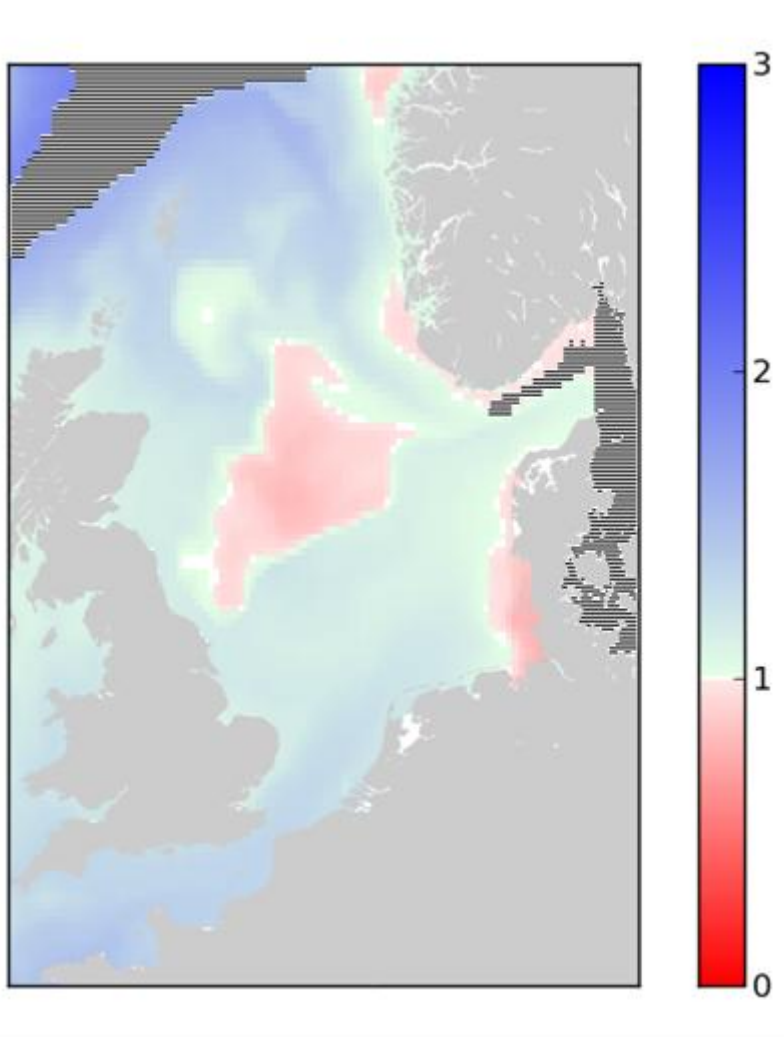


Figure 33: Saturation state of aragonite in the bottom waters in the A1B scenario. Red areas highlight undersaturation, Data deeper than 400m have been shaded due to high uncertainty.

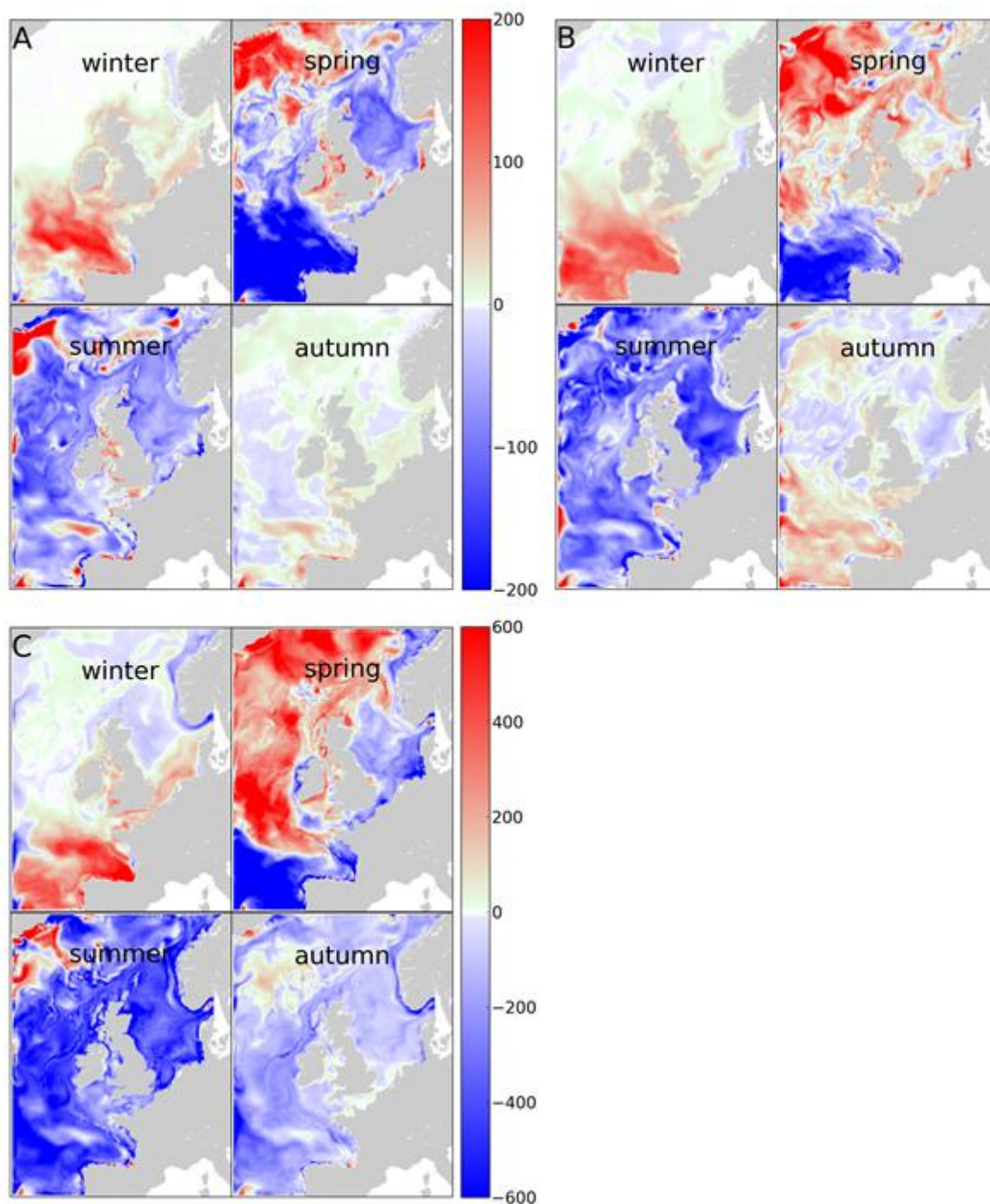


Figure 34: Impacts of climate change and OA in the eco system as projected by the A1B scenario. A: difference in net primary production (depth integrated, mgC/m²/d), (b) absolute difference in the NH₄:DIN ratio in the surface waters (%), (C) difference in zooplankton biomass (depth integrated, mgC/m²).

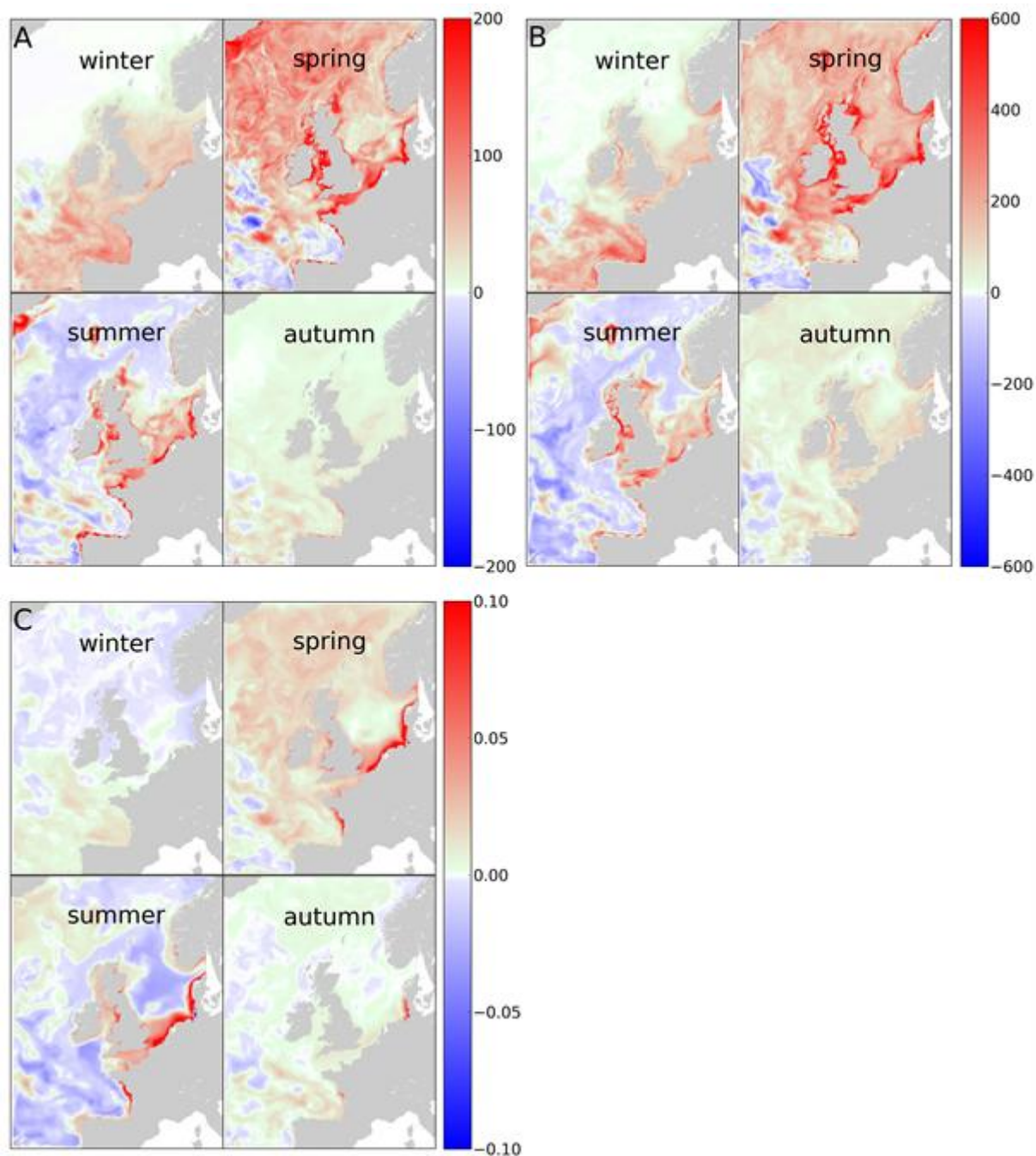


Figure 35: Impacts of the enhanced primary production due to OA (differences between ENH scenario and A1B). A: absolute difference in net primary production (depth integrated, $\text{mgC/m}^2/\text{d}$), B difference in zooplankton biomass (depth integrated, mgC/m^2), C: difference in pH in the surface waters.

This work highlights how the impacts of OA in the shelf ecosystem vary in space and time and how they are interconnected with those of climate change. Despite the average decrease of pH being in line with the mean estimates provided by many global ocean models, this difference is not homogeneous in time and space. While changes in atmospheric CO_2 drive OA, it is not the only factor regulating the carbonate system in the shelf seas. Biological

processes are particularly important to in controlling the seasonality of the impact: in the areas where an increase in net PP is projected the minimum of acidification is observed (e.g. in spring in the Northern Atlantic or in the southern North Sea in summer). Similarly the undersaturation of aragonite projected in bottom waters in the central North Sea is caused by the accumulation of DIC during spring and summer due to community respiration (both pelagic and benthic) and the concurring stratification that prevents ventilation. The increase in temperature plays two contrasting roles. From one side it decreases the solubility of CO₂ in water, promoting the outgassing and therefore preventing further acidification. This is contrasted by a bigger increase in atmospheric pCO₂.

At the same time it increases the values of the dissociation constants of the carbonic acid leading to an increase in the more dissociated form and consequent decrease in pH. This effect is partially responsible of the self-ocean gradient in OA signal: the shelf warms up more than the ocean (Holt et al., 2012) with difference in temperature varying between 1°C and 4°C depending on season and relative difference in pH up to 0.05 units.

Although the uncertainty on the impact of OA on PP is still high, and the parameterization we used in this work is simple, some key messages can be drawn from this study.

The change in net PP due to the OA alone is of the same order of magnitude of the one due to climate change: sometimes they have opposite sign and tend to cancel out (e.g. in the Central North Sea in spring or in the Southern North Sea in summer), sometimes they have the same sign and OA magnifies the climate change impact. This is in agreement with work from (Tagliabue et al., 2011) who tested similar hypotheses at global scale. This impact is transferred up into trophic network at zooplankton level and potentially to higher trophic level.

Enhanced PP does not impact significantly on NH₄:DIN ratio; that is instead mostly affected by the climate change and the related changes in net PP and temperature. In regions where PP increases the NH₄:DIN increases as well because while nitrate is only assimilated by phytoplankton, ammonium is also released via metabolic processes and hence the ratio will increase. In the summer, when temperature is high, the ammonium is oxidized to nitrate via nitrification, and due to the increased summer temperature and the increased amount of ammonium in the water column, nitrification occur faster reverting the sign of the change in the ratio. Also change in nitrification rate due to OA has a smaller impact on the nitrogen speciation than climate change.

ECOSMO model in the North Sea (climate and LTL)

Climate and physical variables. The average change in temperature as projected using the IPSL-ESM is given in Figure According to the ECOSMO, the projected change in annual SST indicates a substantial increase of about 2.8 °C for the period 2070-2099 when compared to the reference hindcast (1980-1999). However, the increase appears not to be equally important throughout the year (Figure 36). While smallest changes are projected for the spring period, the strongest increase appears to be during the summer month with a difference of over 3 °C. The seasonal differences in SST are likely to be ascribed to changes in the stratification where a stronger seasonal thermocline would increase the effect of

climate warming. This is likewise mirrored in the spatial pattern of SST increase with highest increases in the central and northern part of the North Sea. In general, the magnitude of projected SST warming using ECOSMO in the North Sea is comparable to previous climate projections with different downscaling methods such as published by Ådlandsvik (2008) and Holt *et al.* (2012).

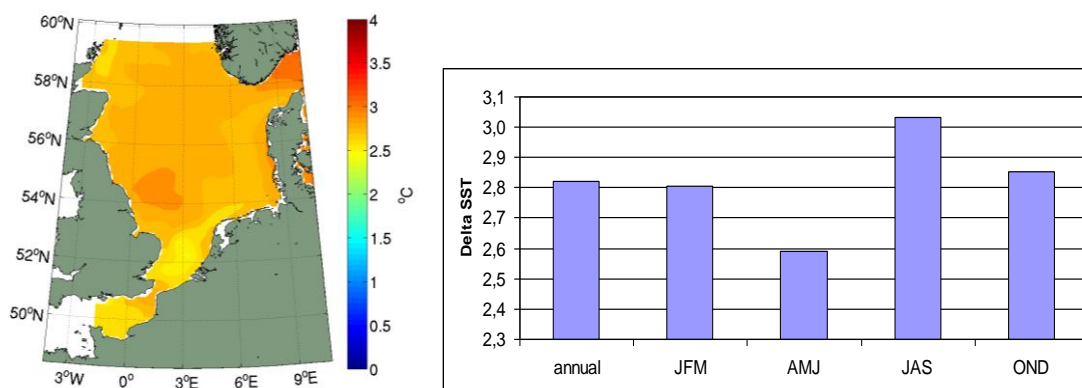


Figure 36 North Sea annual SST change with respect to future (2080-2099) and past (1980-1999) Simulations left: Spatial variability; Right: seasonal differences.

By comparing model results from four simulations forced with different GCMs, we assessed the uncertainty associated with this type of experiments. These simulations did not consider changes in the biogeochemical ocean boundary conditions, since some of the investigated models are not ESM but GCMs only. However, it helps quantifying the uncertainty range in the atmospheric parameters and their impact on regional ocean dynamics and ecosystem productivity.

Although, all 4 future projections (Figure) indicate an increase in North Sea SST, both magnitude and spatial pattern of the warming differs substantially among the simulations. Compared to the IPSL simulation, the SST increase projected in the other simulations is less dramatic with increases around 1-2 °C. Furthermore, in contrast to the IPSL based projection, the results obtained with BCM and ECHAM show the strongest SST increase in the shallow areas of the southern North Sea, while there is only little spatial variability seen in the projections utilizing the NorESM forcing. The differences in the SST can mainly be assigned to differences in the air temperature and short wave radiation, where not only magnitude but also the seasonal cycle can play an important role. Moreover, differences in the wind field need to be considered as a potential reason, these are particularly responsible for spatial variations.

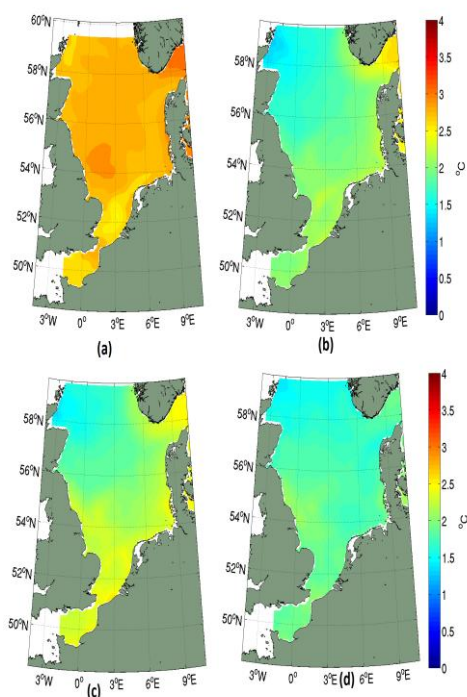


Figure 3731: North Sea annual SST change (a) IPSL, (b) BCM, (c) ECHAM, (d) NorESM calculated as difference between future (2080-2099) and past (1980-1999) simulations.

As for SST, changes in SSS (Figure 38) exhibited large uncertainties related to the choice of the GCM. BCM, ECHAM and NorESM show comparable spatial pattern in projected SSS change, with increasing salinity along the coastlines and decreasing salinities beyond the fronts in the south-eastern part of the North Sea, although different in magnitude. The IPSL forced simulations show contrastingly an overall increase in SSS. Here, the results for both metrics (SST and SSS) underpin not only the general uncertainties accompanied with the use of GCMs, but also indicate that the dynamics in IPSL atmospheric parameter differs substantially from that of the 3 other selected models.

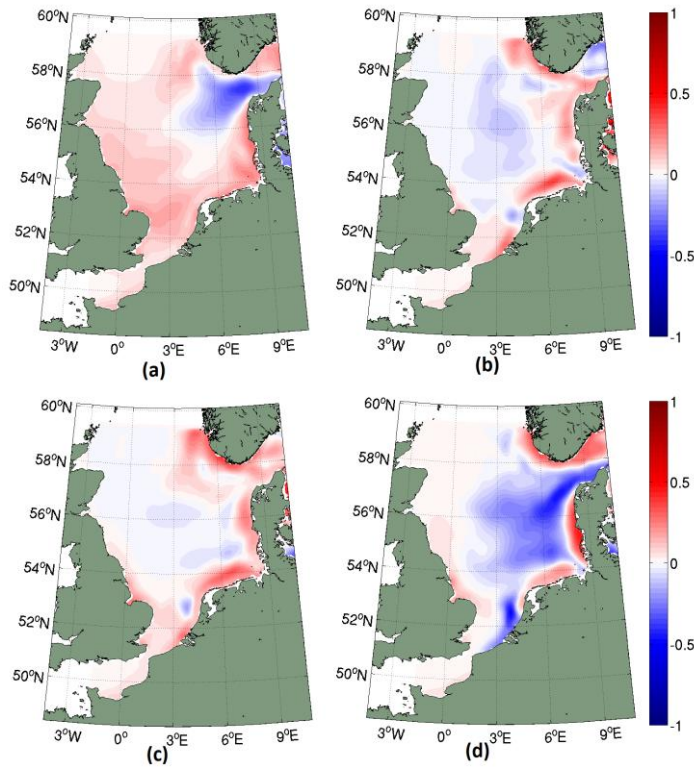


Figure 38. North Sea annual sea surface salinity change (a) IPSL, (b) BCM, (c) ECHAM, (d) NorESM calculated as difference between future (2070-2099) and past (1970-1999) simulations.

Projected LTL and nutrients. In terms of ecosystem productivity, the estimated difference between future and present day production seems to sharpen the prevailing spatial pattern in primary and secondary production (Figure 39.39). This is associated with a decrease in the central and northern North Sea and a slight increase in the high productive areas of the southern North Sea. Here, the change in secondary production appears even stronger than in primary production with a decrease of up to 0.5 in the central North Sea.

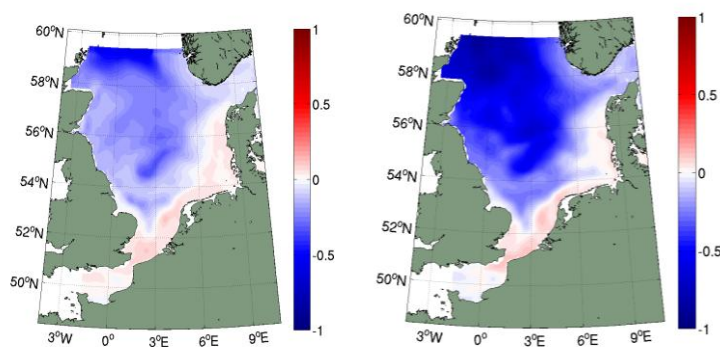


Figure 39. Fractional change of depth integrated annual primary (left) and secondary (right) production (left) between future projection (2080-2099) and reference hindcast (1980-1999).

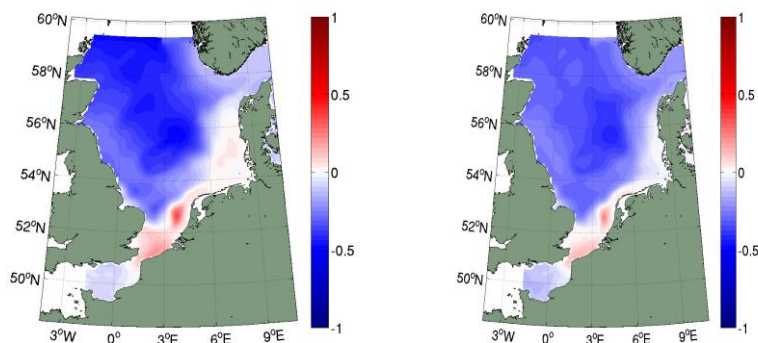


Figure 40. Fractional changes in surface (upper 40m) NO_3 (left) and PO_4 between future projection (2080-2099) and reference hindcast (1980-1999).

Since, primary production in ECSOMO depends mainly on nutrient availability and light, the projected changes in primary production can clearly be assigned to changes in either one of these factors. In figure 40 changes in surface available nutrient (nitrate and phosphate) are given. Here, the pattern reflects the changes in primary production indicating nutrient limitation driving the respective changes. Changes in nutrient availability can be forced by changes in the nutrient supply from the North Atlantic or by changes in the seasonal stratification in the central and northern North Sea. An indication of possible underlying processes important for the projected change in nutrients and subsequently primary production can be obtained from a comparative study concerning impacts of only atmospheric forcing versus atmospheric and ocean forcing (Figure). Here, the results indicate that the changes in PP reveals from the changes oceanic boundary conditions and underpins the importance of the North Atlantic inflow for the North Sea ecosystem dynamics, at least in case of extreme nutrient level decrease, as projected by the IPSL-ESM. Although, we could not perform ensemble simulations with different ESMs in the frame of MEECE, and hence could not assess the uncertainty in projected response to oceanic boundary conditions, we compared projected changes in surface nitrate and phosphate from two ESMs (IPSL-ESM and NorESM) (Figure 42) to assess whether or not the projected extreme decrease in nutrient level is a robust feature. The results indicate that this is not the case. In both ESMs nutrient levels decrease, although the extreme local changes as projected by the IPSL-ESM are not simulated by the NorESM.

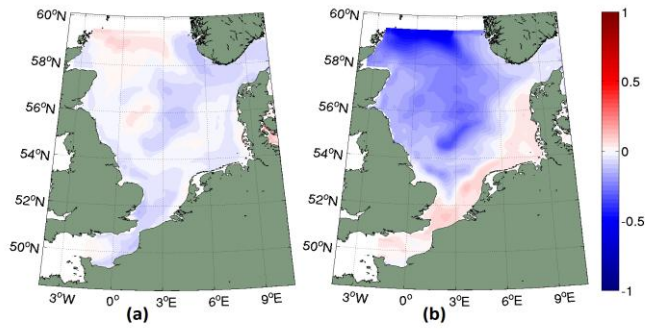


Figure 42. Fractional change of depth integrated primary production between future projection and reference hindcast for (a) ECOSMO forced by IPSL atmospheric forcing only and (b) ECOSMO forced by IPSL atmospheric and ocean forcing.

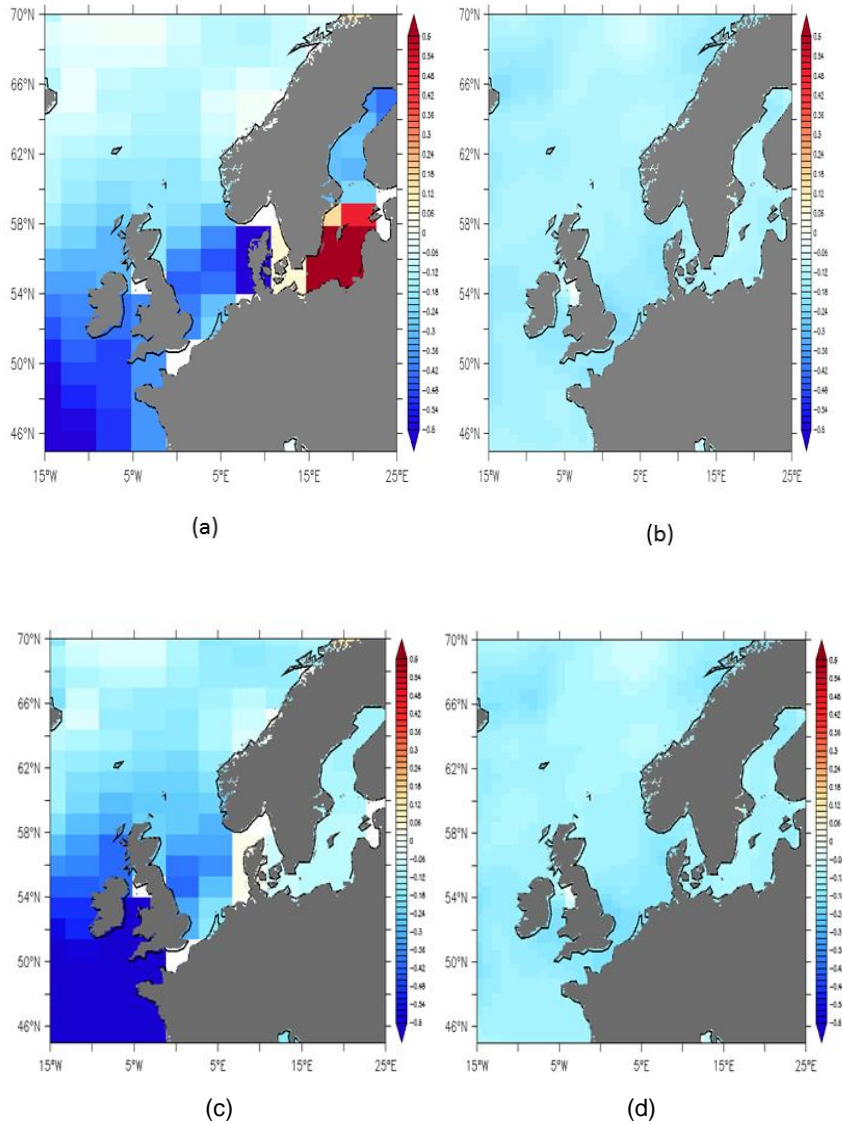


Figure 32 Fractional change of surface nutrients between future projection and reference hindcast for nitrate: (a) IPSL-ESM & (b) NorESM and phosphate: (c) IPSL-ESM & (d) NorESM.

The comparative simulations with different GCM atmospheric forcings were helpful to identify the impact of the atmospheric parameters on projected changes in primary production. The fractional change between future projection and hindcast simulation for all four forcing GCMs are given in Figure 43. As for the physical parameters the simulations reveal large differences ranging from a general decrease (IPSL) to local (NorESM) or overall (BCM, ECHAM) increases in production. In particular, the experiments reveal that, even if spatial pattern in primary production change is similar to IPSL (atmospheric and ocean) (see Figure b) and NorESM (only atmosphere) (Figure b), the underlying dynamics in the respective GCM can be substantially different. As in the example, in one case the oceanic and in the other case the atmospheric forcing drives the projected change.

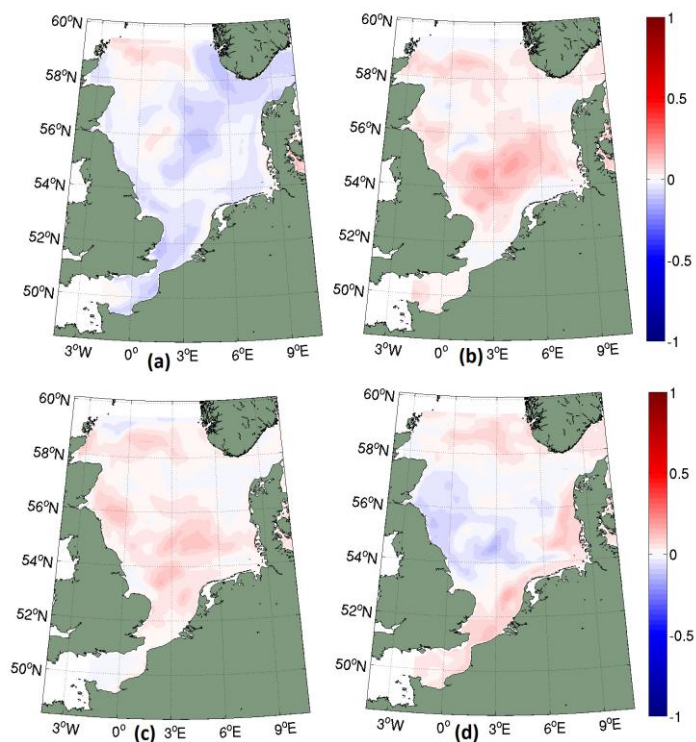


Figure 44. Fractional change in depth integrated primary production (a) IPSL, (b) BCM, (c) ECHAM, (d) NorESM with respect to future (2080-2099) and past (1980-1999) simulations.

Projected Carbonate chemistry changes and ocean acidification changes. Ongoing increase in atmospheric CO₂ is not only causing changes in climatic fields and hence, in physical parameters and ecosystem production but does also impact the air-ocean fluxes of CO₂ and thus oceanic pH. Projected changes in the oceanic pH in the North Sea as given in Figure and Figure indicate clearly an acidification of the North Sea with a decrease in mean pH from 8.09 during the hindcast to 7.87 for the projected future period. The results further indicate that the ongoing acidification trend (Figure) remains almost constant compared to the modelled reference hindcast trend.

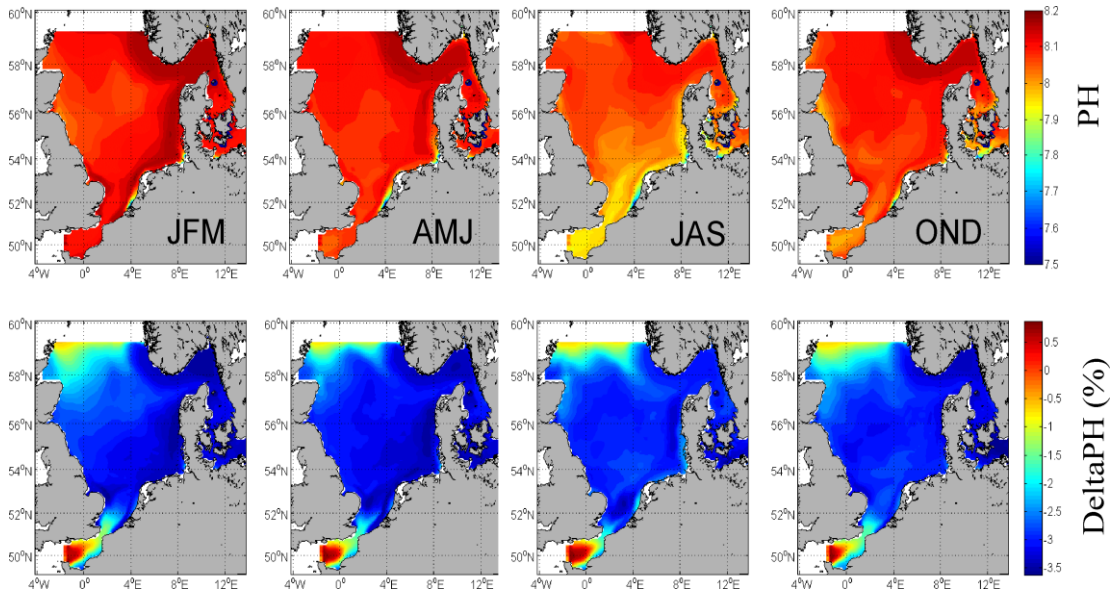


Figure 3345. Estimated seasonal mean PH (1980-1999) upper panels and percentage change (fractional change *100) for the climate projections (2080-2099).

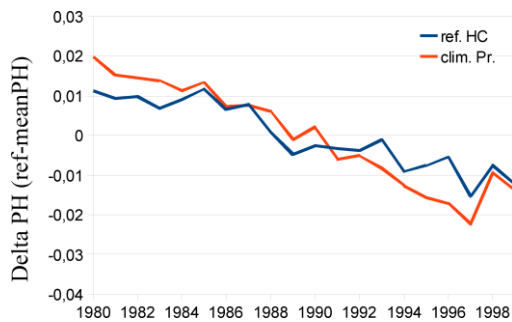


Figure 46. Temporal evolution of annual mean pH in the North Sea relative to the mean pH value (reference hindcast (ref. HC) simulation mean pH: 8.09; climate projection (clim. Pr.) mean pH: 7.87).

Alien Invasive Species: a biogeographic approach

Our projections suggest variable habitat expansion of HABs under the applied assumptions of climate change (Figure 47). In northern European, a considerable expansion in the number of months annually conducive to both types of bloom species is projected, but conditions conducive to expansion of *Prorocentrum* –type HAB species are projected to be greater than those of *Karenia*-type species. While conditions suitable for *Prorocentrum* are projected to lead to greater geographic extent of the blooms, also projected is largely similar numbers of months supportive of these blooms in the regions where they now occur. For conditions herein defined as supportive of increased toxicity (i.e., imbalanced N:P ratios), the overall trends by region and species are similar, but the geographic range is more narrowly defined.

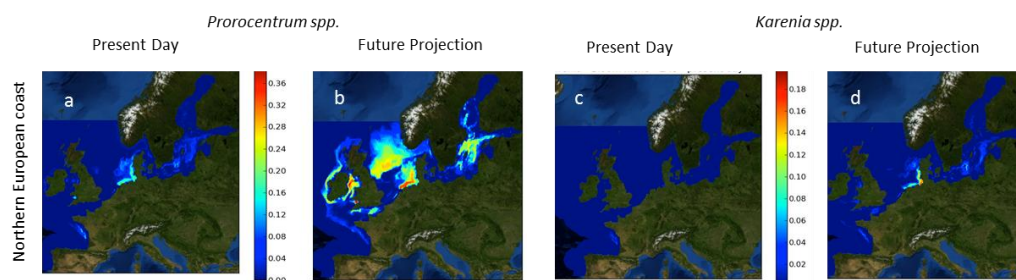


Figure 47. Comparison of output of a coupled-forced-biogeochemical model for northern Europe (panels a-d) depicting the fraction of months suitable for growth of either *Prorocentrum*-type HAB species (panels a,b,e,f) or *Karenia*-type HAB species (panels c,d,g,h), under present day conditions (panels a,e,c,g; encompasses period from 1981-1990) and under future conditions projected using AIB IPCC scenarios for climate change (panels b,f,d,h; encompasses period from 2091-2100).

These patterns were developed from simple, general “rules” and suggest that bloom expansion not only depends on the expansion of abiotic conditions supportive of their growth, but also on the temporal match of expansion of these parameters. In order for blooms to occur, all criteria for growth must be met at the same time and location. There must be a “match” of the physical and chemical conditions. Any scenario which alters one set of matching parameters in time or space without altering the other criteria likely leads to a “mismatch” of conditions and a failure for blooms to develop.

On an individual basis, the increase in temperature and the increase in nutrient conditions suggest an even greater potential for expansion of these blooms, but the overlap of these conditions limits the realization of these effects. For example, as illustrated for *Prorocentrum*-type physical and chemical niches in northern Europe (Fig. 48 left), in both the present day and future scenario, salinity is seemingly suitable year-round for growth, but the optimal conditions in terms of temperature (months 7-10 at present, months 6-12 in the future scenario) and nutrients (months 5-7) are slightly displaced in time. Despite the temporal overlap, in the current scenario there is a significant spatial mismatch that limits the frequency of favouring blooming conditions (Fig. 48 right). The expansion of the physical niche in the A1B scenario leads to a general increase in likelihood of blooming conditions.

The temporal mismatch in suitability of conditions for growth should not be viewed as evidence for no further expansion. Rather, such a difference points to the possibility of expansion should there be a change in the timing of any one of the parameters. Climate forcing may alter the timing of nutrient loads relative to seasonal warming which may in turn alter the alignment of suitable conditions. Such a difference may occur, for example due to extreme weather events that may provide an injection of favourable nutrients later in the year. There is mounting evidence that climate variability and increased frequency of extreme weather events increase due to climate change.

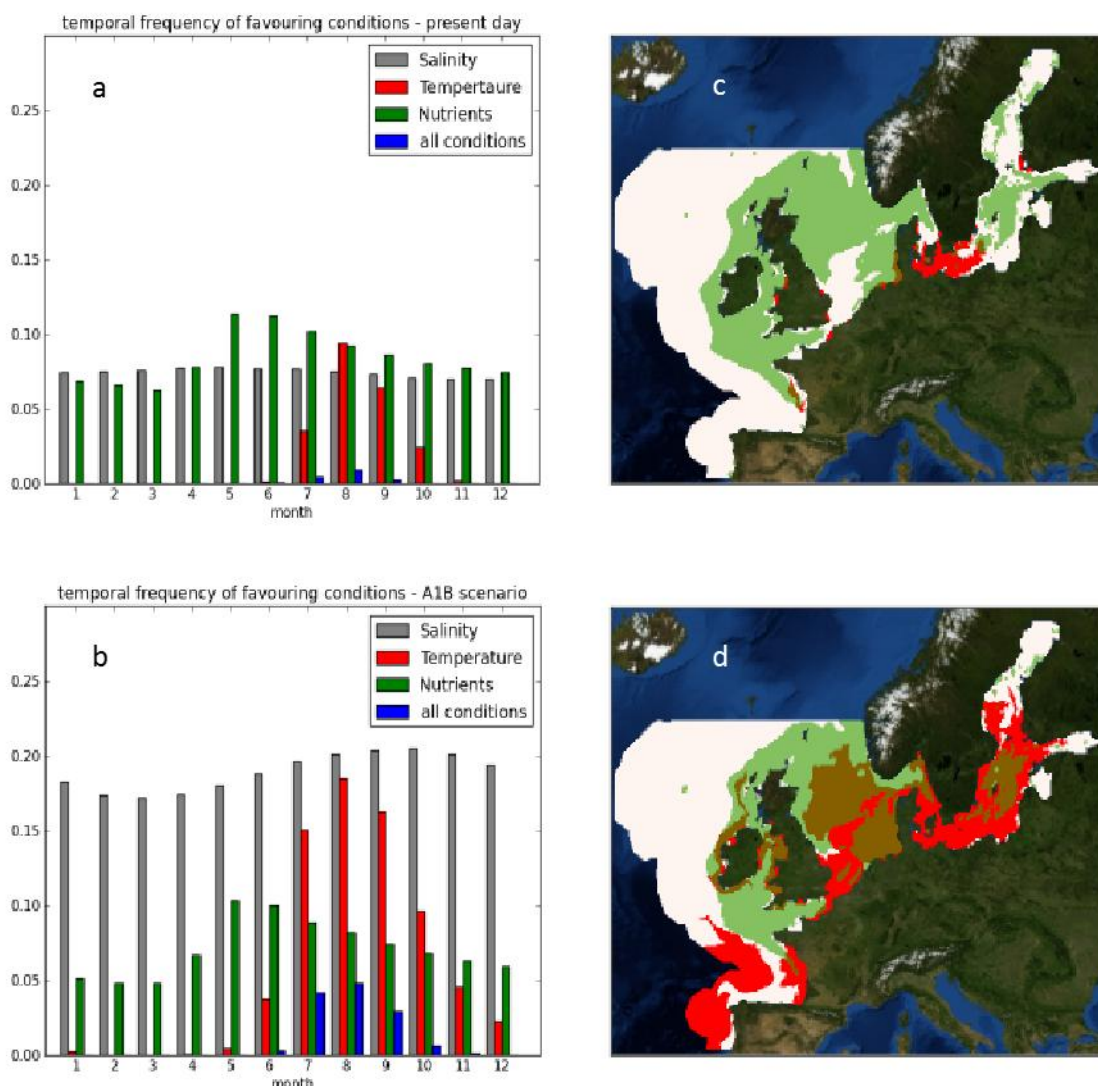


Figure 48. Panel a,b: Comparison of frequency diagrams, by month of the year for suitability of physical and nutrient conditions for *Procentrum*-type HABs in northern European coast under present conditions (a) and under the future scenario (b) described in text. The frequency diagrams depict the fraction of pixels in the ERSEM model that meet the criteria by month. Panels c,d: spatial extension of the physical (salinity and temperature; red) and nutrient ($NH_4 > NO_3$; green) niche and both conditions overlapping (brown) for the month of July under present conditions (year 2001; panel c) and under the future scenario (year 2100; panel d) described in text. Where neither condition is verified, the map domain is white. The regions of the maps indicated in blue are outside the model domain.

Higher Trophic Level: IBM for cod in the North Sea

As defined within MEECE, future projections were accomplished using IPSL-ESM for the time period (2080-2099). As for the lower trophic level simulation, we started the simulation in 2070, although the first 10 years can be considered as a spin-up period. For comparison, we additionally applied NorESM for the time period 2090-2096. In Figure 50, the projected changes for the most relevant environmental variables are shown. We find clear differences between the physical variables SST and U-current velocity (U) (Figure 50a). While for the IPSL-ESM SST changes are very large with almost 3°C and associated with a strong decrease in U, the changes in SST and U projected with NorESM are less severe. In contrast, changes in primary production and hence, in secondary production, seem to be comparable in both magnitude as well as spatial pattern (Figure 50b).

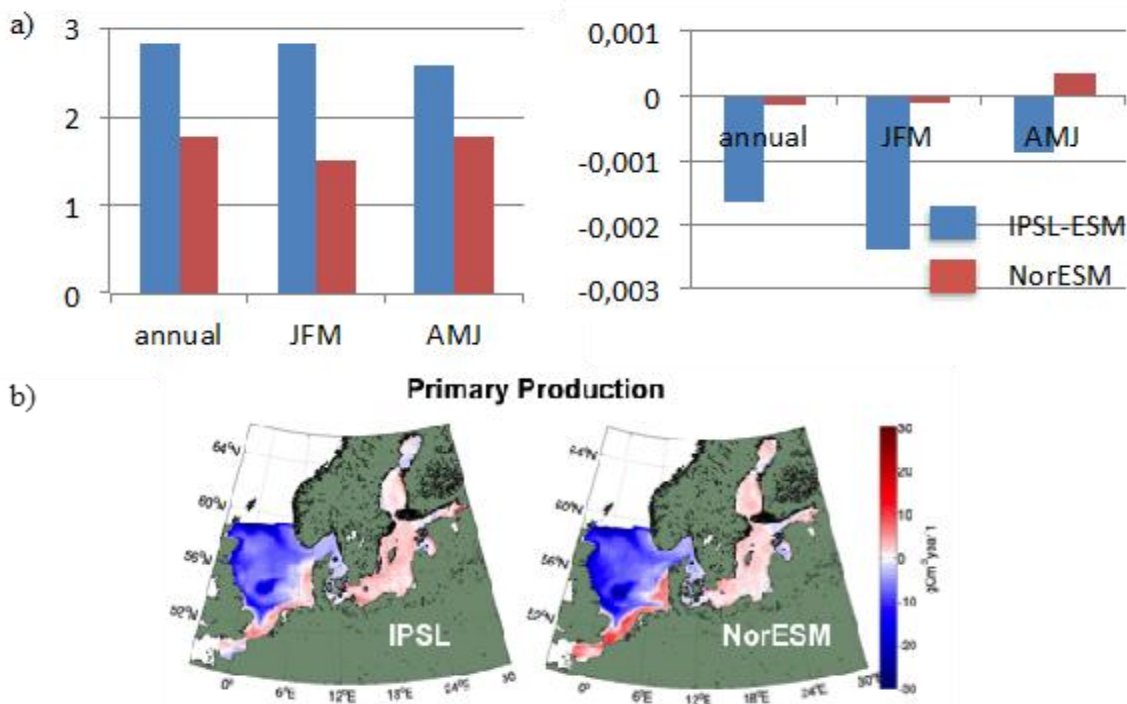


Figure 50: Average change in the magnitude of climate and ecosystem variables calculated as difference between forecast (2090-2096) and hindcast (1980-1999). a) Change in annual and seasonal (winter, spring) SST and u-current velocity; b) change in primary production for IPSL-ESM and NorESM.

The projected changes in PLS for the time period 2090-2096 are given in Figure. The results clearly indicate a general decrease in PLS for both ESM forcings. In coherence with the change in production, the average spatial pattern for both simulations appears comparable and indicates the strongest decrease at the Dogger Bank area. Here, the change in PLS is around 20%.

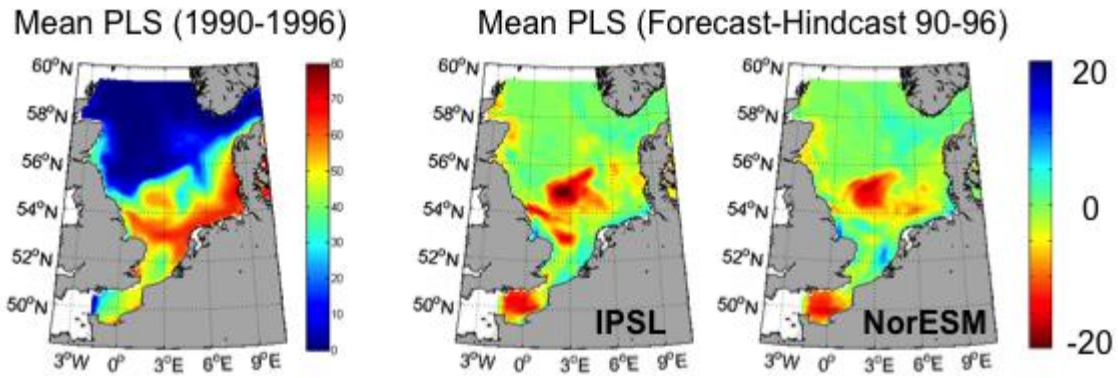


Figure 51. Average (1990-1996) annual PLS and projected changes in 2090-2096 (Forecast-Hindcast)

In Figure , inter-annual variations in PLS (control: black line) and in the respective projected changes are shown. For the longer-term experiment with IPLS-ESM, we found the strongest decrease in PLS associated with the time period prior to the regime shift (2080-2088), while in other years the changes can be relatively small. Considering that the delta change approach does not account for changes in the inter-annual variability of the forcing data, we can conclude that the simulated inter-annual variability in PLS can be attributed to non-linear processes interactions. When comparing the results from the different projections (IPSL-ESM and NorESM), we found that the temporal variations (Figure 52), in contrast to the spatial pattern, reveal clear differences between the two different ESM's.

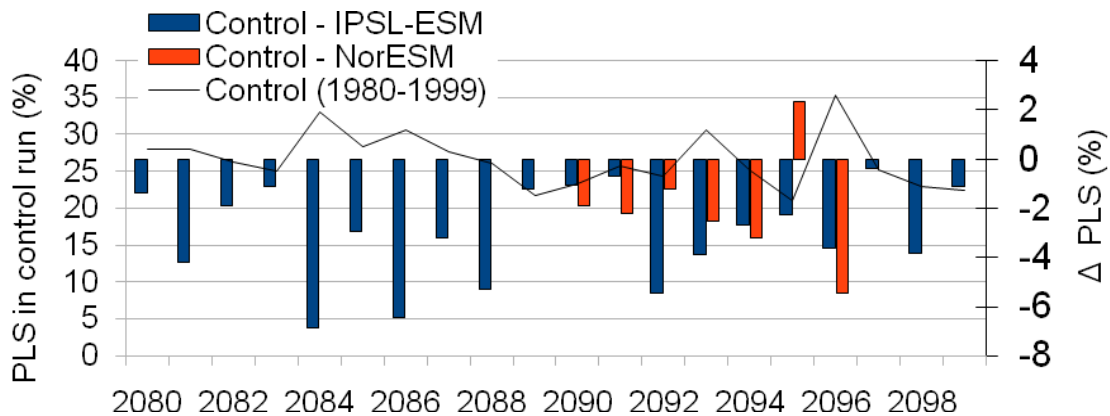


Figure 52. Simulated annual PLS for 1980-1999 (black line) and projected changes in annual PLS (Δ PLS; bars) for both IPSL-ESM (blue) and NorESM (red) forcing.

Higher Trophic Level: Ecosim coupled to GOTM-ERSEM LTL model¹

The linked model runs explore three aspects of environmental change: Effect of changes in fishing mortality to one based on putative MSY, a reduction in the level of shelf sea nutrients

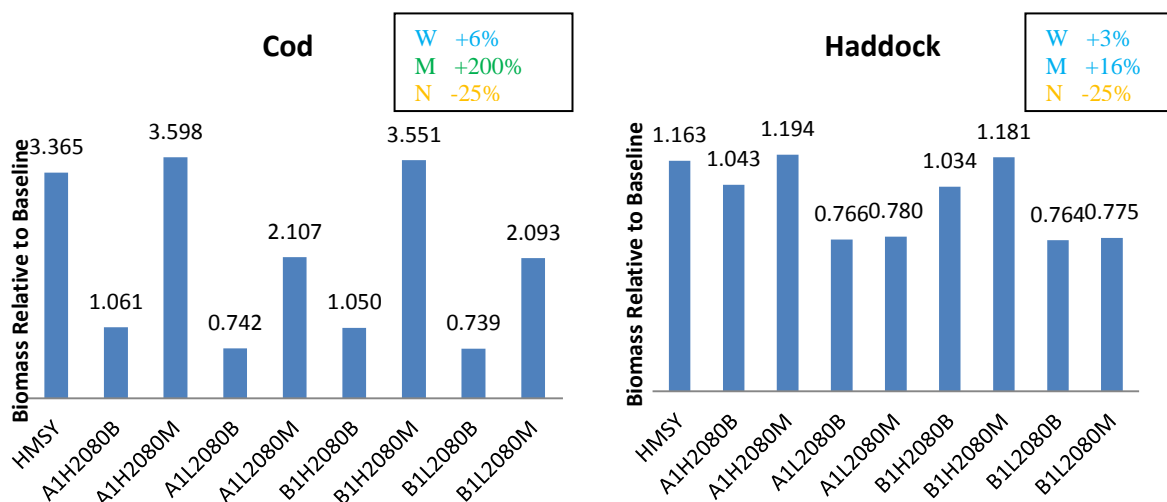
¹ This part of the report is duplicated in D4.3 as it covers both the climate and multiple driver scenarios holistically.

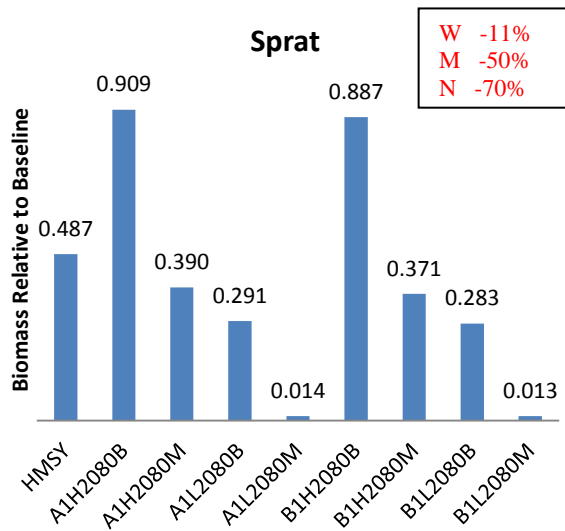
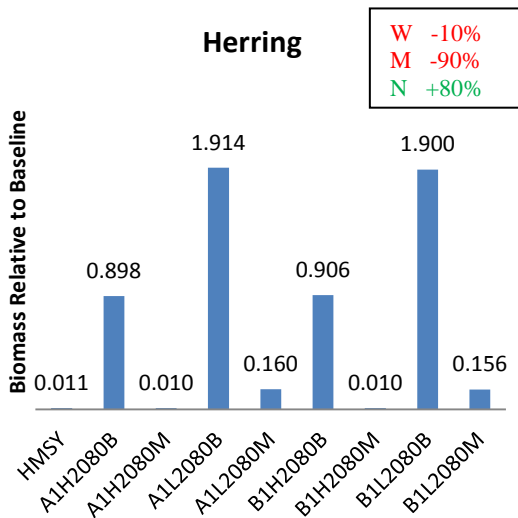
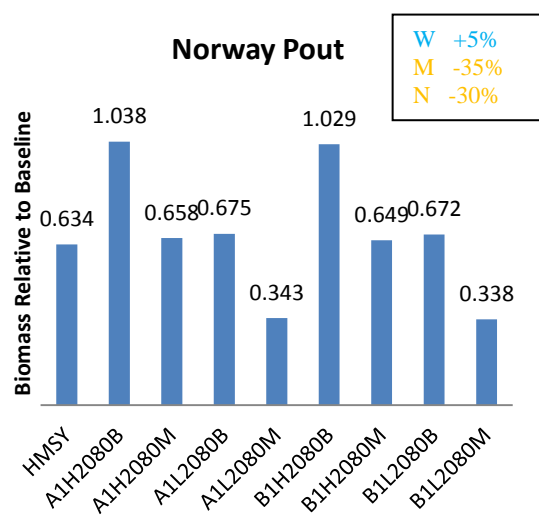
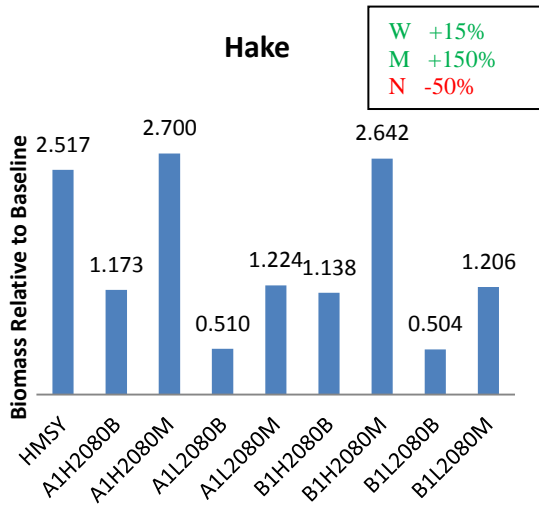
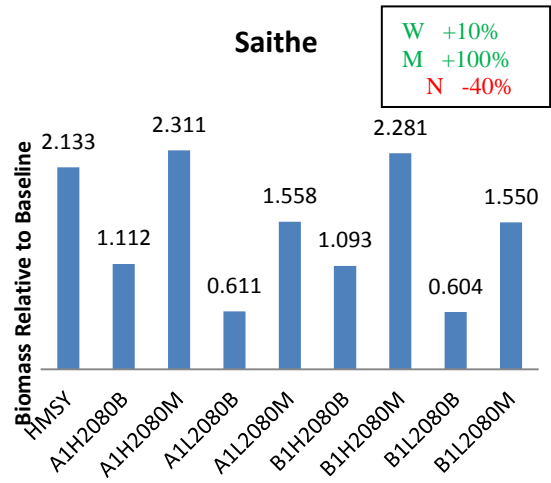
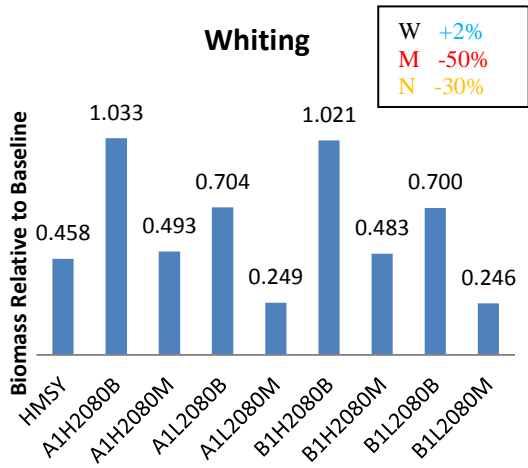
(specifically nitrate and phosphate) and long-term climate change. The order of significance of the effects of the three drivers is as above.

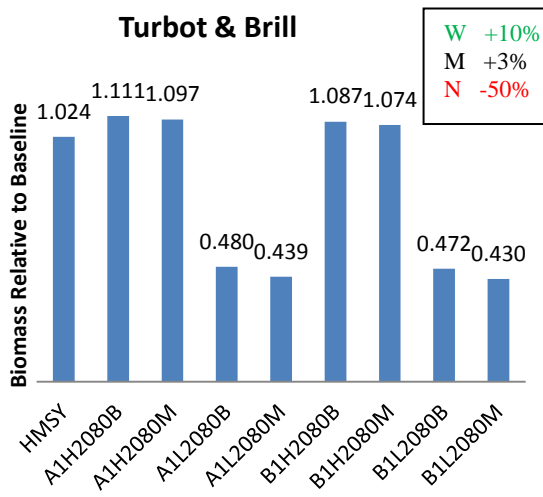
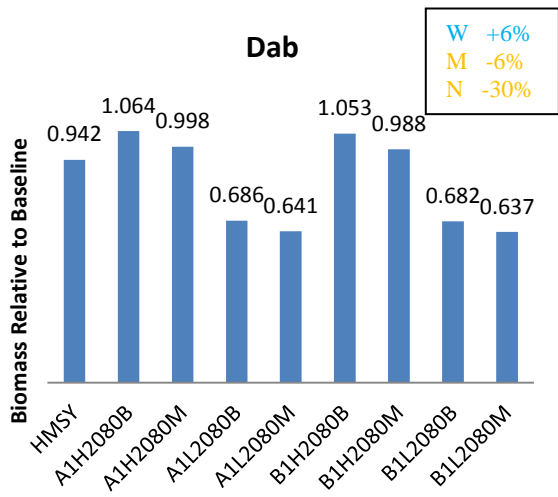
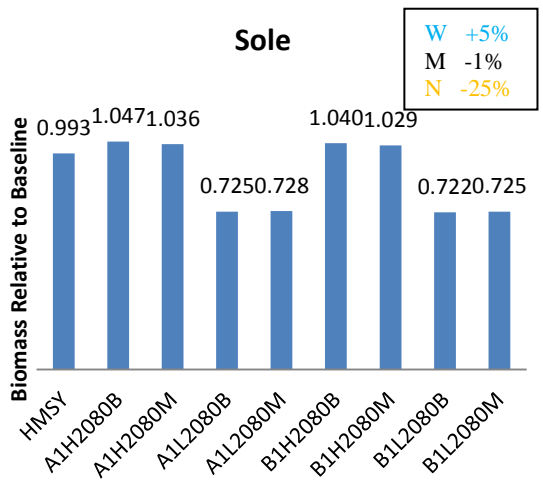
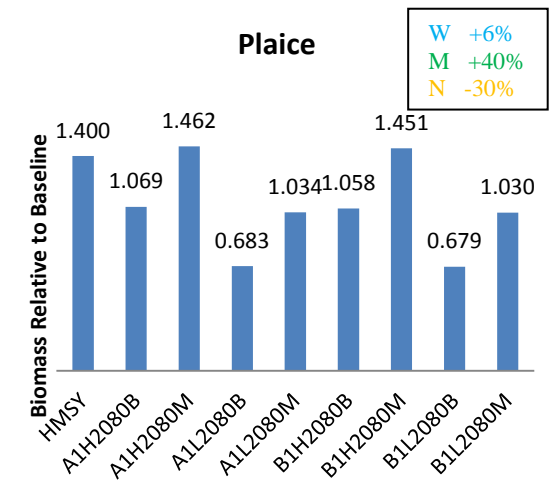
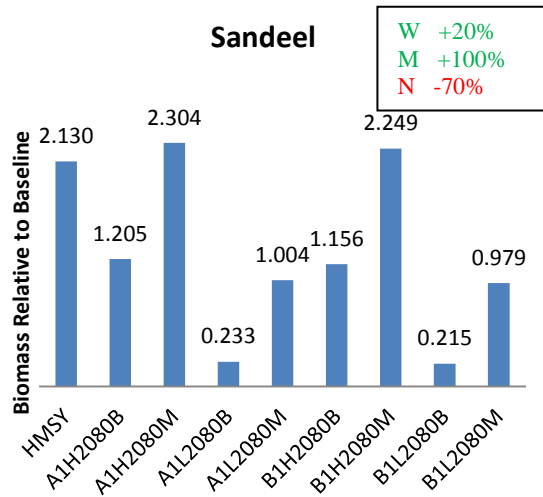
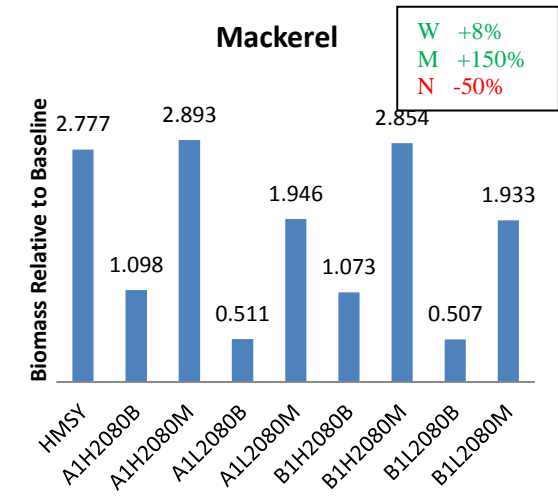
Climate change has the least effect - between zero and 20% change in biomass, with the greatest effect on the highest trophic level species: sharks, rays and seabirds as well as hake and sandeels. The effect on invertebrates was least and benthic fish intermediate. The effect of climate change on pelagic fish was the most complex with sandeels greatly benefitting from global warming but Mackerel suffering a population decline as a result. These results are consistent with the results of figure 23 indicating an increase in large zooplankton biomass (mesozooplankton) in the North Sea area of less than 0.2, except that whereas purely LTL models, such as ERSEM have a fixed proportion death rate, the coupled model has an increasing predation rate on zooplankton resulting from increase in HTL predator population.

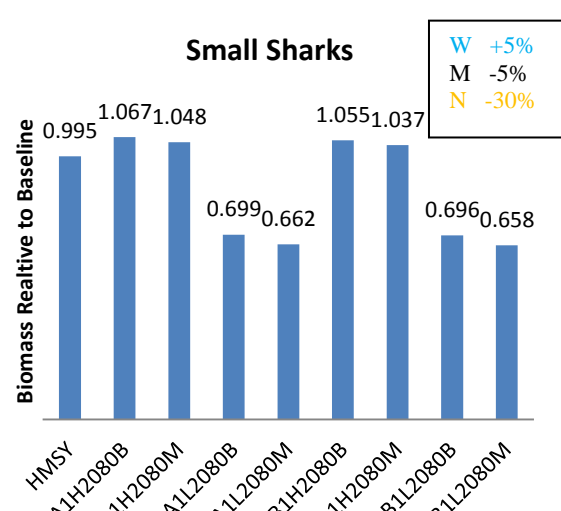
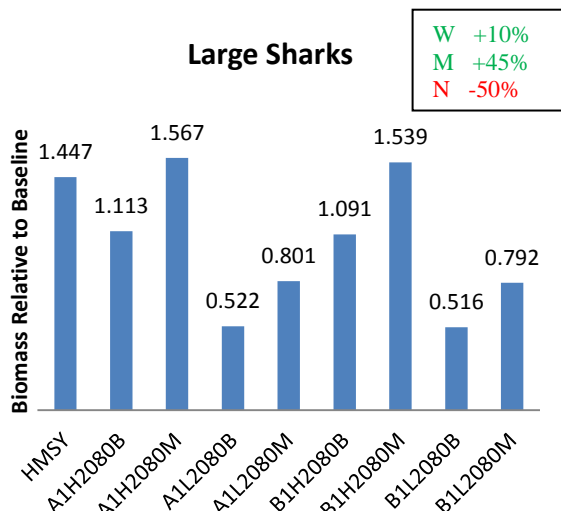
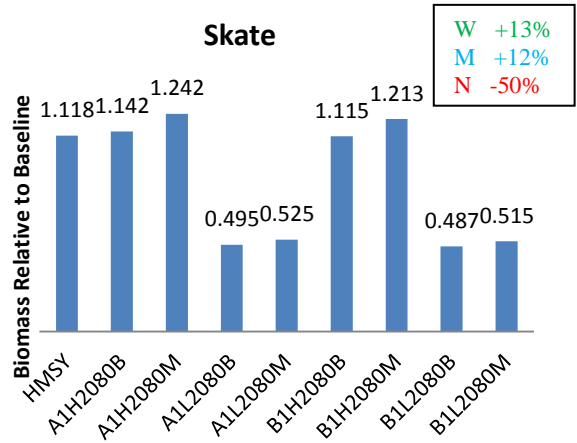
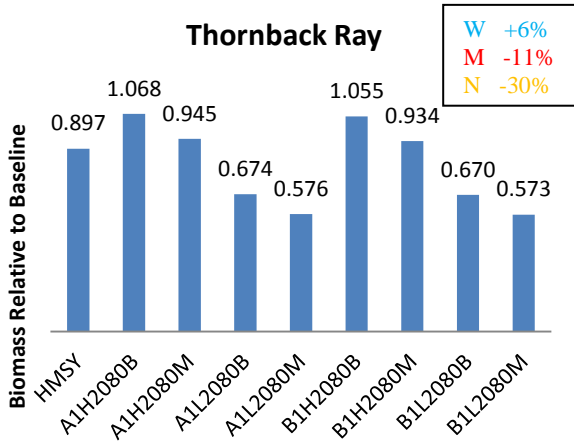
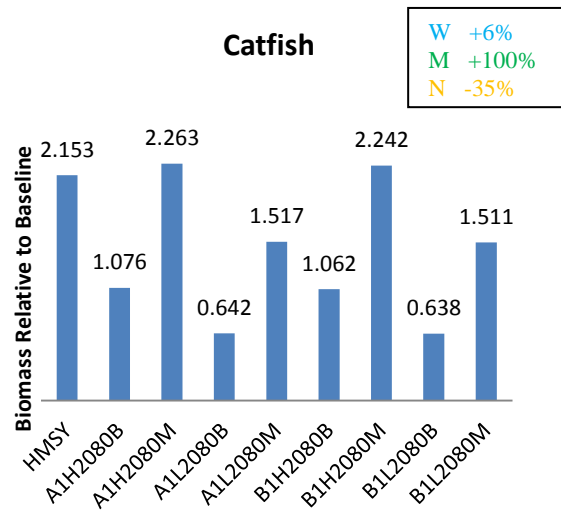
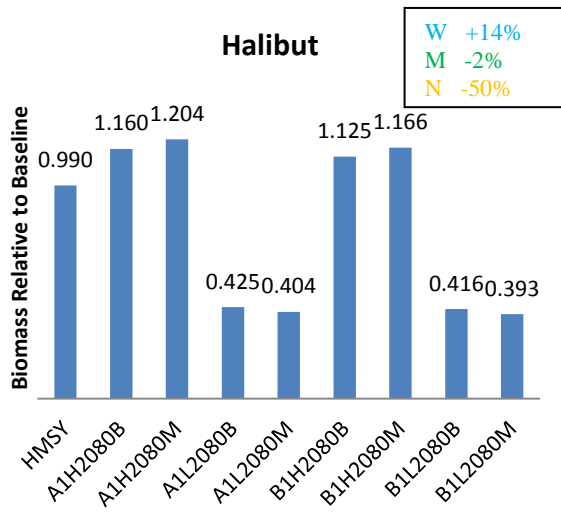
The effect of nutrient reduction was an almost universal reduction in populations of the highest trophic levels with the population levels of around 50% of the high nutrient level for seals, sharks and seabirds. Many commercial species such as Cod and various demersal flatfish showing a 60% to 70% level of biomass, but invertebrates show a small reduction and the Omnivorous zooplankton themselves show little change. These results illustrate that the production of zooplankton is to a large extent nutrient limited but that reduction in productivity at the lower trophic levels is balanced by reduction by predation from higher trophic levels. In other words the system is bottom up as far as nutrients are concerned.

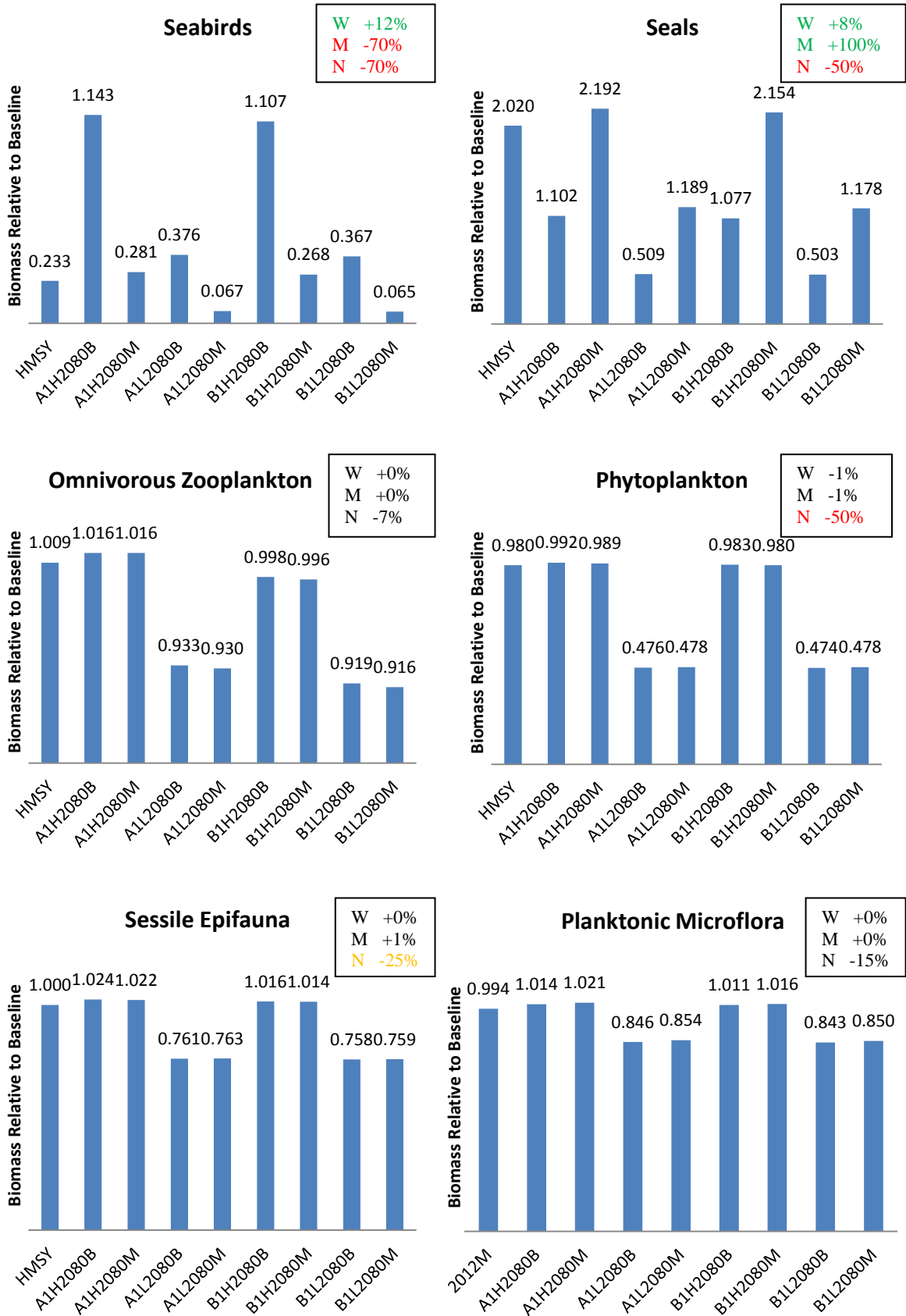
Change in fishing pressure to MSY has a significant long term positive effect on Cod, Saithe, Hake, Mackerel, Sand Eel as well as Catfish and, indirectly, Large Shark and Seals. Cod biomass is a factor of 3 higher (starting from a low baseline of current Cod stocks). Some species are negatively affected through predation / competition: Whiting, Blue whiting, Norway Pout, Herring and Sprat. Flatfish and invertebrates are moderately affected, typically by 20% or less compared to current fishing practices.











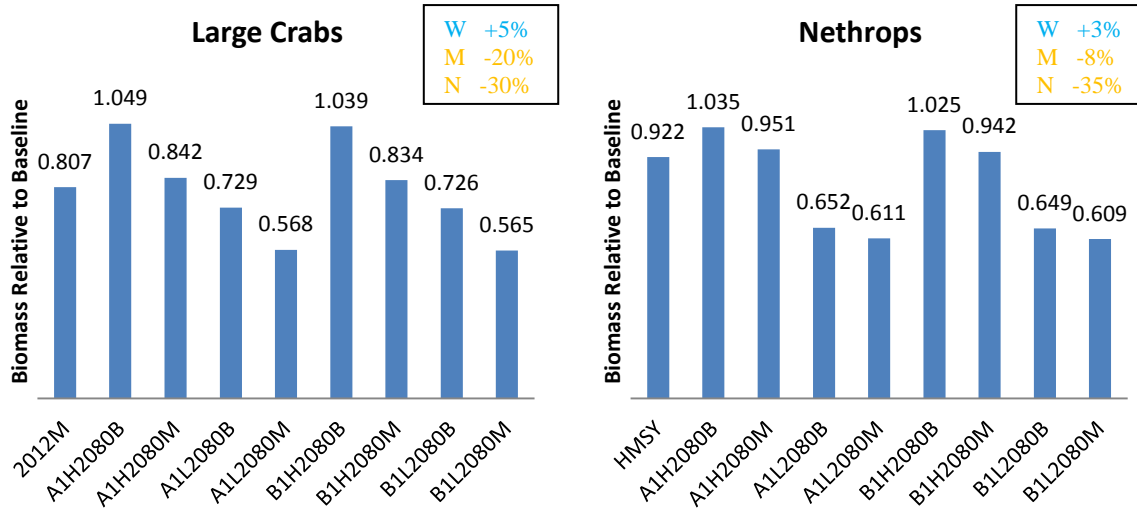


Figure 53: Effect of interaction of climate change, fishing and nutrient reduction scenarios on biomass relative to current baseline levels for a variety of higher trophic level species in the North Sea. Box indicates effect of warming (W) – 3.8 degrees scenario A1B1, switch to MSY (M) and nutrient reduction (N). The levels shown are for the effects separately.

The effects of combining the effects of nutrient reduction, changing the fishing pressure and introducing warming are largely additive with the observed effect of combining MSY fishing and warming very close to the effect of the calculated effect of the combination of the two effects in isolation (fig 54).

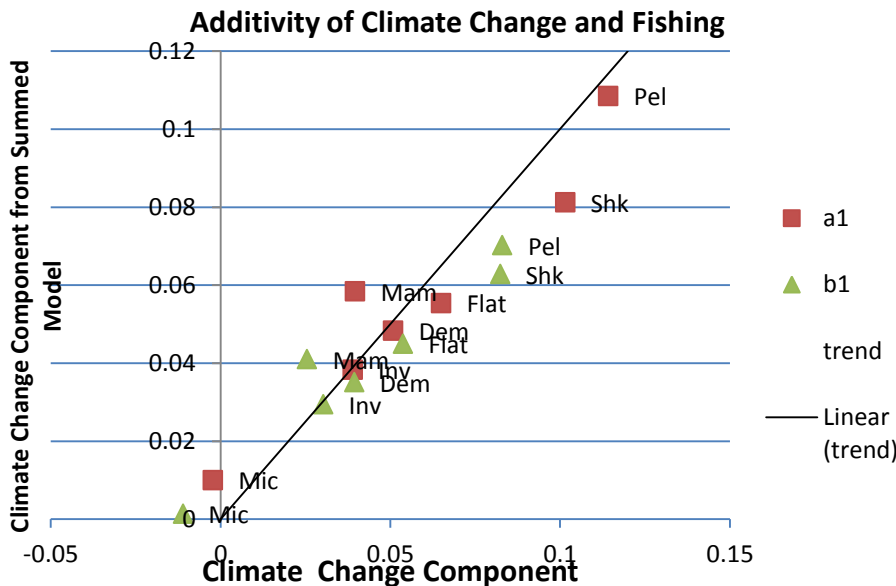


Figure 54. Effect of adding climate change and fishing changes. The effect of climate change in the summed model is compared with the effect from the climate change alone, for the climate change scenarios a1b and b1. A marker below the trend line indicates that the change in biomass in the summed model is less than that predicted from climate change alone. Combined groups are: Pel – pelagic (not sharks), Dem – demersal (not sharks or

flatfish), *Flat* – demersal flatfish species (not sharks or rays), *Shk* – sharks and rays, *Inv* – invertebrates excluding plankton, *Mic* – Microbes and plankton.

7. Discussion

Oceanic climate and lower trophic level in the NE Atlantic (POLCOMS-ERSEM model)

The POLCOMS-ERSEM results for the northeast Atlantic are forced by a single, consistent ocean-atmosphere dataset representing possible future conditions under the SRES A1B emissions scenario. While the simulation is not a prediction of the future, and no assessment of likelihood is presented, it can be used to look at the processes involved and the ecosystem response to potential future conditions.

The main physical changes in the future simulation are an increase in sea surface temperature over the whole northeast Atlantic, a freshening of water over the northwest European continental shelf and in the Bay of Biscay and an increase in surface salinity in the open ocean between Iceland and Norway (Table 4). Seasonal stratification is stronger in the future simulation and, except in the Bay of Biscay, starts earlier in the year.

There is a reduction in the oceanic sources of nitrate and phosphate in the future, arising from increased oceanic stratification. Together with stronger local stratification, this leads to a reduction in the nutrients available for primary production in many on-shelf regions. The spatial distributions of the fractional changes in netPP (Figure 24) and surface phosphate and nitrate (Figure 26) show a high degree of consistency. The longer phytoplankton growing season in the future (Figure 23) does not translate into higher phytoplankton biomass, which generally decreases in the future. The biomass of small zooplankton also decreases while large zooplankton amounts increase. Large phytoplankton start to grow earlier and at a higher rate in the future simulation fueling earlier, stronger blooms of large zooplankton.

Oceanic climate and lower trophic level in the North Sea (ECOSMO)

ECOSMO projects an increase in SST between 2.5 and 3 °C for the IPSL global climate forcing in the North Sea. Our ensemble simulations indicate that warming is a robust feature for all investigated scenarios, while the magnitude of this warming is uncertain. This uncertainty is related to the choice of GCMs and the considered scenario and is of the same order of magnitude as the projected changes. The calculated warming is significantly lower for the projection based on the new AR5 RCP scenarios, at least as seen by the NorESM model. This is very similar to results achieved for the global surface temperature increase. Here, also the new projections (AR5) with the Norwegian climate model (NorESM) projected lower SST increases than the earlier AR4 projections with the previous Norwegian Climate model (BCM). These projected temperature increase might alter habitat conditions and species pattern and alter the species composition in the North Sea.

In addition to the ecosystem changes induced by changing hydrographic conditions, the changes in the atmospheric parameter wind and short wave radiation also have a direct impact on nutrient availability in surface waters and lower trophic level production. The

regional projections performed indicate a significant drop in North Sea primary production when forced by both, atmospheric and oceanic nutrient changes. We could identify that this is mainly driven by a significant decrease in oceanic winter nutrient levels as calculated by the IPSL-ESM. The projected production changes caused by changes of atmospheric conditions were identified to be extremely uncertain for the North Sea system. Both atmospherically induced production increases (BCM, ECHAM and partly NorESM forced) as well as decreases in production (IPSL forced) were modelled. It was not possible to perform downscaling experiments considering different ESMs, however, we could analyse the winter nutrient condition change from the new NorESM simulations and could identify that the projected decrease in nutrients as revealed by the IPSL model simulations is not a robust feature that is produced by all ESMs.

Higher trophic level in the North Sea

The use of spatially explicit IBM to understand past population dynamics in Atlantic cod (and also other fish species) in the North Sea appears to be a useful tool to identify underlying processes. In the analysis we can rely on what already has been observed and measured for the particular species. This can be useful to understand the ecosystem dynamics on the one hand, and also to project population dynamics and recruitment for short-term future time intervals. For long-term future projections, in contrast, the results are difficult to interpret for a number of reasons. First, the IBM parameterisation has been found to critically impact the IBM results (Daewel et al. 2008), since it is unknown to at what degree the species will adapt to the changing climatic conditions. This might concern internal processes like developmental rates, feeding or metabolism, and also external parameters such as spawning behaviour. Second, the comparison between two different ESM forcing reveals similar features in both spatial distribution and amplitude. Since only two experiments have been made for a restricted time period, we cannot estimate the uncertainty range associated with this type of experiments. Nonetheless, considering the fact that the driving environmental parameters as well as the inter-annual variations (Figure 50) differ substantially, we can hypothesize that in the two experiments different processes impact the change in PLS and that the similarities are maybe coincidental for the respective time period. Thus, we can conclude that, together with the high uncertainties already found for the lower trophic level simulations, the uncertainty range for respective projections performed with spatially explicit IBMs is larger than the results indicate. Clearly additional ensemble experiments are necessary to answer the related question concerning the uncertainties on the one hand and to identify the different process-interactions associated with the different setups on the other hand.

The model coupling results have indicated that changes in the environment and fishing pressure could have both a top down and bottom up effect on the North Sea food web. However, whereas the bottom up effect is concentrated up the food web, the top down effects are not transmitted to the microbial parts of the food web, or affect them only very marginally by less than 1%. Furthermore, the most significant effects are as a result of the changes in nutrients rather than the direct effect of changes in temperature. These results should not, however, be taken to be demonstrative of no effect of climate change on higher

trophic levels, rather than the mechanisms of nutrient enrichment / depletion is unlikely to be the most significant one. Other possibilities might include effects on migration of HTL species, effects of shift in nutrient balance having an effect on the metabolism of the HTL species and direct effects of temperature on the metabolism of the HTL species themselves. Empirical evidence of shifts in population following decadal scale changes in temperature resulting from variation in North Atlantic Oscillation suggests other mechanisms are important. It should be noted that other work in the MEECE project has focussed on the effect of environmental and lower trophic level conditions on the survival of fish larvae, however fish larvae in the Ecosim North Sea model are used simply as a food source and are not connected to the mature populations.

It would seem that there is the need to integrate other model components if we are to fully explore the consequences of climate change on HTL populations. One potential improvement is to replace the coupling

Physics Model -> Lower Trophic Level Model -> HTL food web

with

Physics Model -> Lower Trophic Level Model -> Individual based larval and Fish -> HTL food web

The Couplerlib system of managed coupling would be able to do this because it handles data translation, but a specific module for aggregating individual based model data into mean field representation would be required.

The possibility exists for direct incorporation of climatic effects into HTL models, specifically Ecosim. Currently Ecosim has a temperature and salinity variable which can be used to set optimal temperatures and salinities for survival. Potentially the plugin mechanism of model extension could be used to code explicit model relationships for predation and growth as well as survival. Similarly in a 2 dimensional Ecospace model, ocean flux predictions from the physics model could be combined with behavioural information on marine vertebrates to produce a detailed sub-model of migration and fluxes in space. However obtaining the data needed for an elaborate behavioural model in a large food web will be a considerable challenge.

8. Concluding remarks

In relation to future changes on oceanic climate and lower trophic level within the NE Atlantic, there are three important next steps. First, is to better identify the driving mechanisms for the potential future change, particularly where these relate to subtle bio-physical interactions such as the relation between the bloom and the on-set of stratification. Second, is to explore the range of future states. The prospects for building a truly probabilistic view of the future here is limited since there are too many variables of uncertainty in this coupled system (e.g. scenario uncertainty, uncertainty each of the driving and regional models, natural variability). However, detailed knowledge of process response should allow us to put bounds on possible future states given appropriate self-consistent bounds of future conditions. Finally, knowledge of the present day variability and its driving mechanisms is crucial as it is through

this that we may hope to bring forward the statistically significant forecast horizon. This is an important goal for improving the policy relevance of this work.

Particularly for the North Sea, we can conclude that under a future climate scenario produced by the global IPSL-ESM for the A1B scenario, this area is expected to experience: increasing sea surface temperatures, increasing surface salinities, decreasing surface nutrients, and decreasing primary and secondary production (Table 4). The performed ensemble simulations allowed first uncertainty assessments of climate change projections.

Key findings for the North Sea can be summarized as following based on the performed scenarios:

- Projected SST changes are robust in direction (warming) for several forcing GCMs but differ significantly in magnitude.
- Uncertainty in projected warming arising from the utilization of different GCMs is in the order of projected possible changes.
- Projected SSS changes differ in spatial pattern and sign with different forcing GCM.
- Projected changes in primary (and secondary) production differ in pattern and sign for different forcing GCMs (only atmospheric forcing).
- The projected decrease in primary production in the North Sea (full IPSL forcing) could be attributed to the overall decrease of winter nutrients in the North Atlantic region as projected by the IPSL model. However, such a pronounced decrease is not reproduced by all ESMs, the NorESM projections (AR5 simulations) show a much lower decrease in surface nutrients.
- Uncertainty in the amplitude of the projected climate change is large and locally as large as the projected changes.
- The impacts of OA and climate change are strongly intertwined: even when simple parameterizations are implemented, the combination of the effects can lead to unexpected results. OA could either exacerbate or compensate climate change impacts depending on season, area and process.
- IAS distributions are susceptible to climate driven changes in habitat, notably in temperature. Coupled with changing nutrient conditions suggests an even greater potential for expansion of invasive HAB blooms. However the requirement for the overlap of physical and chemical conditions limits the realization of these effects.

Valuable lessons have been learnt from the projections and especially from the ensemble simulations utilizing different GCMs as forcing. For the North Sea these are specifically:

- Wind field variations are essential for the hydro- and ecosystem dynamics in the North Sea.

- Uncertainty in projected changes is large, for some parameter local differences in direction of the changes exist, for all investigated parameter we found significant changes in amplitude.
- The utilization of different GCMs to produce robust future climate projections is essential. Uncertainty is large and projected changes are assumed to be significantly different for the different forcing GCMs.
- The key climatic parameter responsible for productivity changes in the past 6 decades are the wind field (strength and direction) and the Atlantic nutrients. Second order parameters are the solar radiation and river loads.
- For regional climate change impact assessments consistent regional river load scenarios are necessary and consistent information on ocean nutrient changes and hence the utilization of Earths System Models (ESM) instead of GCMs (Global Climate models) is extremely important for the North Sea.
- From AR4 to AR5 the magnitude of projected changes will change, for the Norwegian Climate model we observed a decrease in projected warming and hence regular climate change downscaling exercises are necessary to update to state of the art knowledge about regional impacts of climate change.

Access to selected model results is ensured via the MEECE Atlas. Complete access to hindcast model simulations and selected results from the projections will be ensured via ICES WGOOFE working group and web site (www.wgoofe.org/ICES).

Concerning higher trophic level in the North Sea, the potential larval survival of Atlantic cod is expected to be unchanged in most of areas and to decrease in the central part of the North Sea under future climate change, probably due to the projected decrease of primary production in overall area. In combination with increased temperature, this potentially provokes miss-match situations of first-feeding cod and its prey. The Atlantic cod model is a valuable tool to understand processes related to potential larval survival of this species, including especially match-mismatch dynamics with zooplankton fields. However, additional ensemble simulation and sensitivity studies are necessary to evaluate the uncertainty range associated with future projections of larval fish survival using spatially explicit IBMs.

The wider effect of changes to the North Sea food web is necessarily a complex emergent property of the interactions of the many groups. Modelling an entire system in this way with necessarily simplified models will not produce accurate predictive models for all groups, indeed it may not produce any meaningful predictions at all for some groups where the driving features of the group are not adequately represented by the model. For example although Baleen whales were included in the model, they have not been presented in the results because they are too wide ranging and too long lived to be anything other than a feeding sink for their food species, similarly fish larvae were not included because their population is only meaningful as a population stage in other species / groups. In general though there are some broad conclusions about some of the trends that might be experienced as a result of changes in production: The highest trophic level species respond

positively to less fishing and more nutrients, whereas the effects on demersal and flatfish are smaller. Moving to an MSY based fishing approach clearly benefits the fish that are fished less whilst their competitors may be adversely affected. In other words, the fishing quotas of some groups that are being fished sustainably now may have to be revisited as a result of changes in population of competitors and predators. Smaller pelagic fish are the 'closest' trophically speaking to the plankton whose levels may change and are likely to see the most dramatic effects of any deliberate or inadvertent change in plankton composition.

Table 4. Change of main climate changes and ecosystem response at 2080-2100 relative to 1980-2000 (Scenario A1B) in the North Sea. Legend: For model uncertainty (based on hindcast validation), Low: the model describes interannual, seasonal and spatial variability appropriately, Medium: the model describes the general observed seasonal and spatial variability, High: the model fails in describing the general pattern (seasonal and spatial). For spatial variability, Low: most of areas with same trends, High: some areas with opposite trends with respect to others. Units: SST (°C), pH (surface), netPP: Net Primary Production Depth integrated (mg C/m²/d), Zooplankton (biomass depth integrated) (mg C/m²), HTL (total biomass of all fish species considered). Range is expressed in Percentile 25 and Percentile 75. Absolute change for SST and pH. Fractional change for netPP, Zooplankton biomass and HTL; fractional change = $(A1B_{(2080-2100)}/PD_{(1980-2000)})-1$; see Holt et al. (2012); where -1 to 0: decrease, positive values: increase.

Model: POLCOMS-ERSEM	Change range at 2080-2100 relative to 1980-2000				
Region: Atlantic Margin	SST	pH	netPP	Zoop biomass	HTL
Mean	2.63	-0.23	-0.06	-0.07	N/A
Range	2.42:2.84	-0.3:-0.21	-0.14:0.02	-0.13:-0.01	N/A
Test kruskal-Wallis (p-value)	0.00	0.00	0.00	0.00	N/A
Model Uncertainty	Low		Medium		N/A
Spatial variability	Low	Low	High	High	N/A

Model: POLCOMS-ERSEM	SST	pH	netPP	Zoop biomass
Region: Greater North Sea				
Mean	3.08	-0.27	-0.05	-0.07
Range	2.92:3.29	-0.29:-0.26	-0.10:0.01	-0.10:-0.04
Test kruskal-Wallis (p-value)	0.00	0.00	0.06	0.00
Model Uncertainty	Low		Medium	
Spatial variability	Low	Low	High	Low

Model: GOTM-ERSEM-ECOSIM Region: Greater North Sea	Invertebrates	Pelagic	Demersal	Flatfish	Sharks	Mammals / Birds
Mean	0.04	0.11	0.05	0.07	0.1	0.04
Range	0.0-0.05	-0.10-0.2	-0.17-0.17	0.04-0.16	0.05-0.14	0.02-0.14
Test kruskal-Wallis (p-value)	N/A	N/A	N/A	N/A	N/A	N/A
Model Uncertainty	Medium	High	Medium	Medium	High	High
Spatial variability	High	High	High	High	High	High

Model: ECOSMO-IBM Region: Greater North Sea	SST	pH	netPP	Zoop biomass	HTL (cod, IBM)
Mean	2.82±0.03	-0.22±0.01	-0.125 ±0.027	-0.198±0.064	-0.109
Range	2.81:2.84	-0.221:-0.217	-0.147:-0.105	-0.243:-0.157	-0.158:-0.049
Test kruskal-Wallis (p-value)	6.302e-08	6.302e-08	1.147e-07	2.204e-06	0.0119
Model Uncertainty	Low (medium in some regions)	-	Medium (based on nutrient val.)	Medium (based on nutrient val.)	High
Spatial variability	Médium	-	High	High	High

Model: POLCOMS-ERSEM Region: Celtic Seas	SST	pH	netPP	Zoop biomass	HTL
Mean	2.65	-0.26	0.03	-0.01	N/A
Range	2.52:2.79	-0.28:-0.24	-0.03:0.09	-0.06:0.02	N/A
Test kruskal-Wallis (p-value)	0.00	0.00	0.39	0.15	N/A
Model Uncertainty	Low		Medium		N/A
Spatial variability	Low	Low	High	High	N/A

Model: POLCOMS-ERSEM Region: Bay of Biscay	SST	pH	netPP	Zoop biomass	HTL
Mean	2.22	-0.26	-0.02	-0.01	N/A
Range	2.10:2.38	-0.27:-0.25	-0.09:0.03	-0.07:0.03	N/A
Test kruskal-Wallis (p-value)	0.00	0.00	0.04	0.19	N/A
Model Uncertainty	Low		Medium		N/A
Spatial variability	Low	Low	High	High	N/A

9. References

Ådlandsvik, B. 2008. Marine downscaling of a future climate scenario for the North Sea. *Tellus A* 60: 451-458.

Ahrens, R.N.M., Walters, C.J. & Christensen, V. 2011, Foraging Arena Theory. *Fish and Fisheries* 13(1) 41-59.

Alheit, J., Möllmann, C., Dutz, J., Kornilovs, G., Loewe, P., Mohrholz, V., and Wasmund, N. 2005. Synchronous ecological regime shifts in the central Baltic and the North Sea in the late 1980s. *ICES J.Mar.Sci.* 62: 1205-1215.

Allen, J. I., Holt, J. T., Blackford, J. C., and Proctor, R., 2007a. Error quantification of a high-resolution coupled hydrodynamic-ecosystem coastal-ocean model: Part 2. Chlorophyll-a, nutrients and SPM, *Journal of Marine Systems*, 68, 381-404.

Allen, J. I., Somerfield, P. J., and Gilbert, F. J., 2007b. Quantifying uncertainty in high-resolution coupled hydrodynamic-ecosystem models, *Journal of Marine Systems*, 64, 3-14, 10.1016/j.jmarsys.2006.02.010.

- Artioli, Y., Blackford J.C., Butenschon M., Holt J.T., Wakelin S.L., Thomas H., Borges A.V., Allen J.I., In press. The carbonate system in the North Sea: Sensitivity and model validation. *Journal of Marine Systems*, 102-104, 1-13, doi:10.1016/j.jmarsys.2012.04.006.
- Aumont, O., Maier-Reimer, E., Blain, S., and Monfray, P., 2003. An ecosystem model of the global ocean including Fe, Si, P colimitations, *Global Biogeochemical Cycles*, 17, 1060, doi: 10.1029/2001gb001745.
- Backhaus, J. O. Hainbucher D. A Finite Difference General Circulation Model for Shelf Seas and Its Application to Low Frequency Variability on the North European Shelf. 221-244. 1987. *Three-Dimensional Models of Marine and Estuarine Dynamics*, Elsevier Oceanography Series . Nihoul, J. C. J. and Jamart, B. M.
- Baretta, J.W., Ebanhoh, W. & Ruardij, P. 1997. The European Regional Seas Ecosystem Model (ERSEM) II, *J. Sea Res.* 38:229–483.
- Batten, S. 1996. Comparison of Changes in the Annual Variability of the Seasonal Cycles of Chlorophyll , Nutrients and Zooplankton at Eight Locat = ons on the North- West European Continental Shelf (1960-1994). *Deutsche Hydrographische Zeitschrift*, 48(3), 349–364.
- Batten, S. D., Clark, R., Flinkman, J., Hays, G., John, E., John, A. W. G., Jonas, T., et al. 2003. CPR sampling: the technical background, materials and methods, consistency and comparability. *Progress In Oceanography*, 58(2-4), 193–215. doi:10.1016/j.pocean.2003.08.004
- Beaugrand, G., Keith M Brander , J. Alistair Lindley, Sami Souissi, and Philip C Reid . "Plankton effect on cod recruitment in the North Sea." *Nature* 426 (2003): 661-664.
- Beecham, J., Bruggeman, J. Aldridge, J. and Mackinson, S. A Coupled Model of Upper and Lower Trophic Levels in a Marine Ecosystem. Submitted to *Ecological Modelling*.
- Blackford, J. C., 1997. An analysis of benthic biological dynamics in a North Sea ecosystem model, *Journal of Sea Research*, 38, 213–230.
- Blackford, J.C., J.I. Allen and F.J. Gilbert, 2004. Ecosystem dynamics at six contrasting sites: a generic model study. *Journal of Marine Systems*, 52 (1–4), 191–215, doi:10.1016/j.jmarsys.2004.02.004.
- Blackford, J. and Gilbert, F. 2007. pH variability and CO₂ induced acidification in the North Sea. *Journal of Marine Systems* 64: 229-241.
- Blanchard, J.L. *et al.* 2012 Potential consequences of climate change for primary production and fish production in large marine ecosystems *Phil. Trans. R. Soc. B* doi:10.1098/rstb.2012.0231 (2012).
- Brand, L.E., Campbell, L., Bresnan, E. Karenia, 2012. The biology and ecology of a toxic genus. *Harmful Algae* 14, 156-178.
- Borges, A.V., 2005. Do we have enough pieces of the jigsaw to integrate CO₂ fluxes in the coastal ocean? *Estuaries*, 28(1): 3-27.
- Burchard, H. Bolding K., Villarreal M.R., 1999. GOTM—a general ocean turbulence model. Theory, applications and test cases, Tech. Rep. EUR 18745 EN, European Commission.

- Burchard, H., Bolding K., W. Kuhn W., Meister A., Neumann T., Umlauf L., 2006, Description of a flexible and extendable physical-biogeochemical model system for the water column, *J. Mar. Sys.*, 61, pp 180-211.
- Cadee, G.C. and Hegeman, J., 2002. Phytoplankton in the Marsdiep at the end of the 20th Century; 30 years monitoring biomass, primary production, and Phaeocystis blooms *Journal of Sea Research*, 48: 97-110.
- Christensen, V., Walters, C.J. & Pauly, D. 2005. Ecosim with Ecopath: a user's guide, November 2005 edition. Report Fisheries Centre, University of British Columbia, Vancouver, Canada.
- Clark, R. A., Fox, C. J., Viner, D., & Livermore, M. 2003. North Sea cod and climate change - modelling the effects of temperature on population dynamics. *Global Change Biology*, 9(11), 1669–1680. Retrieved from <http://doi.wiley.com/10.1046/j.1365-2486.2003.00685.x>
- Daewel, Ute, Myron A. Peck, and Corinna Schrum. "Life history strategy and impacts of environmental variability on early life stages of two marine fishes in the North Sea: an individual-based modelling approach." *Canadian Journal of Fisheries and Aquatic Sciences* 68, no. 3 (2011): 426-443.
- Daewel, Ute, Myron A. Peck, Wilfried Kuehn, Mike St. John, Irina Alekseeva, and Corinna Schrum, 2008. Coupling ecosystem and individual-based models to simulate the influence of climate variability on potential growth and survival of larval sprat in the North Sea. ." *Fisheries Oceanography* 17, no. 5: 333–351.
- Damm, Peter 1997. Die saisonale Salzgehalts- und Frischwasserverteilung in der Nordsee und ihre Bilanzierung. No. 28.
- Dickson, R., Meinke, J., Malmberg, S.-A., and Lee, A.J. 1980. The "Great Salinity Anomaly" in the Northern North Atlantic 1968-1982. *Progress In Oceanography* 20: 103-151.
- Dippner, J.W. 1993. Larvae survival due to eddy activity and related phenomena in the German Bight. *Science* 4: 303-313.
- Edwards, M., Beaugrand, G., Reid, P.C., Rowden, A.A., and Jones, M.B. 2002. Ocean climate anomalies and the ecology of the North Sea. *Mar Ecol Prog Ser* 239: 1-10.
- Fairall, C. W., Bradley, E. F., Hare, J. E., Grachev, A. A., and Edson, J. B., 2003. Bulk parameterization of air-sea fluxes: updates and verification for the COARE algorithm, *Journal of Climate*, 16, 571-591.
- Flather, R.A., 1981. Results from a model of the northeast Atlantic relating to the Norwegian Coastal Current. In *The Norwegian Coastal Current Vol. 2*, edited by R. Saetre and M. Mork, pp. 427–458, Bergen University, Bergen, Norway.
- Force, N. S. T., 1993. North Sea Quality Status Report, OSPAR.
- Fox, Clive J., et al. "Mapping the spawning grounds of North Sea cod (*Gadus morhua*) by direct and indirect means." *Proceedings of The Royal Society B* 275, no. 1642 (2008): 1543-1547.
- Fransz, H. G., Colebrook, J. M., Gamble, J. C., & Krause, M. 1991. The Zooplankton of the North Sea. *Journal of Sea Research*, 28(1/2), 1–52.

- Garcia, H.E., R.A. Locarnini, T.P. Boyer and J.I. Antonov, 2006. World Ocean Atlas 2005, Volume 4: Nutrients (phosphate, nitrate, silicate). S. Levitus, Ed. NOAA Atlas NESDIS 64, U.S. Government Printing Office, Washington, D.C., 396 pp.
- Geider, R. J., MacIntyre, H. L., and Kana, T. M., 1997. A dynamical model of phytoplankton growth and acclimation: response of the balanced growth rate to light, nutrient limitation and temperature, *Mar. Ecol.-Prog. Ser.*, 148, 187-200.
- Gleckler, P. J., Taylor, K.E., Doutriaux, C. 2008. Performance metrics for climate models, *J. Geophys. Res.*, 113(D6), D06104
- Glibert, P.M., Burkholder, J.M., Kana, T.M. 2012. Recent advances in understanding of relationships between nutrient availability, forms and stoichiometry and the biogeographical distribution, ecophysiology, and food web effects of pelagic and benthic *Prorocentrum* spp. *Harmful Algae*. 14, 231-259.
- Gomez-Gesteira, M., Beiras, R., Presa, P. and Vilas, F., 2011. Coastal processes in northwestern Iberia, Spain. *Continental Shelf Research*, 31(5): 367-375.
- Gowen, R. J., and Bloomfield, S. P., 1996. Chlorophyll standing crop and phytoplankton production in the western Irish Sea during 1992 and 1993, *J. Plankton Res.*, 18, 1735-1751.
- Gowen, R. J., Mills, D. K., Trimmer, M., and Nedwell, D. B., 2000. Production and its fate in two coastal regions of the Irish Sea: the influence of anthropogenic nutrients, *Mar. Ecol.-Prog. Ser.*, 208, 51-64.
- Harten, A. 1983. High resolution schemes for hyperbolic conservation laws. *Journal of Computational Physics* 49: 357-393.
- Heil, C.A., Glibert, P. M., Fan, C. *Prorocentrum minimum* (Pavillard) Schiller –A review of a harmful algal bloom species of growing worldwide importance. *Harmful Algae* 4, 449-470 (2005).
- Hjort, J. "Fluctuations in the great fisheries of northern Europe viewed in the light of biological research." *Rapp. P.-V. Reun. Cons. Int. Explo. Mer* 20 (1914): 1-228.
- Holt, J. T., Allen, J. I., Proctor, R., and Gilbert, F., 2005. Error quantification of a high resolution coupled hydrodynamic-ecosystem coastal-ocean model: part 1 model overview and assessment of the hydrodynamics *Journal of Marine Systems*, 57, 167-188.
- Holt, J., Wakelin, S. and Huthnance, J., 2009. Down-welling circulation of the northwest European continental shelf: A driving mechanism for the continental shelf carbon pump. *Geophysical Research Letters*, 36: doi:10.1029/2009GL038997.
- Holt, J.T. *et al.* 2009. Modelling the global coastal ocean, *Phil. Trans. Roy. Soc. A* 367, 939-951 (2009)
- Holt, J., Wakelin, S., Lowe, J., and Tinker, J., 2010. The potential impacts of climate change on the hydrography of the northwest European Continental shelf. *Progress in Oceanography*, doi:10.1016/j.pocean.2010.1005.1003.
- Holt, J., Butenschön, M., Wakelin, S. L., Artioli, Y., and Allen, J. I. 2012. Oceanic controls on the primary production of the northwest European continental shelf: model experiments under recent past conditions and a potential future scenario, *Biogeosciences*, 9, 97-117, doi:10.5194/bg-9-97-2012,

- Holt, J., Butenschön, M., Wakelin, S.L., Artioli, Y., and Allen, J.I. 2012. Oceanic controls on the primary production of the northwest European continental shelf: model experiments under recent past conditions and a potential future scenario. *Biogeosciences* 9: 97-117.
- Huisman, J., van Oostveen, P. and Weissing, F.J., 1999. Critical depth and critical turbulence: Two different mechanisms for the development of phytoplankton blooms. *Limnology and Oceanography*, 44(7): 1781-1787.
- Huthnance, J.M., Holt, J.T. and Wakelin, S.L., 2009. Deep ocean exchange with west-European shelf seas. *Ocean science*, 5(4): 621-634.
- ICES, 2012. Annex 5 Report on Key Run for the North Sea Ecopath with Ecosim Ecosystem Model, 1991–2007. In ICES 2012. Report of the Working Group on Multispecies Assessment Methods (WGSAM), 10–14 October 2011, Woods Hole, USA. ICES CM 2011/SSGSUE: 10. 229 pp.
- Janssen, F. Statistische Analyse mehrjähriger Variabilität der Hydrographie in Nord- und Ostsee Möglichkeiten zur Validation und Korrektur systematischer Fehler eines regionalen Ozeanmodells. PhD-thesis, University of Hamburg, Hamburg, Germany.
- Janssen, F., Schrum, C., and Backhaus, J. 1999. A climatological data set of temperature and salinity for the Baltic Sea and the North Sea. *Ocean Dynamics* 51: 5-245.
- Joint, I., and Pomeroy, A., 1993. Phytoplankton Biomass and Production in the Southern North-Sea, *Mar. Ecol.-Prog. Ser.*, 99, 169-182.
- Joint, I., Wollast, R., Chou, L., Batten, S., Elskens, M., Edwards, E., Hirst, A., Burkill, P., Groom, S., Gibb, S., Miller, A., Hydes, D., Dehairs, F., Antia, A., Barlow, R., Rees, A., Pomroy, A., Brockmann, U., Cummings, D., Lampitt, R., Loijens, M., Mantoura, F., Miller, P., Raabe, T., Alvarez-Salgado, X., Stelfox, C., and Woolfenden, J., 2001. Pelagic production at the Celtic Sea shelf break, *Deep-Sea Res. Part II-Top. Stud. Oceanogr.*, 48, 3049-3081.
- Kalnay, E., Kanamitsu, M., Kistler, R., Collins, W., Deaven, D., Gandin, L., Iredell, M., Saha, S., White, G., Woollen, J., Zhu, Y., Leetmaa, A., Reynolds, R., Chelliah, M., Ebisuzaki, W., Higgins, W., Janowiak, J., Mo, K.C., Ropelewski, C., Wang, J., Jenne, R., and Joseph, D. 1996. The NCEP/NCAR 40-Year Reanalysis Project. *Bulletin of the American Meteorological Society* 77: 437-471.
- Kjørboe, T., Munk, P., and Richardson, K. 1987. Respiration and growth of larval herring *Clupea harengus*: relation between specific dynamic action and growth efficiency. *Mar. Ecol. Prog. Ser.* 40: 1-10.
- Lenhart, H. J., Mills, D. K., Baretta-Bekker, H., van Leeuwen, S. M., van der Molen, J., Baretta, J. W., Blaas, M., Desmit, X., Kuhn, W., Lacroix, G., Los, H. J., Menesguen, A., Neves, R., Proctor, R., Ruardij, P., Skogen, M. D., Vanhoute-Brunier, A., Villars, M. T., and Wakelin, S. L., 2010. Predicting the consequences of nutrient reduction on the eutrophication status of the North Sea, *Journal of Marine Systems*, 81, 148-170, 10.1016/j.jmarsys.2009.12.014.
- Lewis, K., Allen, J. I., Richardson, A., J, and Holt, J. T., 2006. Error quantification of a high resolution coupled hydrodynamic-ecosystem coastal-ocean model: part3, Validation with Continuous Plankton Recorder data, *Journal of Marine Systems*, 63, 209-224.

- Mackinson, S and Daskalov, G. 2007. An ecosystem model of the North Sea to support and ecosystem approach to fisheries management: description and parameterisation. Cefas Science Series Technical Report 142. 195pp.
- Mackinson, S., Daskalov, G. 2007. An ecosystem model of the North Sea to support an ecosystem approach to fisheries management: description and parameterisation. Sci Ser. Tech. Rep., Cefas Lowestoft, 142: 196pp.
- Merino G., *et al.* Can marine fisheries and aquaculture meet fish demand from a growing human population in a changing climate? *Global Environmental Change* doi:10.1016/j.gloenvcha.2012.03.003 (2012)
- Mcquatters-gollop,A., Edwards,M., Pradhan,Y., Mee,L.D., Lavender,S.J., and Attrill,M.J. 2007. A long-term chlorophyll data set reveals regime shift in North Sea phytoplankton biomass unconnected to nutrient trends. *Marine Biology* 52: 635-648.
- Moll,A. and Radach,G. 2003. Review of three-dimensional ecological modelling related to the North Sea shelf system: Part 1: models and their results. *Progress In Oceanography* 57: 175-217.
- Munk,P., Larsson,P.O., Danielssen,D.S., and Moksness,E. 1987. Variability in frontal zone formation and distribution of gadoid fish larvae at the shelf break in the northeastern North Sea. *Mar.Ecol.Prog.Ser.* 177: 221-233.
- Orlanski,I. 1976. A simple boundary condition for unbounded hyperbolic flows. *Journal of Computational Physics* 21: 251-269.
- Pätsch, J., and Lenhart, H.-J., 2004. Daily loads of nutrients, total alkalinity, dissolved inorganic carbon and dissolved organic carbon of the European continental rivers for the years 1977-2002. , *Berichte aus dem Zentrum für Meeres- und Klimaforschung; Reihe B: Ozeanographie*, 48, 159pp.
- Peters, R. H. 1983. *The Ecological Implications of Body Size* (Cambridge Studies in Ecology). (E. Beck, H. J. B. Birks, & E. F. Connor, Eds.) (p. 344). Cambridge University Press. Retrieved from <http://www.amazon.com/Ecological-Implications-Cambridge-Studies-Ecology/dp/052128886X>
- Pitois,S.G. and Fox,C.J. 2006. Long-term changes in zooplankton biomass concentration and mean size over the Northwest European shelf inferred from Continuous Plankton Recorder data. *ICES Journal of Marine Science* 63: 785-798.
- Radach,G. and Pätsch,J. 1997. Climatological annual cycles of nutrients and chlorophyll in the North Sea. *Journal of Sea Research* 01.
- Richardson,K., Visser,A.W., and Pedersen,F.B. 2000. Subsurface phytoplankton blooms fuel pelagic production in the North Sea. *J.Plankton Res.* 22: 1663-1671.
- Rydberg, L., Aertebjerg, G., and Edler, L., 2006. Fifty years of primary production measurements in the Baltic entrance region, trends and variability in relation to land-based input of nutrients, *Journal of Sea Research*, 56, 1-16, 10.1016/j.seares.2006.03.009.
- Schrum,C. and Backhaus,J.O. 1999. Sensitivity of atmosphere-ocean heat exchange and heat content in the North Sea and the Baltic Sea. *Tellus A* 51: 526-549.

- Schrum, C., Alekseeva, I., and St. John, M. 2006. Development of a coupled physical-biological ecosystem model ECOSMO: Part I: Model description and validation for the North Sea. *Journal of Marine Systems* 61: 79-99.
- Sharples, J., 2008. Potential impacts of the spring-neap tidal cycle on shelf sea primary production. *Journal of Plankton Research*, 30(2): 183-197.
- Smith, G. and K. Haines, 2009. Evaluation of the S(T) assimilation method with the Argo dataset. *Quarterly Journal of the Royal Meteorological Society*, 135, 739–756, doi:10.1002/qj.395.
- Song, Y., and Haidvogel, D., 1994. A semi-implicit ocean circulation model using a generalized topography-following coordinate system, *Journal of Computational Physics*, 115, 228-244.
- Steele, J. H., 1956. Plant production on the Fladen Ground, *Journal of Marine Biology Association UK*, 35, 1-33.
- Taylor, K.E. 2001. Summarizing multiple aspects of model performance in a single diagram. *J. Geophys. Res.* 106: 7183-7192.
- Tagliabue, A., Bopp, L., Gehlen, M., 2011. The response of marine carbon and nutrient cycles to ocean acidification: Large uncertainties related to phytoplankton physiological assumptions. *Global Biogeochemical Cycles* 25,
- Thomas, H., Bozec, Y., Elkalay, K. and de Baar, H.J.W., 2004. Enhanced Open Ocean Storage of CO₂ from Shelf Sea Pumping. *Science* 304: 1005-1008.
- Turrell, W.R., Henderson, E.W., Slessor, G., Payne, R., and Adams, R.D. 1992. Seasonal changes in the circulation of the northern North Sea. *Continental Shelf Research* 12: 257-286.
- van Raaphorst, W. and Veer, H.W. 1990. The phosphorus budget of the Marsdiep tidal basin (Dutch Wadden Sea) in the period 1950-1985: importance of the exchange with the North Sea. *Hydrobiologia* 195: 21-38.
- Vargo, G.A., *et al.* Nutrient availability in support of *Karenia brevis* blooms in the central West Florida Shelf: What keeps *Karenia* blooming? *Cont. Shelf Res.* 28, 73-98 (2008).
- Vörösmarty, C. J., Fekete, B. M., Meybeck, M., and R., L., 2000. A simulated topological network representing the global system of rivers at 30-minute spatial resolution (STN-30). *Global Biogeochemical Cycles*, 14, 599-621.
- Wakelin, S.L., Holt, J.T., Blackford, J.C., Allen, J.I., Butenschön, M., Artioli, Y., (2012). Modeling the carbon fluxes of the northwest European continental shelf: validation and budgets. *J. Geophys. Res.* 117, C05020, doi:10.1029/2011JC007402.
- Wakelin, S.L., J.T. Holt and R. Proctor, 2009. The influence of initial conditions and open boundary conditions on shelf circulation in a 3D ocean-shelf model of the North East Atlantic. *Ocean Dynamics*, 59, 67–81 doi:10.1007/s10236-008-0164-3.
- Watson, R. and Pauly, D., 2001. Systematic distortions in world fisheries catch trends. *Nature*, 414(6863): 534-536.
- Young, E.F. and J.T. Holt, 2007. Prediction and analysis of long-term variability of temperature and salinity in the Irish Sea. *Journal of Geophysical Research*, 112 C01008, doi:10.1029/2005JC003386.